Targeting the Adaptability of Heterogeneous Aneuploidy Populations

By

Guangbo Chen

Submitted to the graduate degree program in Molecular and Integrative Physiology and the Graduate Faculty of the University of Kansas in partial fulfillment of the requirements for the degree of Doctor of Philosophy.

_____

Co-Chairperson Dr. Rong Li

_____

Co-Chairperson Dr. Michael Wolfe

_____

Dr. Marco Blanchette

_____

Dr. Scott Hawley

_____

Dr. Joe Lutkenhaus

Date Defended: Jan 6, 2015

The Dissertation Committee for Guangbo Chen

certifies that this is the approved version of the following dissertation:

Targeting the adaptability of heterogeneous aneuploidy population

_____

Co-Chairperson Rong Li

_____

Co-Chairperson Michael Wolfe

Date approved: 02/23/2015

Abstract

Aneuploid genomes, characterized by unbalanced and diverse chromosome stoichiometry (karyotype), are associated with cancer malignancy and drug-resistance of human pathogenic fungi. My PhD projects studied three aspects of aneuploidy that are logically linked to each other: the production of aneuploidy by environmental stress; the impact of the heterogeneous aneuploidy population generated by stress on adaptability; the potential therapeutic strategy towards these heterogeneous aneuploidy populations with high adaptability, a root for the clinical challenge in treating aneuploidy diseases such as cancer.

We investigated whether pleiotropic stress could induce the production of aneuploidy in budding yeast. We showed that while diverse stresses can induce an increase in chromosome instability (CIN), proteotoxic stress, caused by transient Hsp90 inhibition or heat-shock, drastically elevated CIN to produce karyotypically mosaic cell population. The latter effect is linked to an evolutionarily conserved role for Hsp90 chaperon complexes in kinetochore assembly.

We found the induction of aneuploidy population potentiates adaptability. Continued growth in the presence of Hsp90 inhibitor resulted in emergence of drug-resistant colonies with chromosome XV gain. This drug-resistance phenotype is a quantitative trait involving copy number increases of at least two genes located on chromosome XV. Short-term exposure to Hsp90 stress, which produced an aneuploidy population with heterogeneous karyotypes, potentiated fast adaptation to unrelated cyto-toxic compounds through different aneuploid chromosome stoichiometries.

We designed an evolutionary trap to harness the adaptability of heterogeneous aneuploidy populations with high adaptability. Using a combination of experimental data and a general statistical model, we showed that the degree of phenotypic variation, thus evolvability, escalates with the degree of overall growth suppression irrespective of stress mechanisms. Such scaling explains the challenge of treating aneuploidy diseases with diverse different karyotypes by imposing a single mode of inhibition, yet specific karyotype features can be highly targetable. Motivated by this finding, we proposed an "evolutionary trap" targeting both karyotypic diversity and fitness of the population. This strategy entails a selective condition "channeling" a karyotypically divergent population into one with a predominant and drugable karyotypic feature. We provided a proof-of-principle test with mechanistic explanation in budding yeast and demonstrated the potential efficacy of this strategy toward aneuploidy-based azole resistance in the human pathogen *Candida albicans*.

Karyotype channeling also happens naturally in tumors, which is resulted from adaptation to the tissue micro-environment and/or the need for oncogenic transformation. This natural karyotypic selection may be leveraged by drug treatment targeting the selected karyotype feature. Thus, the strategy proposed here may be utilized for designing a class of treatment regime distinct from current therapies.

Dedicated to my dear parents,

Yongtai Chen & Zhenmei Liang

献给我亲爱的父母，

陈永泰和梁贞梅

Acknowledgement

Dr. Rong Li, who is my mentor through the PhD, provided training and supports that are essential for my advancement in science. My committee members guided the training processes.

For experiments, I would like to thank: N. Pavelka, B. Rubinstein and H. Li for help with data analysis, J. Zhu, B. Fleharty and J. Haug for experimental assistance, S. Lindquist for helpful discussion, and T. potapova and B. Slaughter for comments on the manuscript. CF strains and disomies are kind gifts from F. Spencer and A. Amon, respectively. This work was supported by NIH grant RO1GM059964 to R.L.

Table of Contents

Chapter 1: Introduction -- Aneuploidy, an Type of Widely Observed Mutations

The contents are adapt from:

Chen G*, Rubinstein B, Li R. 2012. Whole chromosome aneuploidy: big mutations drive adaptation by phenotypic leap. *Bioessays* **34:** 893-900**.** *(Cover story)*

**** correspondence author***

Aneuploidy is a widespread genetic variation in nature

Error in genome transmission is usually harmful to the fitness of an individual cell or organism, but in a population with a large number of individuals, imperfect genome transmission produces genetic variants, which are essential for adaptive evolution under selection. The most commonly considered genetic variants during evolutionary processes are point mutations. Chromosome segregation also produces genetic variants, not in single gene sequences but in the copy number of chromosomes, which contain hundreds of genes. This genetic variation is referred to as whole chromosome aneuploidy[2-5]. We note that "aneuploidy" in this dissertation refers to whole chromosome number variation without the inclusion of segmental chromosome aneuploidy. By changing the dosage of many genes, aneuploidy leads to dramatic consequences.

Early studies on aneuploidy related it solely to the disease state, which predicts that aneuploidy is unlikely to be persistent in the population as a result of the detrimental effect on fitness. In recent years, the advent of genome technology, especially comparative genome hybridization and DNA sequencing, reveals a different picture (Table 1). In lab strains of *S. cerevisiae*, it was estimated that 8% of the strains from the genome-wide ORF knockout library are aneuploid[6]. In wild yeasts isolated from the environment such as oak tree soil, aneuploidy was also identified[7]. In industrial strains, the deviation of DNA content from euploidy is a common feature documented decades ago[8]. High-resolution genomic analysis techniques such as array-based comparative genomic hybridization (aCGH) and next-generation sequencing has revealed the detailed genome structure and copy number variation, which include whole chromosome aneuploidy, in strains used for diverse industrial applications, such as sake and beer brewing[7,9,10], wine fermentation[10], and sherry-wine aging[11]. In pathogenic yeast/fungi, aneuploidy is associated with drug resistance[2,12]. For example, more than 50% fluconazole-resistant *Candida albican*s isolates from patients were found to harbor either whole chromosome or segmental duplication of Chr 5[13]. Whole chromosome

aneuploidy was also found in fluconazole-resistant strains of another pathogenic yeast, *Cryptococcus neoformans*[14].

Table 1: Examples of aneuploidy associated with environmental stress

Species	Conditions		Associated stress
Saccharomyces cerevisiae	Lab	Gene deletion	various growth defect
		Evironmental stress	proteotoxic stress
	Industrial	sake production (1/9) *	ethanol, high sugar (osmotic stress)
		wine production (4/26) *	ethanol, acetaldehyde, high sugar
		beer brewing (3/4) *	ethanol, high sugar
Candida albicans		fluconazole resistance(21/42)*	membrane defect
Cryptococcus neoformans		fluconazole resistance	membrane defect
Leishemania		different species	
Human		most cancer	growth restriction, immune attack
		liver	metabolic stress

* Frequency of aneupoidy reported in the parentheses (Aneuploids/Total tested)

Beyond yeast and fungi, aneuploidy has been documented in many other contexts. It is long thought that due to their erroneous transmission during meiosis, aneuploid karyotypes are unlikely to be maintained during long-term adaptation and speciation in natural history. However, this view of sexual reproduction barrier for aneuploidy is challenged by recent findings. Leishmaniasis is a form of clinical pathology ranging from disfiguring cutaneous lesions to fatal visceral infection, caused by different *Leishmania* protozoan parasites associated with varied pathology features[15]. Interestingly, it was found that four different *Leishmanias* have little variation in DNA sequence, yet exhibit dramatic difference in chromosome copy numbers[16]. The aneuploid *Leishmania* can perform sexual reproduction nonetheless[17], but the mechanistic details have yet to be elucidated.

In multicellular organisms such as mammals, aneuploidy is present in both the germline and somatic tissues. Germline aneuploidy is rare and when present it causes severe developmental abnormalities. In humans, chromosome number variation in fertilized oocytes causes rare birth defects such as Down's syndrome (trisomy 21, incidence at 1 in 2,000 births), Edwards syndrome (trisomy 18, 1 in 6,000 births), and Patau syndrome (trisomy 13, less than 1 in 10,000 births). However, it is intriguing that several studies reported that aneuploidy is highly prevalent in the early blastomeres of developing human or mouse embryos[18,19], raising a question as to at what stage aneuploidy impairs developmental programs and how

aneuploid cells are cleared during later development. On the other hand, aneuploidy in somatic cells is not rare at all. Aneuploidy is a hallmark of cancer, one of the leading causes of death. It is present in more than 70% tumors[20-22]. Evidence indicates that aneuploidy may drive the tumorigenesis through its adaptive effect in a cell population. But somatic aneuploid is not limited to cancer cells – work in recent years revealed that several normal human tissues bear a surprisingly high-level diversity of karyotypes. For example, normal human liver contains 25%-50% aneuploids[23]. In the fetal brain, it was estimated that 30-35% neurons are aneuploidy[24,25]. Compared with animal organisms, plant such as *Arabidopsis thaliana*, tolerates germline aneuploidy well and can cause substantial phenotypic variations[26,27]. In summary, aneuploidy is observed from yeasts to human. With the increasing application of quantitative DNA technology, it is likely that further evidence to emerge from diverse contexts illustrating the wide existence of aneuploidy.

Why is aneuploidy, which defines an "abnormal" genome, widespread in nature?

1) "Abnormal" karyotypes can be beneficial under abnormal environment.

The effect of aneuploidy on fitness is context specific[3]. Aneuploidy is thought to bring abnormality due to an imbalance in gene dosage. It is assumed that the "normal" functionality of molecular complexes or pathways made of more loosely interacting molecules relies on the correct stoichiometry of their protein components. When the normal stoichiometry is skewed, the functionality, such as efficiency, timing or specificity, of the system would be reduced or altered in someway. However, normalcy is relative and in the context of physiology it refers to the preferred state or the state of highest fitness under a given condition. Thus, a cell with a genome imbalanced (i.e. with suboptimal stoichiometry) for one condition, say the "normal" environment, may indeed have the altered functionality that gives rise to optimal fitness

under an altered, for instance, stressful condition[3,28]. In many cases, the prevalence of aneuploidy as discussed above was found indeed in association with stress (Table 1). For example, the wine brewing/aging process imposes potent proteotoxic stress due to high concentrations of ethanol and acetaldehyde[11]. Fluconazole impairs the synthesis of ergosterol, an essential component of *Candida albicans*' membrane[29]. Even the normal tissue environment in an animal organism is usually repressive for cellular proliferation, which cancer cells must overcome (see following).

The mechanism by which aneuploidy can bring adaptive phenotypic change has been extensively studied in single cell organisms. In different manners, aneuploidy can cause expression change manifested on both mRNA[1,6,28,30-33] and protein[28,34] levels. Although altered chromosome stoichiometry leads to expression changes of many genes, in some cases the adaptive effect of aneuploidy can be attributed to dosage change of a single gene. For example, homozygous deletion of *RPS24A* gene on yeast Chr V causes a growth defect. However, large, fast-growing colonies occasionally appear among a group of small colonies. It was found that cells in these large colonies had gained a copy of Chr IX, carrying the *RPS24B* gene that is 97% identical in sequence to *RPS24A*[6]. An advantage of achieving adaptive functions through aneuploidy over that through mutations of specific genes is that genes contributing to the same physiological outcome may be present on the same aneuploid chromosome, and this allows combination of adaptive dosage changes of two or several genes through a single chromosome dosage change. In *C. albicans*, the fluconazole resistance associated with Chr V duplication can be mimicked by increasing the dosage of *ERG11* (encoding the drug target) and *TAC1* (encoding a regulator of the drug efflux system), which are both located on this chromosome[13,29].

The dosage change of genes located on an aneuploid chromosome can also bring adaptive traits by altering the expression of genes on other chromosome. Myo1 is a motor protein required for constriction of the bud neck during cytokinesis, whose gene deletion leads to cytokinesis failure and in most cases lethality[35]. In the rare *Δmyo1* survivors, some are able to restore cytokinesis through gradual thickening

of the cell wall at the bud neck. In these adapted strains, the expression of several genes involved in cell wall biogenesis was increased up to 16-fold compared to that in the isogenic wild-type haploid strain. Interestingly, these genes are located on multiple different chromosomes, but a commonly amplified chromosome in these strains is Chr XVI. It turned out that Chr XVI carries the genes encoding two upstream regulators of cell wall biogenesis, Rlm1 and its upstream activator Mkk2, a MAP kinase kinase[29]. Thus, through altering the dosage of regulatory factors aneuploidy can cause broad gene expression changes well beyond a direct DNA dosage effect.

Even though aneuploidy can bring adaptive traits into the population, it is also noticed that in any given environment, such as the presence of proteotoxic stress[1,36] or a DNA damaging agent[28,37], or low temperature[28], most aneuploid karyotypes tested are not adaptive, but only some aneuploid karyotypes show enhanced growth compared to the euploid. This reminds us of the fact that phenotypic changes generated by mutations are usually deleterious[38]; nonetheless mutations are a necessary ingredient of the force that drives adaptive evolution. In other words, chromosome number variation or any other type of mutations does not guarantee enhanced cell fitness, but rather the adaptive value of genetic variation is best appreciated on the population level, where the adaptive variant is selected through competition.

2) Aneuploidy impacts organismal versus cellular fitness differently in multicellular species.

Despite evidence in unicellular organisms demonstrating how changes in chromosome stoichiometry bring about adaptation, it remains elusive whether similar mechanisms exist in metazoans. It has been shown that aneuploidy leads to gene expression variation in mammalian cell lines in a manner similar to that in yeast[32,33,39], but the counter argument has been that aneuploidy causes debilitating diseases such

as Down's syndrome and cancer. One way to reconcile this paradox is to distinguish cellular fitness from organismal fitness.

A)

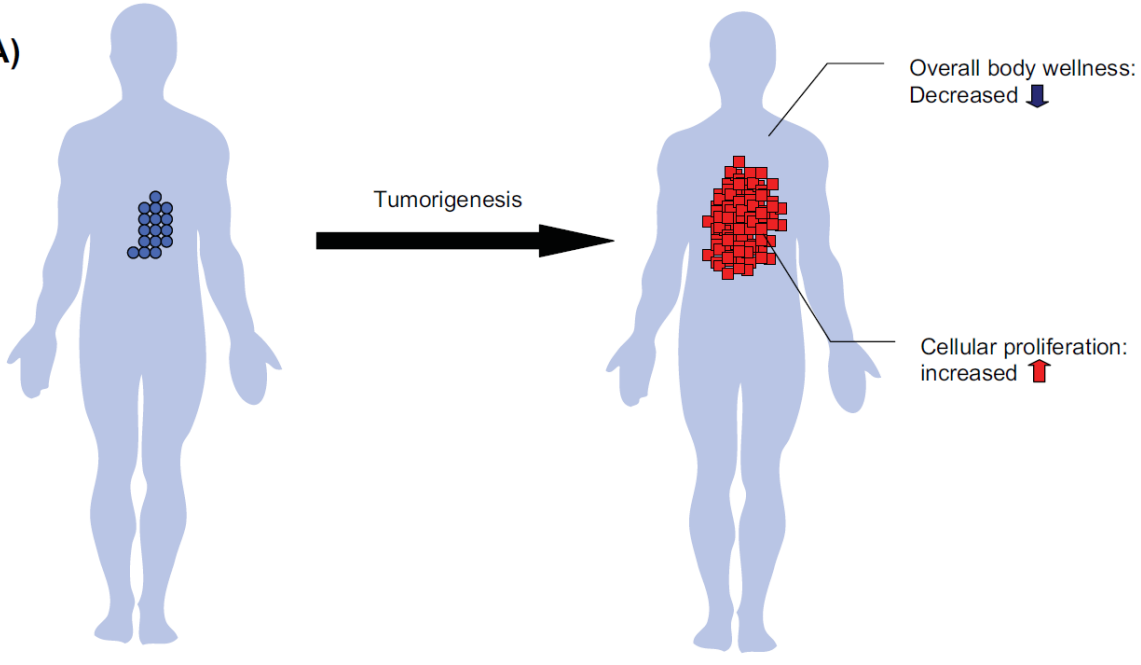

B)

Role of aneuploidy in disease

	Organismal Aneuploidy	Cellular Aneuploidy
Example	Down's Syndrome	Cancer
Cellular karyotype competition	No	Yes
Cellular fitness /proliferation	↑ Example: Enhanced myeloproliferation compared to euploid ↓ Example: Reduced angiogenesis	↑ Through competition, the adaptive karyotype is seleceted. Example: Chr 8 duplication in APL
Overall body wellness	↓	↓

Figure 1. Aneuploidy can exert opposing effect on overall body wellness and cellular fitness in disease.

A: In tumorigenesis, the cellular fitness/proliferation of tumor tissue is enhanced at the expense of overall body wellness. **B:** Aneuploidy can have different roles on cellular versus organismal level. Organismal aneuploidy originates from karyotype alteration in parental germ line/gametes. Cellular aneuploidy results from errors in somatic cell mitosis.

In natural history, the appearance of multi-cellularity loosed the tie between organismal evolution and celluar evolution. The former considers relative fitness between individuals, whereas the later considers fitness between cells in the same individuals. In order to survive organismal competition, strict developmental programs tightly control cell proliferation, death and morphogenesis in order to form and maintain homeostasis of functional structures. Thus, organismal fitness occurs at the expense of the proliferative ability or even viability of individual component cells. Oncogenic mutations, on the other hand, promote the cellular proliferation and survivability of cancer cells at the expense of the fitness of the host organism (Figure 1A). For example, the Ras protein, which controls cellular mitogenic signals, is mutated to hyperactive forms in 25% of cancers and renders abnormally high growth potential for the cancer cells harboring the mutations[40]. The extrinsic barrier to cell proliferation, such as limited vesicular accessibility, can also be lifted by enhanced expression of VEGF in tumors[40]. These examples highlight the apparent conflict between cellular versus organismal fitness.

Whole organism aneuploidy such as Down's syndrome originates from karyotype alteration in parental germ cells, which leads to drastic gene expression changes that disrupt the intricate developmental program evolved during long-term natural history, resulting in disease of the organism[41]. On the other hand, tumorigenesis involves fierce selection and competition between normal cells and cancer cells as well as between cancer cells of diverse karyotypes[42,43]. As the tissue environment for cancer cells is hostile, this presents the natural selective force for different types of genetic variants that could survive and improve the fitness of the cell population at the expense of organismal fitness. As the well known cancer hallmark, karyotype abnormality is a major source of genetic variation in cancer [21,44].

The direct causative relationship between specific karyotype and overproliferation phenotype of tumor has been captured in a handful cases (Figure 1B). Trisomy 8 was observed in 12% of human acute promyelocytic leukemia (APL) [45,46]. It was long speculated that trisomy 8 brings the growth advantage

through introduction of an additional copy of the oncogene, *MYC*. Interestingly, in an APL mouse model, 64% of the cases were trisomy for chromosome 15, which also contains the mouse *MYC*. *MYC* retrovirus transduction facilitates myeloid leukemogenesis and suppressed gain of chromosome 15. Meanwhile, the induction efficiency for APL in *MYC* heterozygous background was reduced. Remarkably, in *MYC* heterozygous mouse where APL was inducted, a preferential amplification of the chromosome 15 containing the wild-type *MYC,* but not the one missing the gene, was observed. These data strongly suggest that the elevated copy number of *MYC* through aneuploidy directly participates in the progression of APL[47]. Another case comes from the well-characterized Down's syndrome-associated predisposition to leukemia. Down's syndrome patients have a reduced incidence of most tumors compared with euploid population[48,49], but their incidence of pediatric acute megakaryoblastic leukemia (AMKL) is increased 500 times[50]. Accordingly, the mouse model of Down's syndrome, which contains trisomic chromosome region syntenic to human chromosome 21, also shows excessive cell proliferation in myeloid linage, which may progress into AMKL[51]. Later, it was found that by deleting the trisomic copy of *Erg*, a transcription factor necessary for platelet development and stem cell function, the myeloproliferation was restored to normal[52]. This case highlights that a karyotype (trisomy 21) that is detrimental in organismal level, can nontheless increased fitness and proliferation at cellular level under certain context (Figure 1B). In spite of a few well-studied cases, the direct causative link between karyotype and tumor phenotype in many cases remains elusive due to the high level karyotype complexity associated with even a single cancer. This may reflect the existence of different ecological niche in a tumor [42]. In addition, different karyotypes can bring adaptation to the same stress, as shown recently in budding yeast[28,30]. The tools that monitor the karyotype in single cell level, such as spectral karyotyping (SKY) or single-cell sequencing[53], will provide insight into how karyotype heterogeneity evolves during the tumor progression or cancer treatment. An ability to dissect the contribution of specific karyotypes to tumor phenotypes in a karyotypically heterogeneous population will be crucial for understanding the role of aneuploidy in tumorigenesis.

Chromosome instability can be induced by stress

The broad existence of aneuploidy raises the question: how are aneuploids generated? Mitotic error has long been known as a result of lesions in the genes controlling the chromosome segregation processes[54,55]. Genes that cause CIN when mutated are called CIN genes, many of which encode components of kinetochore, centrosome or mitotic checkpoint, which directly participate in chromosome segregation process. In mammals, there is considerable evidence CIN gene mutations are tumorigenetic, even though the exact tumorigenetic karyotypes that arise in the presence of these mutations have not been identified. For example, Mad2 overexpression in mouse, which delays mitotic progression, promotes the occurrence of aneuploidy and leads to a wide spectrum of tumors[56]. Human genetics also discovered mutations in checkpoint component BUB1B[57], or centrosomal protein CEP57[58] cause mosaic variegated aneuploidy and hereditary cancer. However, CIN that is too high can inhibit tumorigenesis. In mouse, the haploinsufficiency of CENP-E, a kinechore component, modestly increase CIN in various tissues[59]. It drastically increases the incidence of spleen and lung tumors in aged animals. However, in liver, it inhibits the formation of spontaneous cancer. As liver's basal level of CIN is high[60,61], it is speculated that CIN level that is too high to even maintain the tumorigenetic karyotype can suppress the tumor formation[59].

The intimacy between the appearance of aneuploidy and stress (table 1) raised the possibility that stress may be another way to induce the production of aneuploids. In Chapter 2, using a selective-neutral artificial chromosome, I showed that environmental stress, especially Hsp90 inhibition, can induce the production of aneuploids. Importantly, as a consequence, the karyotype diversity potentiates the population adaptability to diverse environmental stress. Karyotype diversity is an important property observed in certain pathogenesis process, such as tumor and candidemia, which endows the cell

population with superior adaptability against therapeutic regimes. I further investigated how to target the adaptability of heterogeneous aneuploidy populations, with the results presented in Chapter 3.

Chapter 2: The Production of Aneuploidy by Stress and Its Consequence on Adaptability

Chen G, Bradford WD, Seidel CW, Li R. 2012. Hsp90 stress potentiates rapid cellular adaptation through induction of aneuploidy. *Nature* **482:**246-50**.**

Abstract

Aneuploidy, a state of having uneven numbers of chromosomes, is a form of large-effect mutation able to confer adaptive phenotypes under diverse stress conditions[2,3]. Here we investigate whether pleiotropic stress could in turn induce aneuploidy in budding yeast. We show that while diverse stresses can induce an increase in chromosome instability (CIN), proteotoxic stress, caused by transient Hsp90 inhibition or heat-shock, drastically elevated CIN to produce karyotypically mosaic cell population. The latter effect is linked to an evolutionarily conserved role for Hsp90 chaperon complexes in kinetochore assembly[62,63]. Continued growth in the presence of Hsp90 inhibitor resulted in emergence of drug-resistant colonies with chromosome XV gain. This drug-resistance phenotype is a quantitative trait involving copy number increases of at least two genes located on chromosome XV. Short-term exposure to Hsp90 stress potentiated fast adaptation to unrelated cyto-toxic compounds through different aneuploid chromosome stoichiometries. These findings demonstrate that aneuploidy is a form of stress-inducible mutation in eukaryotes, capable of fueling rapid phenotypic evolution and drug resistance, and reveal a new role for Hsp90 in regulating the emergence of adaptive traits under stress.

How cells maintain stable phenotypes and yet can adapt to diverse stress conditions through heritable change is a question with broad implications in evolution and disease progression. In prokaryotes, while the genome is propagated with high fidelity under normal conditions, extensive studies have demonstrated that different modes of genetic variation can be directly induced by stress, fueling stress adaptation [64]. Recent work has revealed that one form of adaptive mutation in eukaryotic cells is the alteration of chromosome copy number, or aneuploidy [2,3,28]. Aneuploid yeast has been observed in diverse laboratory[3], industrial [7,10,11] and natural [7] environments. Aneuploidy leads to expression changes of many genes at levels that largely scale with gene copy number changes, bringing about dramatic phenotypic variation in a karyotype-specific manner under diverse growth conditions [28]. These findings suggest that to maintain phenotypic stability, karyotype stability must be ensured, and indeed intricate mechanisms have evolved to achieve highly accurate chromosome segregation to prevent CIN during mitotic proliferation. Furthermore, as aneuploids are known to exhibit growth disadvantage compared to euploids under stress-free conditions [1,28], the pre-existing karyotype diversity in a euploid population is likely to be limited for rapid adaptation when exposed to stressful environments. This raises the question of whether the cellular mechanisms ensuring chromosome transmission fidelity may be relaxed under stress, thus allowing the emergence of karyotypic diversity to fuel rapid cellular adaptation.

To test whether stress conditions in general could increase the rate of whole chromosomal instability, we exposed haploid yeast cells to chemicals inducing various types of pleiotropic stress for 12-14 hours and quantified chromosome loss rate by using the selection-neutral, chromosome fragment (CF)-based colony color assay (Figure 1a, Figure 2 and page 97 appendix) [65]. This initial screen revealed that many stress conditions, including hydrogen peroxide (oxidative stress), cycloheximide (translational stress), tunicamycin (ER stress), etc., elevated the chromosome loss rate to a level similar to that caused by benomyl, a microtubule inhibitor (Figure 1a). Surprisingly, radicicol, an Hsp90 inhibitor [66], was by far the most effective CIN inducer: the chromosome loss rate (7.4×10^{-2}/cell division) was hundreds of times above the control (2×10^{-4}/cell division), even at a radicicol concentration (10 μg/ml or 27 μM) with only minor

effect on growth (Figure 1a, Figure 3). Quantitative PCR (qPCR) confirmed that red colonies induced by radicicol had lost the whole CF (Figure 4a). Two of the 13 tested red colonies were confirmed to have also gained chromosome (Chr) X or Chr XI (Figure 4b, c).

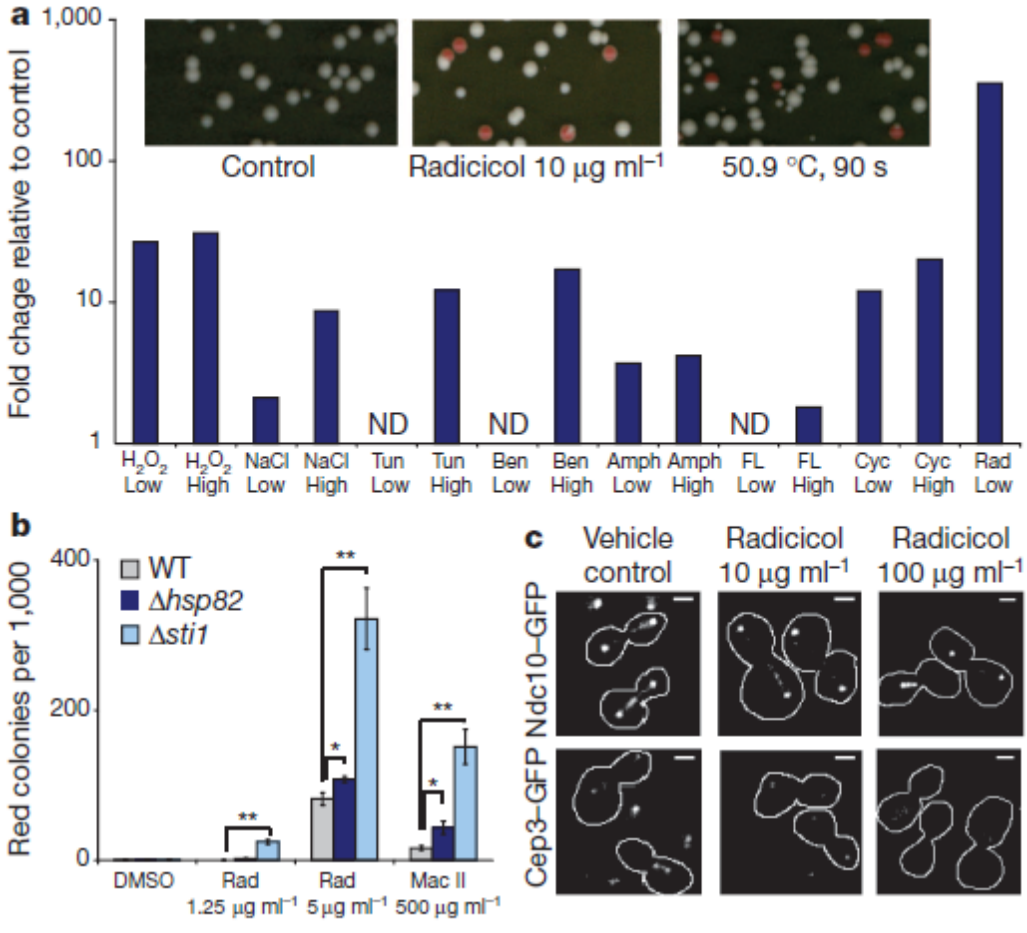

Figure 1. Diverse stress conditions, especially Hsp90 inhibition, induce chromosomal instability.

(a) Up: Colony appearance on YPD plates after cells were exposed to no stress (left), 16 hr of 10 g/ml radicicol treatment (middle) or 90 sec heat shock at 50.9 °C. White colony color indicates retentions of CF; red indicates CF loss. Down: CF loss rates during exposure to diverse stress were inferred from red colony frequencies normalized to that of the vehicle-control population. N.D.: increase not detected over control. See Figure 2, 3. **(b)** Deletion of *HSP82* or *STI1* sensitized the CIN-inducing effect of radicicol and macbecin II. Red colony frequencies normalized to that of wild-type DMSO control were averaged among 4 replicates, shown with standard error of the mean (SEM). *, $p<0.05$; **, $p<0.01$, two-tail t-test. **(c)** Representative images showing kinetocore localization of Ndc10-GFP and Cep3-GFP under different

conditions as indicated. Radicicol diminished Cep3-GFP localization at the kinetocore. Scale bar: 2µm. See Figure 5 for additional images and quantification.

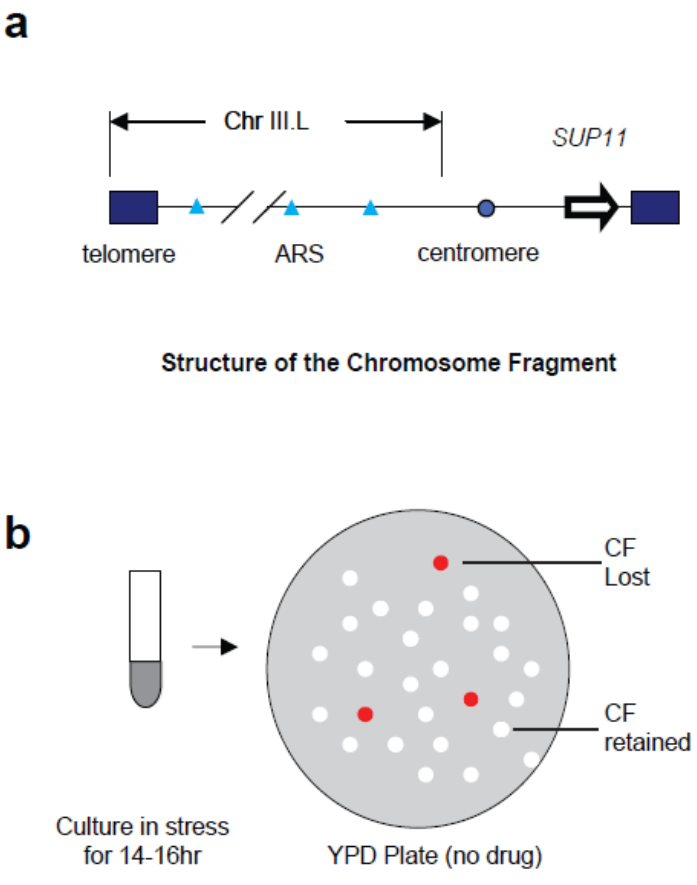

Figure 2. Experimental Scheme for measuring CF loss rates induced by diverse stress conditions.

(a) The structure of the artificial chromosome. ARS: autonomously replicating sequence. The gene suppressing the red pigment accumulation (*SUP11*) is located on the short arm, while the long arm is composed of an additional copy of Chr III left arm (Chr III.L). **(b)** Cells carrying CF, which give rise to white colonies, were grown in the presence of a specific chemical at two sub-lethal concentrations (low and high, Figure 3) for 14-16 hour and then plated onto stress-free rich media (YPD). The OD reading of the liquid culture after incubation, total number of colonies on YPD plates and the number of red colonies, which lost CF, were recorded (Figure 3).

Name	Ctrl (DMSO)	H_2O_2 Low	H_2O_2 High	NaCl Low	NaCl High	Tun Low	Tun High	Ben Low	Ben High	Amph Low	Amph High	FL Low	FL High	Cyc Low	Cyc High	Rad Low
Concentration (w/v or v/v)	1%			37.5g/L	75g/L	5µg/ml	10µg/ml	30µg/ml	60µg/ml	0.4µg/ml	0.8µg/ml	100µg/ml	200µg/ml	0.5µg/ml	1µg/ml	10µg/ml
Concentration (in molar)		1.125mM	2.25mM	0.65M	1.3M	6µM	12µM	104µM	208µM	430nM	860nM	327µM	654µM	2µM	4µM	27µM
Total Colonies	40752	3875	1614	3038	1435	628	1868	2955	2874	3423	2685	1898	1560	1355	2780	592
Red Colonies	47	22	6	5	3	0	5	1	11	8	3	1	2	5	10	111
Red Colony Frequency ($1x10^{-3}$)	1.1	5.7	3.7	1.6	2.1	0.0	2.7	0.3	3.8	2.3	1.1	0.5	1.3	3.7	3.6	187.5
OD_{final}	7.0	0.7	0.4	5.3	0.6	1.1	0.6	4.3	0.7	4.5	0.5	2.3	2.4	1.1	0.5	6.5
Number of Cell Cycles	5.1	1.8	1.0	4.7	1.6	2.5	1.6	4.4	1.8	4.5	1.2	3.5	3.6	2.5	1.4	5.0
Chr. Loss Rate ($1x10^{-3}$/division)	0.2	5.6	6.5	0.4	1.8	N.D.	2.5	N.D.	3.6	0.8	0.9	N.D.	0.4	2.5	4.2	74.4

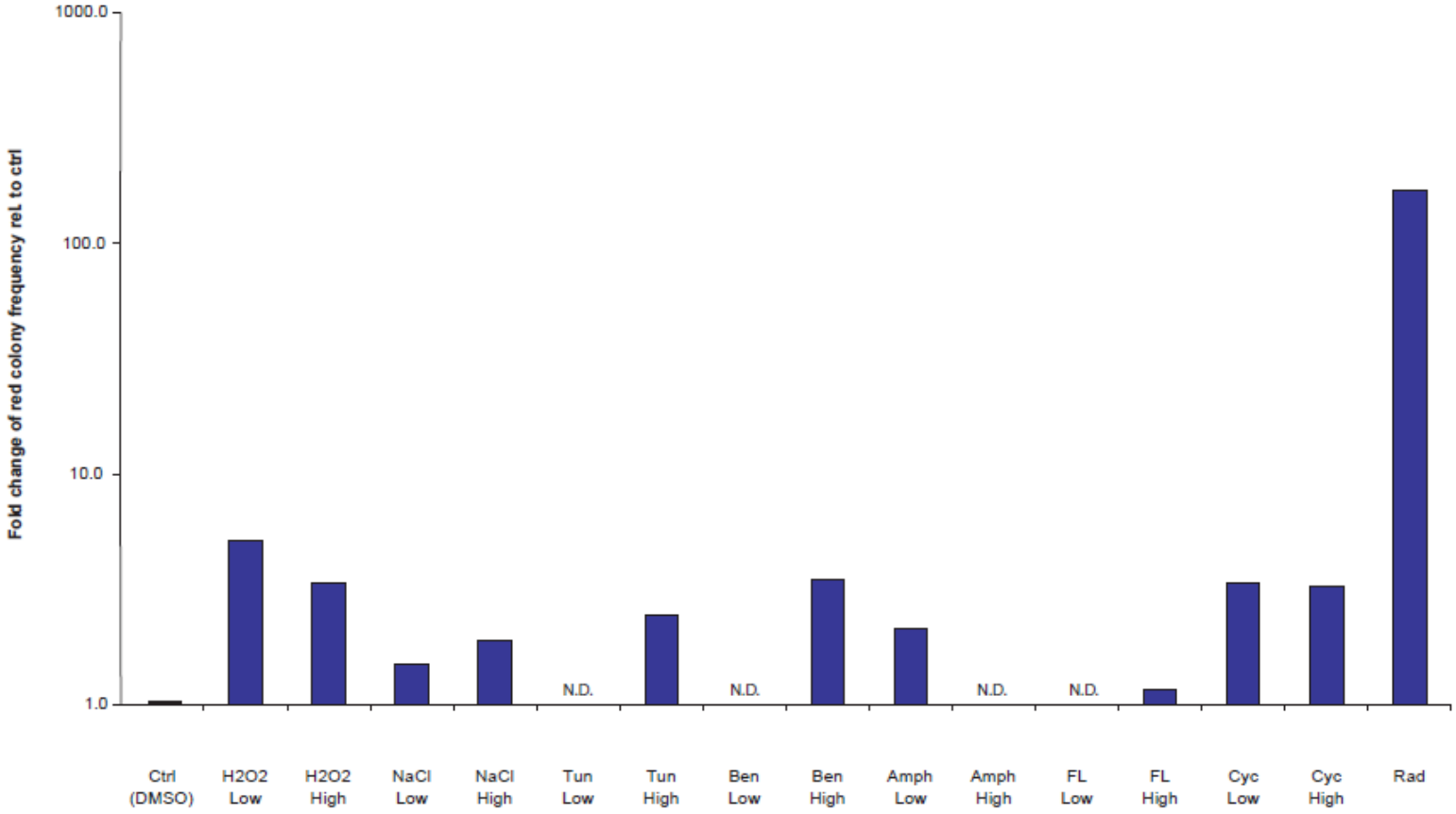

Figure 3. Diverse stress conditions, especially Hsp90 inhibition, increase the red colony frequency.

Top, the parameters of the colony color assay used to estimate the CF loss rate were reported. Bottom, red colony frequencies (number of red colonies over total colonies), were reported. Many stresses elevated CF loss rate. The CIN effect usually came along with strong inhibition of cell proliferation. However, radicicol, a Hsp90 inhibitor, led to a CF loss rate ~300x higher than the vehicle control and ~20x higher than benomyl, with only relatively minor growth inhibition. Data were normalized to vehicle-control. N.D.: no detection of red colony frequency increase over control.

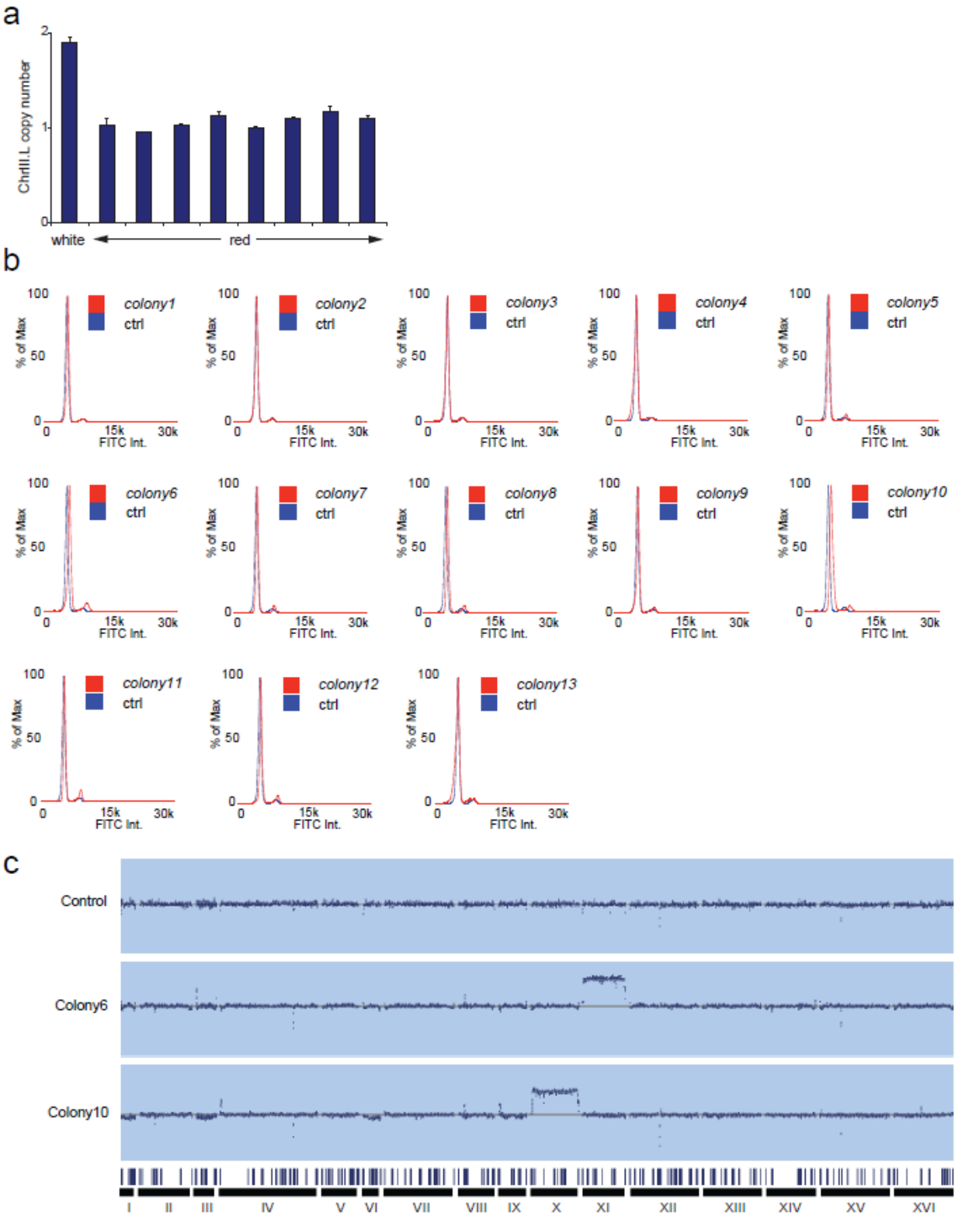

Figure 4. Hsp90 stress induces whole chromosome aneuploidy.

(a) Both arms of artificial chromosome were lost in red cells induced by 10µg/ml radicicol treatment. The copy numbers of chromosome 3L, which is present on both endogenous Chr III and the chromosome

fragment (CF), are shown in relative to Chromosome 3R. The red color of the colony suggested the loss of *SUP11*. The loss of both *SUP11* (on the CF short arm) and one copy of Chr 3L (the CF long arm) suggested that the whole CF artificial chromosome was lost in red colonies. Structure of CF is presented in Figure 2a. Data were obtained with the qPCR assay. **(b, c)** Whole chromosome aneuploidy of other chromosomes was identified among the red colonies generated after the 10μg/ml radicicol treatment. **(b)** DNA flow-cytometry analysis of 13 different red colonies treated by radicicol is shown, in comparison with ones treated with vehicle control. No polyploidization was observed. **(c)** Comparative genomic hybridization results of a euploid control, colony 6 and colony 10 are presented with dots representing the probe intensity log2ratios over euploid. Repetitive elements were mapped to show regions where the copy number cannot be inferred from aCGH data [21,22].

A similar aneuploidy-inducing effect was also observed with macbecin II, a structurally distinct Hsp90 inhibitor (Figure1b) [67]. Deletion of one copy of Hsp90 genes, *HSP82* showed enhanced CF loss compared to the wild type in the presence of radicicol or macbecin II (Figure1b). Interestingly, deletion of *STI1*, the yeast homolog of mammalian *Hop* and a co-chaperone of Hsp90, resulted in significantly elevated CIN even at a concentration of radicicol too low to induce CIN on its own (Figure 1b, Figure 5a). Heat is a common environmental stress known to tax Hsp90 function [68]. Heat-shock for 90 seconds at 50.9°C induced subsequent CF loss at a rate comparable to that by pharmacological inhibition of Hsp90 (Figure 1a). These results confirmed that Hsp90 stress is a potent inducer of aneuploidy. Hsp90 chaperon complexes are crucial facilitators of many cellular functions[69]. Previous biochemical studies suggested that Hsp90 is important for the activation of Ctf13 and assembly of the CBF3 inner kinetochore complex [62]. Most CBF3 complex components, as well as the two co-chaperones involved in Ctf13 activation, showed haploinsufficiency toward radicicol (Figure 5b). Radicicol disrupted the kinetochore localization of Cep3 but had less effect on Ndc10, thus altering the stoichiometry of CBF3 complex at the kinetochore (Figure 1c, Figure 5c, d, e). In addition to the CBF3 complex, Hsp90 interacts with several other pathways that could affect chromosome transmission fidelity, including the spindle assembly checkpoint [70] (see below).

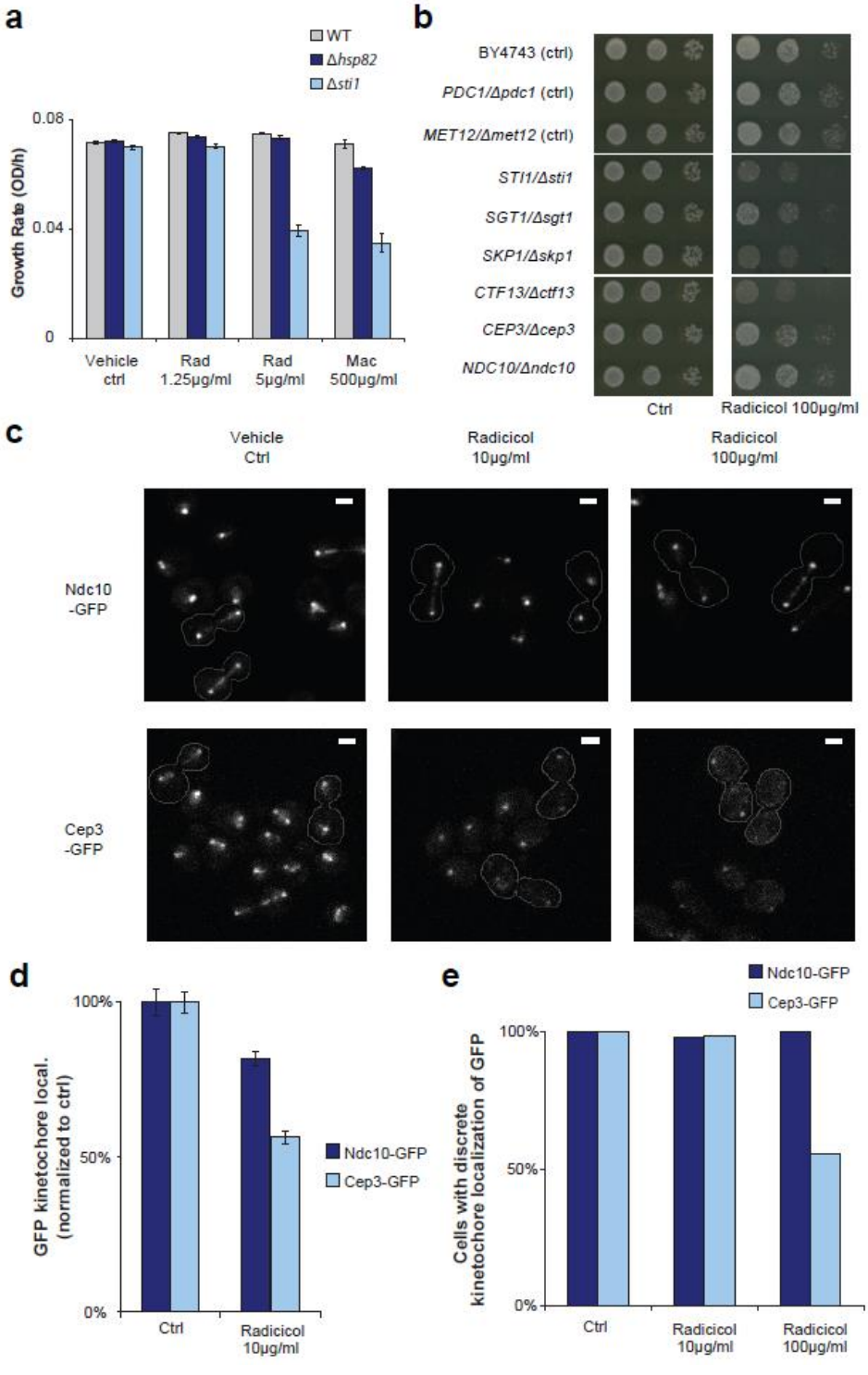

Figure 5. Radicicol reduces Hsp90 function and impairs CBF3 complex assembly.

(a) Δ*sti1* showed higher sensitivity than Δ*hsp82* to the presence of pharmacological inhibition of Hsp90. The maximum growth rate of wild type (WT), Δ*hsp82* and Δ*sti1* are shown. Bar graphs show mean±SEM.

n=4. **(b)** All but one components of CBF3 complex exhibited haploinsufficiency in the presence of radicicol. Sgt1 is the co-chaperone bridging the Hsp90-Sti1 complex to kinetochore [23]. Different strains were spotted at 10x serial dilutions from left to right. **(c)** Hsp90 stress disrupted the stoichiometry of kinetochore components. The localization of Ndc10-GFP and Cep3-GFP in different conditions is shown in a field larger than that in Figure 1c. Scale bar =2μm. **(d)** Quantification of the intensities of kinetocore GFP signals in anaphase cells under conditions as indicated. Bar graphs show mean±SEM. n>20 cells/strain/condition. **(e)** The percentages of cells with discrete kinetochore localization of Ndc10-GFP or Cep3-GFP were quantified. n>30 cells/strain/condition.

Hsp90 taxation has previous been proposed to impact evolution by releasing phenotypic variation from pre-stored genetic diversity in the population and by transposon mobilization [69,71]. Does Hsp90 inhibition also promote adaptation through induction of aneuploidy? As a first test, a diploid strain was grown in the presence of high concentration of radicicol and 3 largest radicicol-resistant (Rad^r) colonies were selected and reconfirmed (Figure 6a, Figure 7 and page 101 in appendix). Karyotyping revealed that all 3 Rad^r colonies were aneuploid with a dominant karyotype feature: all 3 Rad^r colonies, which adapted independently, contained one or two additional copies of Chr XV (Figure 6a). A haploid Chr XV disomy strain, generated by genetic manipulation [1], also showed strong resistance to radicicol (Figure 6b). A previous genome-wide screen identified a set of genes exhibiting haploinsufficiency toward macbecin II, among which 2 of the top genes are located on Chr XV: *STI1* and *PDR5*, a pleiotropic drug pump [70]. We deleted a single copy of *STI1* or *PDR5* gene from Rad^r colony 3, trisomy for Chr XV. Growth measurements showed that either deletion abolished more than 50% of the growth rate gained by Chr XV trisomy over diploid in the presence of radicicol (Figure 6c). A single copy of *STI1* and/or *PDR5* was then introduced into the parental diploid strain. An extra copy of each gene mildly but significantly increased radicicol resistance, but their combination drastically improved radicicol resistance (Figure 6c, Figure 8). These results indicate that Chr XV gain directly confers radicicol resistance through increased copy number of *STI1* and *PDR5*, and possibly also other genes carried on this chromosome (e.g., *SGT1*).

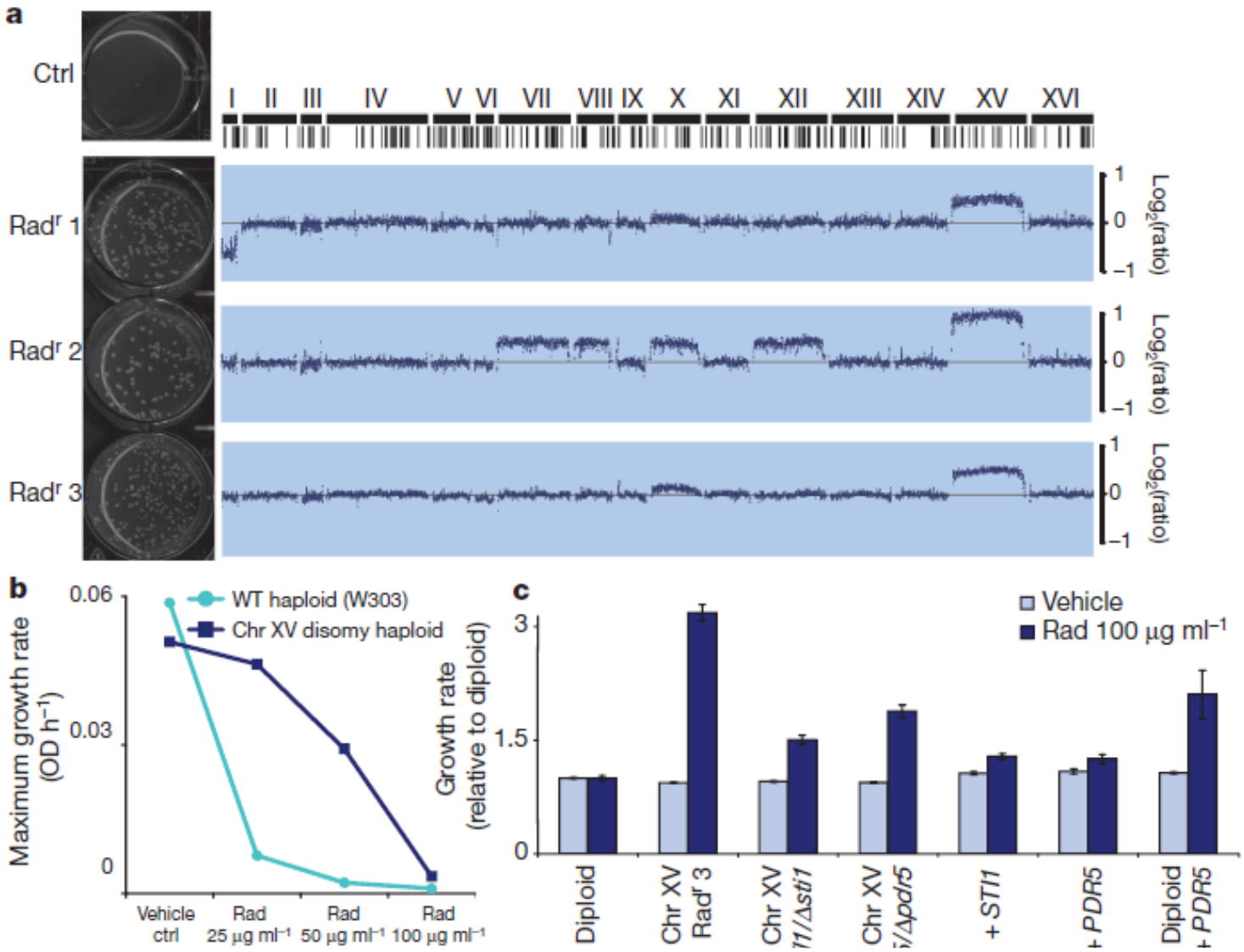
a
Ctrl
Rad^r 1
Rad^r 2
Rad^r 3
I II III IV V VI VII VIII IX X XI XII XIII XIV XV XVI
Log2(ratio)
b
WT haploid (W303)
Chr XV disomy haploid
Maximum growth rate (OD h−1)
Growth rate (relative to diploid)
0.06
0.03
0
Vehicle ctrl
Rad 25 μg ml−1
Rad 50 μg ml−1
Rad 100 μg ml−1
c
Vehicle
Rad 100 μg ml−1
3
1.5
0
Diploid
Chr XV Rad^r 3
Chr XV /Δsti1
Chr XV /Δpdr5
+ STI1
+ PDR5
Diploid + PDR5

Figure 6. Aneuploidy is the predominant genetic change conferring adaptation to radicicol

(a) Left: Replating and growth of control (ctrl) or three adapted radicicol resistant (Rad^r) strains on 100μg/ml radicicol plates after 3 days incubation. See the experimental scheme in Figure 7. Right: All 3 re-confirmed Rad^r colonies were aneuploids with different levels of Chr XV gain. Intensity log2ratios over euploid are shown. Repetitive elements are shown as vertical lines. **(b)** Haploid Chr XV disomy generated by genetic manipulation shows higher growth rate than euploid in radicicol. **(c)** Increased gene dosages of *STI1* and *PDR5* encoded on Chr XV are partially required and sufficient for radicicol resistance. The maximum growth rates were averaged for 4 replicates and normalized to diploid, shown with SEM.

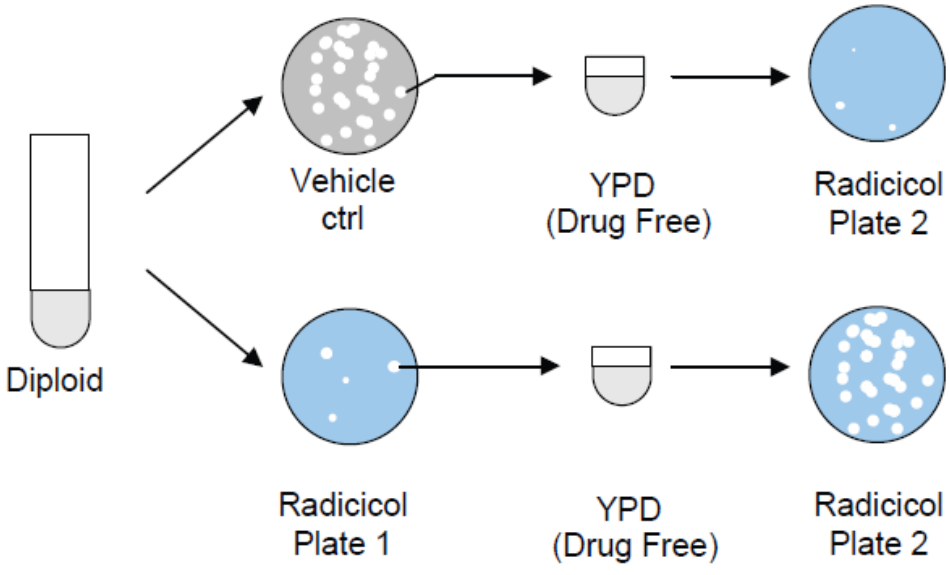

Figure 7. Evolution experiment to select for stable radicicol resistant colonies

Briefly, a diploid strain was first grown on plate containing high concentration of radicicol (100µg/ml) or vehicle control; three of the largest radicicol resistant colonies along with a colony from the vehicle plate were cultured overnight in drug-free media to wash out non-genetic effect and then retested for radicicol resistance (See page 101 for experimental details in appendix).

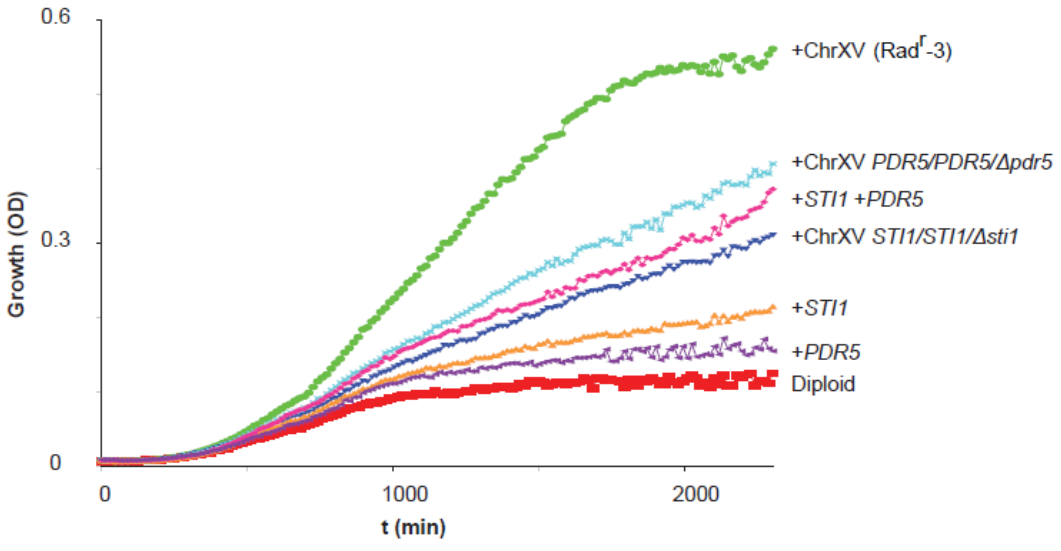

Figure 8. Increased gene dosages of *STI1* and *PDR5* encoded on Chr XV are partially required and sufficient for conferring radicicol resistance.

Representative growth curves for the indicated strains in 100 µg/ml radicicol are shown.

We next tested if the karyotype diversity produced by Hsp90 stress-induced CIN could fuel adaptation to various other stress conditions. A karyotypically mosaic yeast cell population (~1/3 of the population were aneuploid with different karyotypes, Figure 9c) was generated by growing a diploid strain under moderate Hsp90 stress (20μg/ml Radicicol) for 2 days. This population was then tested for enhanced adaptability toward other stress conditions, including the presence of growth inhibiting concentrations of fluconazole, tunicamycin, or benomyl, over a control homogeneous euploid population (see experimental scheme in Figure 9a). The radicicol-pretreated population did not show any growth advantage over the control diploid (vehicle pre-treated) on drug-free plates (Figure 10a, Ctrl). However, on each of the different drug-containing plates, the radicicol pre-treated populations demonstrated drastically enhanced colony viability and frequency to form large drug-resistant colonies than the vehicle-pretreated population (Figure 10a, b, c).

Twenty one colonies were picked from the vehicle control plates bearing the radicicol-pretreated population, and out of these 12 were aneuploid, whereas none (0/9) from the control plate bearing the vehicle-pretreated population were aneuploid (Figure 10d, e, Figure 9d, e). The vast majority (17/18) of the large colonies karyotyped from the drug plates bearing the radicicol-pretreated population were aneuploid (Figure 10e). The drug-resistant colonies from the vehicle-pretreated population were also aneuploid (Figure 10d). Importantly, the aneuploid colonies resistant to the same drug showed obvious karyotypic commonalities and tend to cluster together based on karyotype similarity (Figure 10e, Figure 11). For example, 4 of the 5 aneuploid colonies from fluconazole plates karyotyped gained an extra copy of Chr VIII, which carries *Erg11*, encoding an ergostrol biosynthetic enzyme known to confer fluconazole resistance in *Candida albicans* [29]. Losing a copy of Chr XVI is a predominant karyotype change among the tunicamycin-resistant colonies (seen in 10/12 karyotyped, Figure 10d). Of the 12 benomyl-resistant colonies, 10 demonstrated karyotype clustering with 6 of them losing one Chr XII, but it appears that more than one karyotypic pattern could confer benomyl resistance. This however is consistent with our previous observation of phenotypic convergence of distinct karyotypic patterns [28]. All the above common

karyotype features were significantly (Mantel-Haenszel tests) enriched in drug resistant colonies but not the starting radicicol-pretreated population prior to selection on drug plates (Figure 10d, e, Figure 9e), suggesting an association of specific karyotypes with resistance to certain drugs.

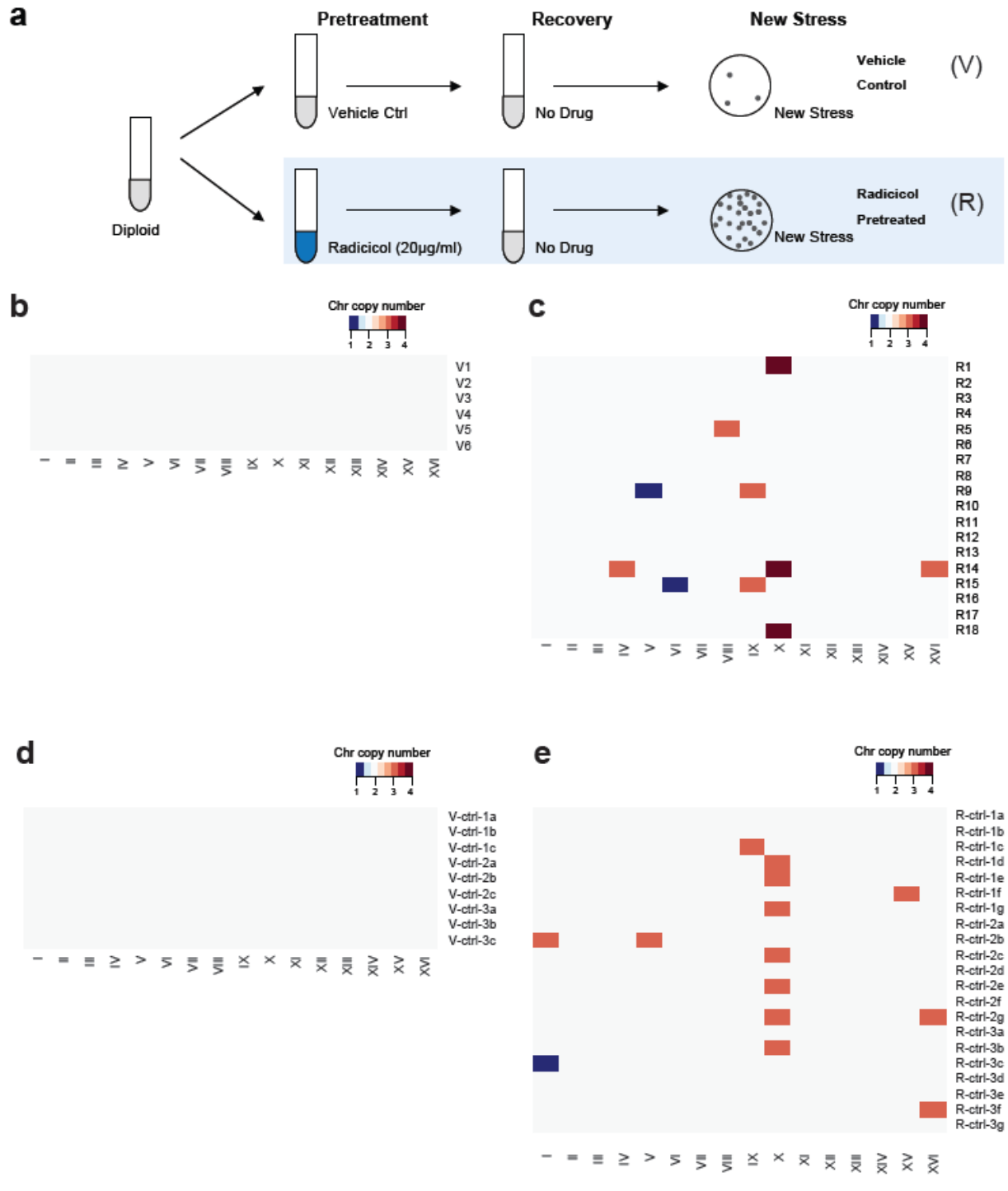

Figure 9. Moderate and short-term Hsp90 inhibition drastically increases the karyotype diversity in the population.

(a) Experimental scheme to test the effect of moderate and short-term Hsp90 inhibition on the adaptability of population to new stresses. A diploid culture was established from a single colony and split into two groups, which are pretreated for 2 days with either vehicle control (V) or radicicol (R). They were then recovered in a drug-free environment for 24 hours to diminish non-genetic effects. The two groups were then plated on media containing 3 new stress-causing agents separately. The experiment was repeated three times. **(b, c)** The population after moderate and short-term Hsp90 inhibition showed drastically higher karyotype diversity. Immediately after the 2-day pre-treatment as mentioned above, the cell cultures treated by vehicle control (V group) or radicicol (R group) were plated onto YPD plates without drug. Single colonies were karyotyped by qPCR. **(b)** The karyotypes of 6 colonies from V group were characterized showing all 6 remained euploid. **(c)** The karyotypes of 18 colonies from R group were characterized showing 6 of the 18 were aneuploid with different karyotypes. **(d, e)** The karyotype diversity induced in radicicol pre-treatment was partially maintained after the recovery phase. The cell cultures pre-treated by vehicle control (V group) or radicicol (R group) were plated onto YPD plates with vehicle control after the recovery phase. **(d)** The karyotypes of 9 colonies from V group on vehicle control plates were characterized showing maintenance of euploidy. **(e)** The karyotypes of 21 colonies from R group on vehicle control plates are shown. Compared with Figure 9c, the karyotype diversity was reduced. This is likely attributed to the competition between cells bearing different karyotypes during the recovery phase. All karyotypes in this figure were determined by the qPCR assay.

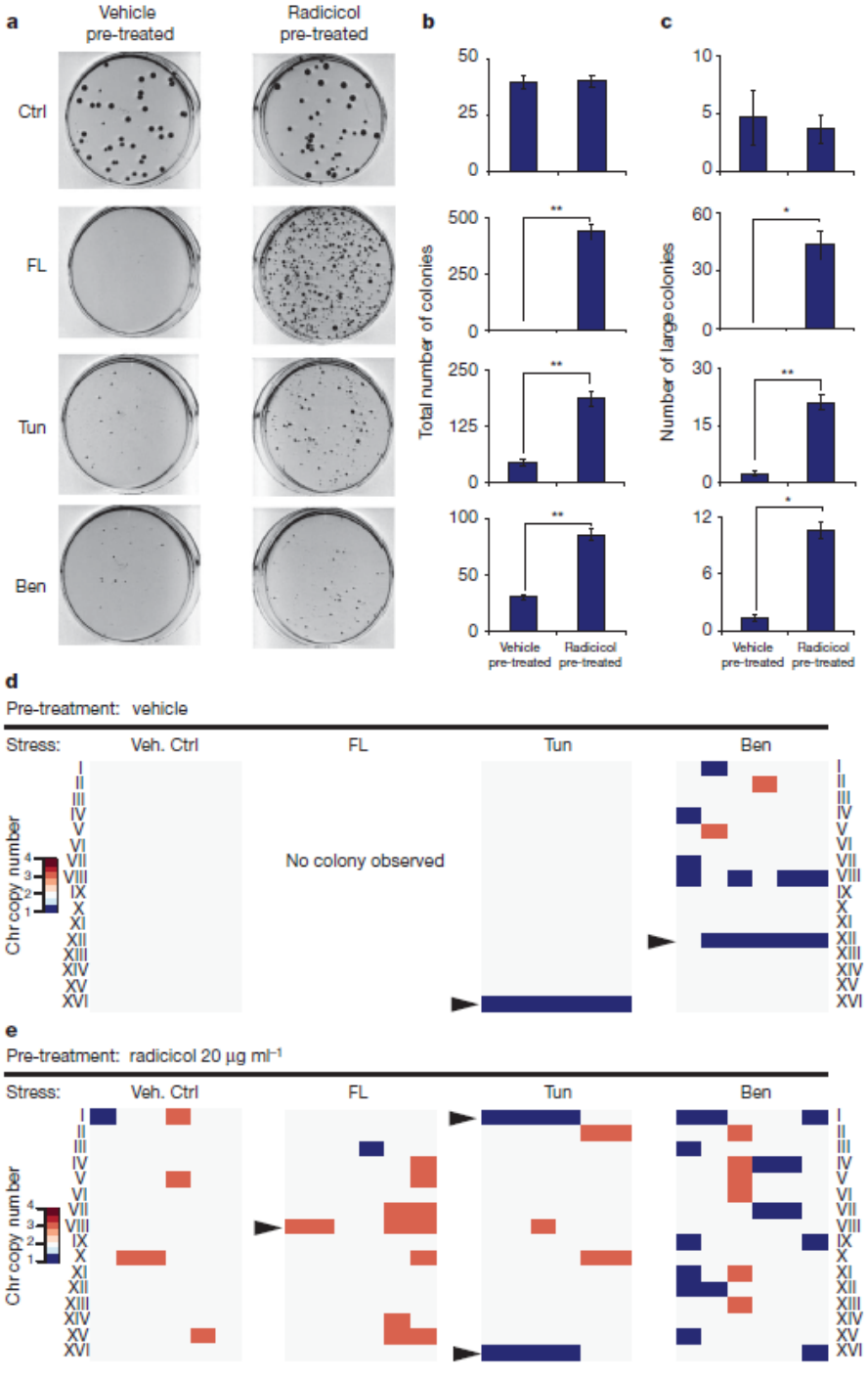

Figure 10. Prior Hsp90 inhibition potentiates adaption to other stress conditions through divergent aneuploid karyotypes

(a) Plates of vehicle-pretreated (V) group and radicicol-pretreated (R) group on different media as indicated. ~40 cells were plated on DMSO (Ctrl); ~40,000 cells were plated onto each drug plate. FL: 32 g/ml fluconazole; Tun: 2.5 g/ml tunicamycin; Ben: 30 g/ml benomyl. **(b)** Quantification of the number of viable colonies. Shown are mean±SEM from triplicate experiments. **(c)** The sizes of all colonies (including both R and V groups) grown on each type of plates were measured. The distributions of top 10% largest colonies between the two groups are shown. *, $p<0.05$; **, $p<0.01$, two-tail paired t-test. **(d)** The karyotypes of 6 V colonies from 3 replicate experiments of each type as determined by qPCR [6]. **(e)** The karyotypes of 6 independent R colonies from 3 replicate experiments of each type determined by qPCR. Arrowheads point to aneuploid chromosomes whose gain or loss frequency among resistant colonies was significantly higher than the starting populations ($p<0.01$, Mantel-Haenszel tests).

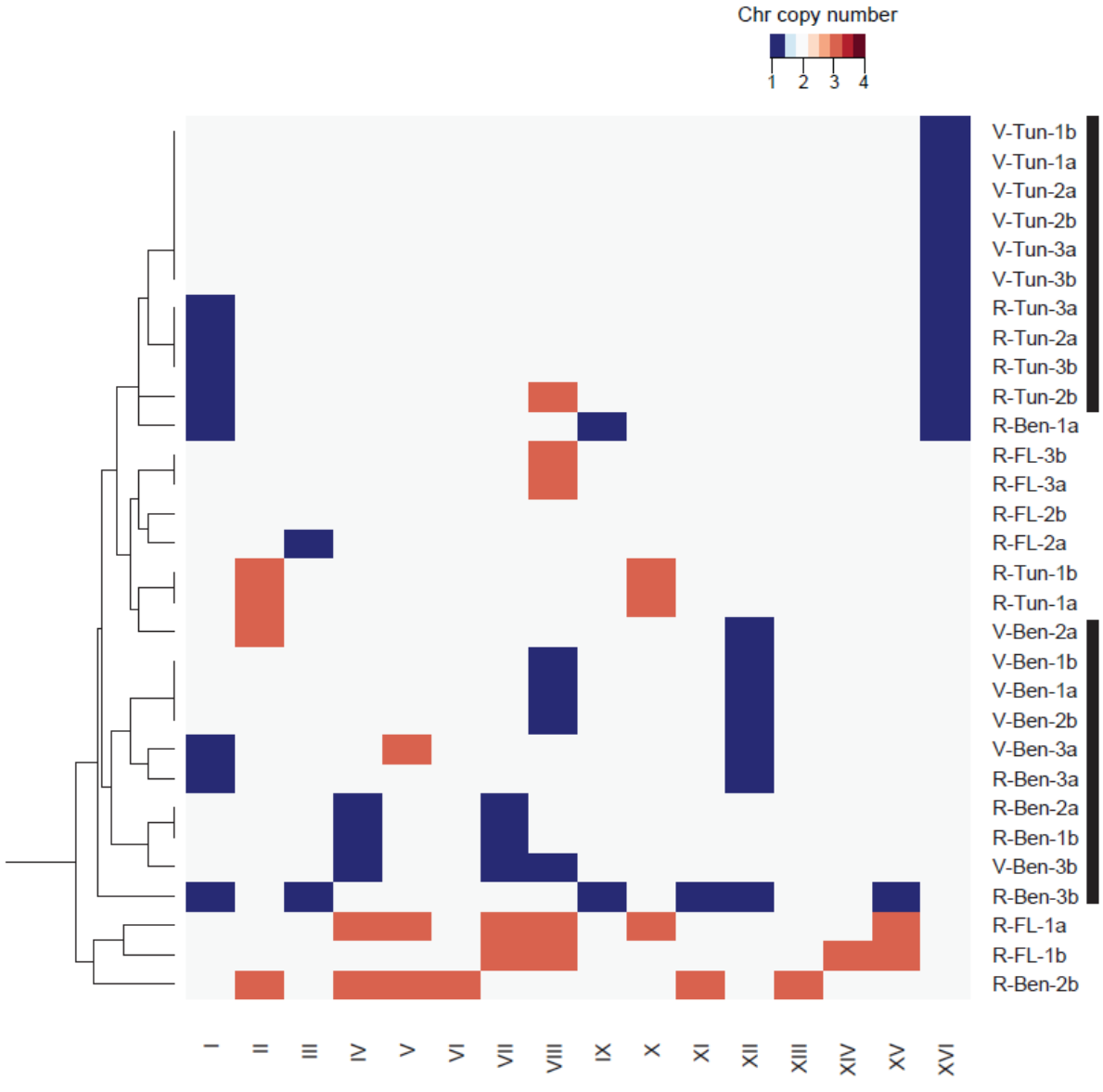

Figure 11. Independent drug-resistant colonies formed in the same new environment tend to share the same karyotype

Resistant colonies formed in the same stress tend to be clustered together by their karyotype. Two major clusters, containing resistant colonies to tunicamycin and benomyl, respectively, are highlighted by bars. The hierarchical clustering was performed in R using the complete linkage method using the Euclidean distances.

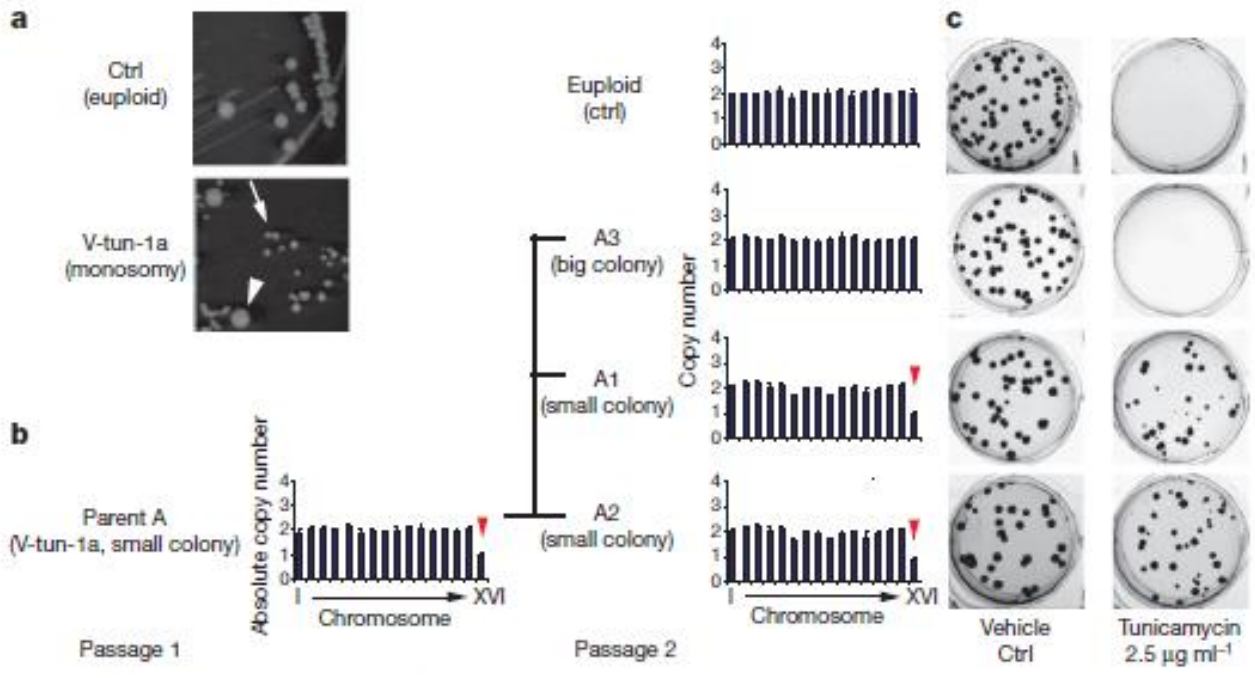

Figure 12. Karyotype requirement and dynamics associated with tunicamycin resistance.

(a, b) Chr XVI monosomy (small colonies (arrow)) is unstable and produces large euploid progenies (arrowhead). Shown are a representative image of the colonies (observed after 3 day growth on YPD) **(a)** and karyotypes of the Parent A and the progeny colonies (A1-3) determined by qPCR **(b)**. **(c)** Chr XVI monosomy progenies (A1 and A2) but not euploid progeny (A3) displayed tunicamycin resistance. Note that the size difference between small and large colonies on control plates was no longer apparent after 7-day growth.

To further assess the selective advantage of aneuploidy and karyotype dynamics under varying stress levels, two single Chr XVI monosomy colonies from a tunicamycin plate were streaked on drug-free plates. Colonies of two distinct sizes emerged, with the small ones being predominant (Figure 12a). Karyotyping showed that the small colonies represented Chr XVI monosomy, whereas the rare large colonies had gained back the missing Chr XVI and returned to diploid (Figure 12b, Figure 13a). Tunicamycin resistance was tightly linked to Chr XVI monosomy: all of the small colonies were tunicamycin resistant while the growth of the big colonies was abolished by tunicamycin (Figure 12c, Figure 13b, c, d). This result shows that an adapted aneuploid population also has the potential to return to euploid state when the stress condition is attenuated, suggesting that aneuploidy is not only a readily accessible mutation with large phenotypic impacts but is also reversible.

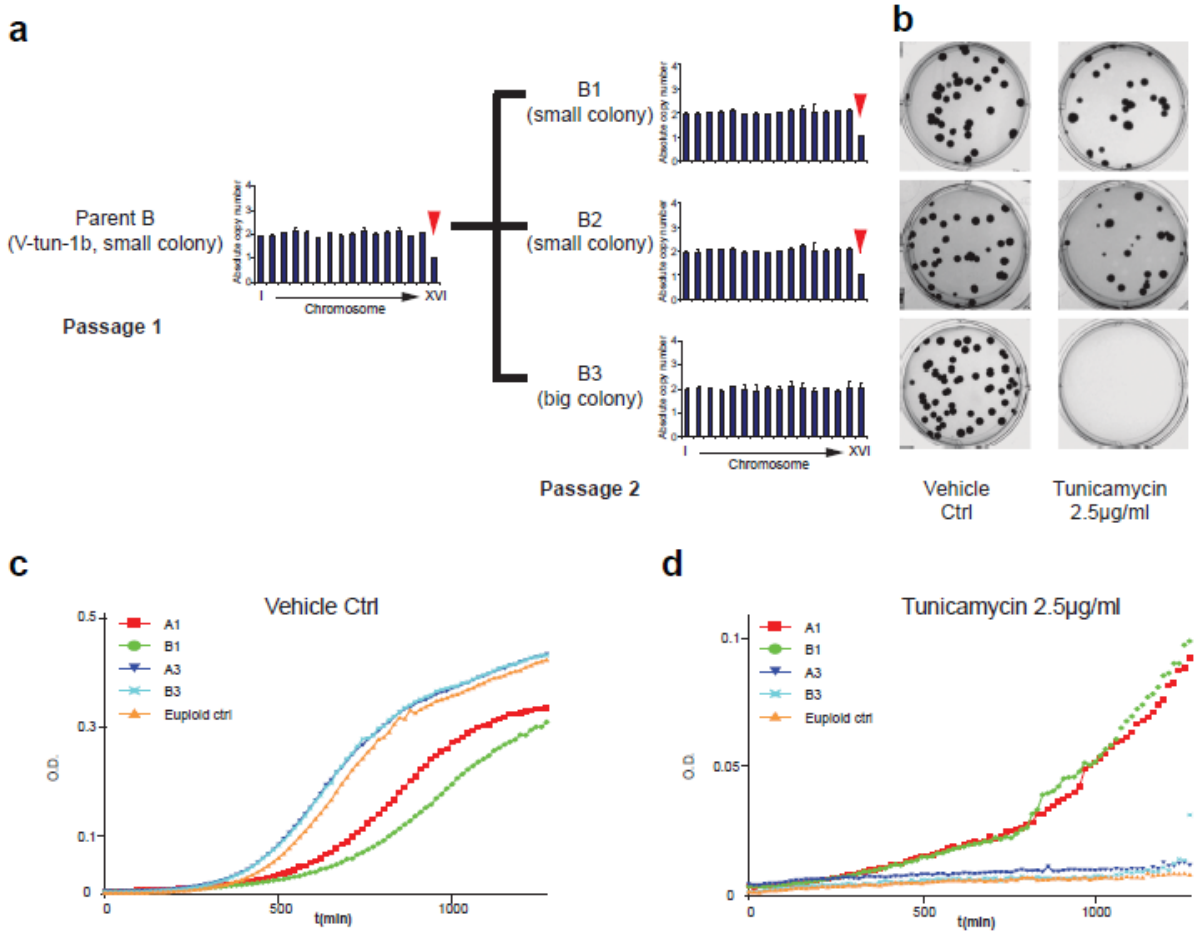

Figure 13. Chr XVI monosomy is unstable in stress-free environment and produces large (diploid) and small (Chr XVI monosomy) colonies

(a) Colony size variation is due to karyotype instability of Chr XVI monosomy. Shown here are karyotypes of the Parent B and the progeny colonies B1-3 as determined by qPCR karyotyping. Sizes of these colonies on YPD plates are noted. See Figure 12 for similar result on Parent A lineage. Parent A and B are direct progenies of the colony V-Tun-1a and 1b, respectively, in Figure 10. **(b)** Only Chr XVI monosomy progenies but not euploid progenies retain tunicamycin resistance. Same numbers of cells were plated onto control and tunicamycin plates. **(c, d)** Growth curves of the euploid progenies (A3 and B3) and the ChrXVI monosomy progenies (A1 and B1) in YPD liquid media containing vehicle **(c)** or 2.5 g/ml tunicamycin **(d)** are shown.

The results demonstrated that stress-induced chromosome instability, leading to aneuploidy, is a mechanism of stress-induced mutagenesis in eukaryotes with high adaptive value to diverse perturbations. By far Hsp90 inhibition is the most potent inducer of aneuploidy among the stress conditions tested. This may be due to a broad but critical involvement of Hsp90 in pathways governing chromosome transmission fidelity and cell division [70]. For example, the mitotic checkpoint gene *MAD2* is a genetic interaction hub sensitive to Hsp90 perturbation [70]. *MAD2* deletion was also sufficient to lead to rapid emergence of fluconazole-resistant colonies bearing an extra copy of Chr VIII [36]. As Mad2 requires the CBF3 complex for its activity at the kinetochore [72], the exceptionally high-level CIN induced by Hsp90 inhibitors may be explained by a combined effect of interference with both kinetochore assembly and the checkpoint monitoring spindle defects. It is presently unknown whether the other stress conditions induce CIN through similar or different cellular targets.

The Hsp90 chaperon complex specializes in modulating the stability and function of many important regulatory and structural proteins [70]. As a result, Hsp90 acts as a capacitor facilitating evolutionary adaptation by unleashing the effects of pre-existing mutations when Hsp90 activity is taxed under mild stress [68,69]. Strong Hsp90 inhibition also induces phenotypic variation through transposon activation in *Drosophila* [71]. The results presented in this work reveal a new role for Hsp90 in adaptive evolution - as the guardian of chromosomal stability, the inhibition of which could trigger *de novo* karyotypic diversity leading to rapid adaptation through aneuploidy. We note that our observed induction of aneuploidy required more potent Hsp90 inhibition than that required to reveal phenotypic effects of pre-existing mutations [68]. As the function of Hsp90

chaperon complex in kinetochore assembly is conserved in mammalian species [63,73], the Hsp90 stress-induced aneuploidy may be a mechanism of cellular adaptation affecting a wide range of organisms.

Chapter 3: Target the adaptability of heterogeneous aneuploidy populations

Chen G, Mulla WA, Kucharavy A, Tsai HJ, Rubinstein B, Conkright J, McCroskey S, Bradford WD, Weems L, Haug J, Seidel CW, Berman J, Li R. 2014 (under revision for *Cell*)

Abstract:

Aneuploid genomes, characterized by unbalanced and diverse chromosome stoichiometry (karyotype), are associated with cancer malignancy and drug-resistance of human pathogenic fungi. The phenotypic diversity resulting from karyotypic diversity endows the cell population superior adaptability to both natural stressors and clinical treatments. We show here using a combination of experimental data and a general statistical model that the degree of phenotypic variation, thus evolvability, escalates with the degree of overall growth suppression irrespective of stress mechanisms. Such scaling explains the challenge of treating aneuploidy diseases with diverse different karyotypes by imposing a single mode of inhibition, yet specific karyotype features can be highly targetable. Motivated by this finding, we propose an "evolutionary trap" targeting both karyotypic diversity and fitness of the population. This strategy entails a selective condition "channeling" a karyotypically divergent population into one with a predominant and drugable karyotypic feature. We provide a proof-of-principle test with mechanistic explanation in budding yeast and demonstrate the potential efficacy of this strategy toward aneuploidy-based azole resistance in the human pathogen *Candida albicans*. Targeting selected karyotypes may also be a viable approach for treating those tumors with a prevalent karyotypic signature.

Introduction

Germline evolution shapes the organismal tree in changing environments during the long course of natural history, while acute environmental fluctuation drives asexual cellular evolution [42,74]. Cellular evolution is often associated with dynamic structural changes in the genomes of microbes or cancer cells, allowing rapid adaptation to host defense mechanisms or the emergence of drug resistance. Aneuploidy (chromosome copy number imbalance) is a type of genome alteration widely observed during cellular evolution of eukaryote species, such as laboratory [6,30,36], industrial [7,10,11,75] and pathogenic [13,14,76,77] yeasts, as well as protozoan parasites such as leishmania [78-80] and trypanosome [81,82]. Emerging evidence also points to aneuploidy as an important driver for the evolution of human cancer [44,47,52,83,84]. Due to its impact on the expression of many genes, aneuploidy brings about large phenotypic change that can be either detrimental or beneficial in a karyotype and environmental condition-dependent manner.

Aneuploid populations are often characterized by heterogeneity characterized by the coexistence of many different karyotypes. Diverse stress conditions, such as Hsp90 chaperone taxation [36] and anti-fungal treatment [85] as well as stress caused by many gene mutations [55], elevate the rate of chromosome segregation errors and generate karyotypically and phenotypically divergent populations. The resulting genetic diversity provides the raw material for evolutionary selection and endows the aneuploid population high adaptive potential [36,86,87]. This underscores the exceptional challenge of treating disease-causing cell populations characterized by large karyotype heterogeneity and instability [53,85,88-90].

One idea that has been explored for potential therapy against aneuploid populations is to find drugs strongly exacerbating a common deficiency of aneuploids irrespective of specific karyotype [91]. For example, a study found that, in a pool of aneuploid yeast strains each with a defined disomy karyotype, many showed prominent growth defect toward agents that perturb proteome homeostasis such as hygromycin B (a translation inhibitor) or geldanaycin (an Hsp90 inhibitor) [1]. This was attributed to overloading of the protein quality control system as a result of excessive gene expression from the gained aneuploidy chromosome [34]. In support of this explanation, a broad signature of environmental stress response (ESR) was reported in the transcriptome of all disomy strains generated by genetic manipulation [1,92]. However, some of the disomy strains with ESR signature exhibited resistance, as opposed to sensitivity, toward proteotoxic agents, and one of the karyotypic features, increased copy number of chromosome XV (Chr XV), emerged as the adaptive variant when a diploid strain was evolved in the presence of a Hsp90 inhibitor (Chen et al. 2012a and also see Results of this study). In addition, when a highly heterogeneous aneuploid population was treated with various drugs that imposed strong immediate inhibition, long-term culturing enabled evolutionary selection for a few variants that endured the initial suppression and then repopulated the population to render it drug-resistant [36]. These findings highlight the fallacy of short-term efficacy in drug treatments when dealing with heterogeneous populations already poised for rapid adaptation.

In this study, we aim for an innovative approach that accounts for the evolutionary dynamics and achieves long-term growth suppression or extinction of aneuploid cell populations consisting of a wide spectrum of aneuploid karyotypes. Our analyses show on a general level that a heterogeneous aneuploid population cannot be suppressed by a single type of stress condition but may become highly targetable once the karyotype diversity is drastically confined. These

findings led us to design a two-component strategy targeting both the population's adaptability and fitness. We provide a proof-of-principle test of this strategy in the budding yeast and demonstrate its potential efficacy in dealing with aneuploidy-based resistance to fluconazole - the first-line drug against systemic fungal infection.

Results

Scaling of phenotypic variation with growth suppression under diverse stress conditions

To investigate whether certain stress conditions may be consistently effective toward aneuploids with various karyotypes, we performed a re-analysis of the growth data from a previous study subjecting a panel of 38 aneuploid yeast strains (*S. cerevisiae*) with diverse and random chromosome stoichiometry to phenotypic profiling across a wide range of conditions with varying stress type and level [28]. Growth conditions were ranked by their general effectiveness toward the aneuploid strains as measured by the mean growth ratio relative to the euploid control ($\log_2$[aneuploid growth/ euploid growth]) (Figure 1A). This analysis revealed a surprising trend: those conditions more toxic to the aneuploidy cohort (lower mean growth ratio) also produced a larger fitness spread among the aneuploids, such that even under highly toxic conditions (e.g. in the presence of 4-Nitroquinoline 1-oxide (4-NQO) or thiolutin), while many aneuploids failed to grow, some aneuploids endured or thrived. The standard deviation (spread) and mean of the growth ratio (overall growth suppression) of diverse aneuploids are strongly correlated across diverse stress conditions (Figure 1B). This same trend could also be observed with the set of disomy aneuploid strains isolated in a previous study [1] treated with increasing concentrations of different drugs (Figure 1C).

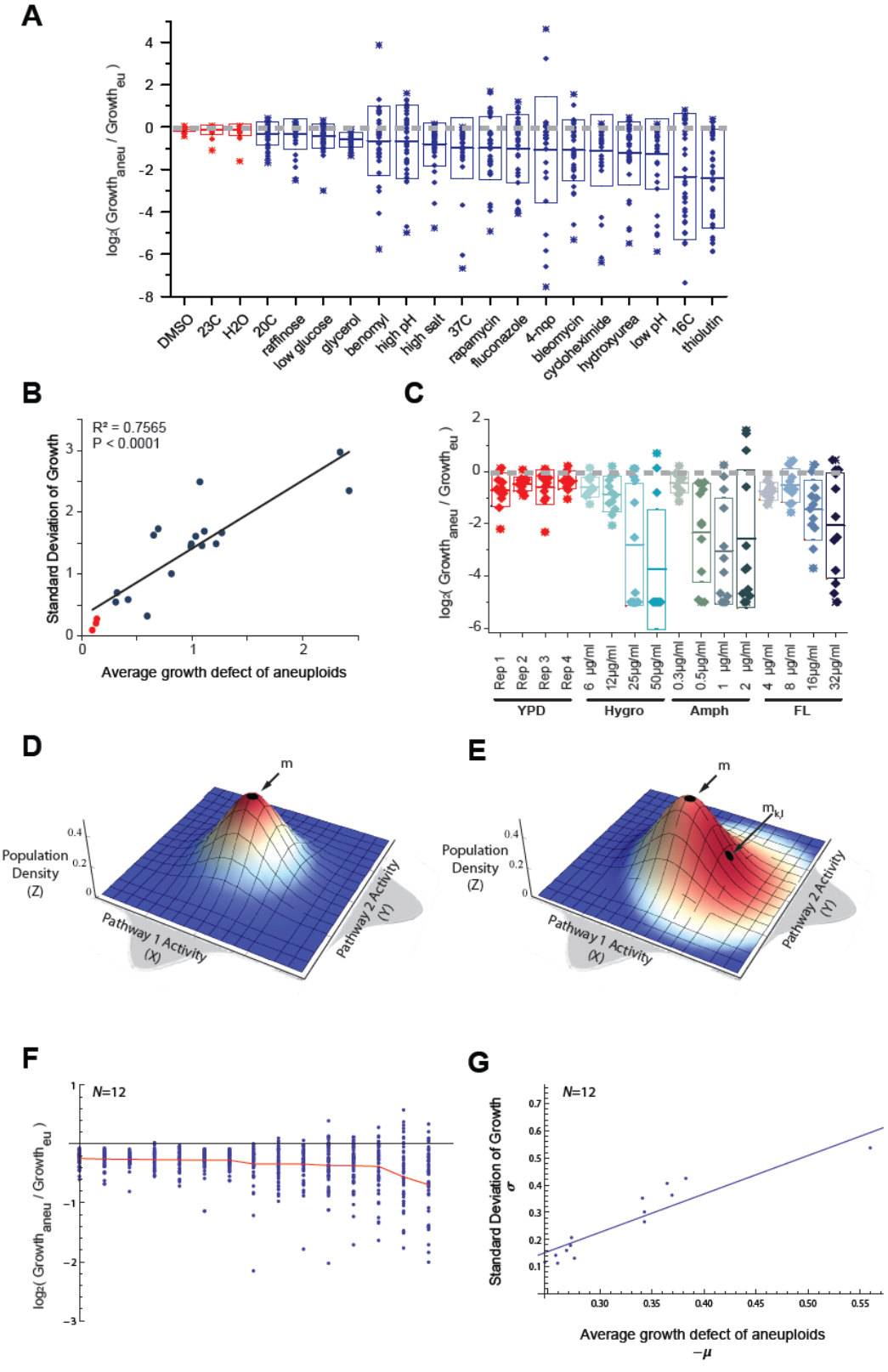

Figure 1. Scaling of phenotypic variation with growth suppression in aneuploids under diverse stress conditions.

(A) The growth of 38 aneuploid strains relative to the euploid, as log2ratio of aneuploid growth (OD increase) over the euploid (haploid, diploid or triploid) with the nearest ploidy, are binned by growth conditions and ranked by the average growth defect compare. Each point in a box plot represents an aneuploidy strain. The half-length of each box represents the standard deviation of relative growth among aneuploids and the middle line represents the average. Note that the horizontal dashed line across 0 represents the euploid control, and under every condition there is a group of aneuploids with fitness close to or surpassing that of the euploid. **(B)** Phenotypic variation among the aneuploids, measured as the standard deviation of relative growth, scales with average growth defect of the aneuploid cohort across diverse stress conditions. **(C)** The growth of 12 disomy strains relative to the haploid control under increasing concentrations of hygromycin B (Hygro), amphotericin B (Amph) or fluconazole (FL). Box plot representation is as described for (a). **(D-E)** Schematic representation of the model is shown for the simple case of N = 2. The distribution of the cell population on the X-Y dimension has a mountain-like shape due to normal distribution along the X and Y dimensions (shown in grey), representing activity distributions of two independent pathways across karyotypes. The Z axis represents population density. Deep blue to deep red code for increasing fitness. **(D)** Graph represents the stress-free condition, where the euploid is located at the center of the activity field (position **m**) assumes highest fitness. **(E)** Graph represents a stress condition, where the optimal fitness point shifts from **m** to $\mathbf{m}_{k,l}$, reflecting the activity change necessary for adaptation. Consequently, the euploid (located at point m) no longer holds maximal fitness, whereas higher fitness is assumed by certain aneuploids (those occupying redder regions). **(F)** Example simulation results of the model of 50 random aneuploids under diverse stress conditions (governed by varying type k and magnitude l) for a 12 dimension space (N = 12), with relative

growth displayed as the experimental data in (A). The red line shows the decrease of average $\log_2$ growth ratio from the simulated aneuploid population. Note the appearance of adaptive aneuploids under high-stress conditions (toward the right of the graph) and the correlation between the spread and growth suppression. **(G)** Plots of model simulations demonstrating the scaling between mean and standard deviation of relative growth. Each dot represents one stress condition from (**F)**.

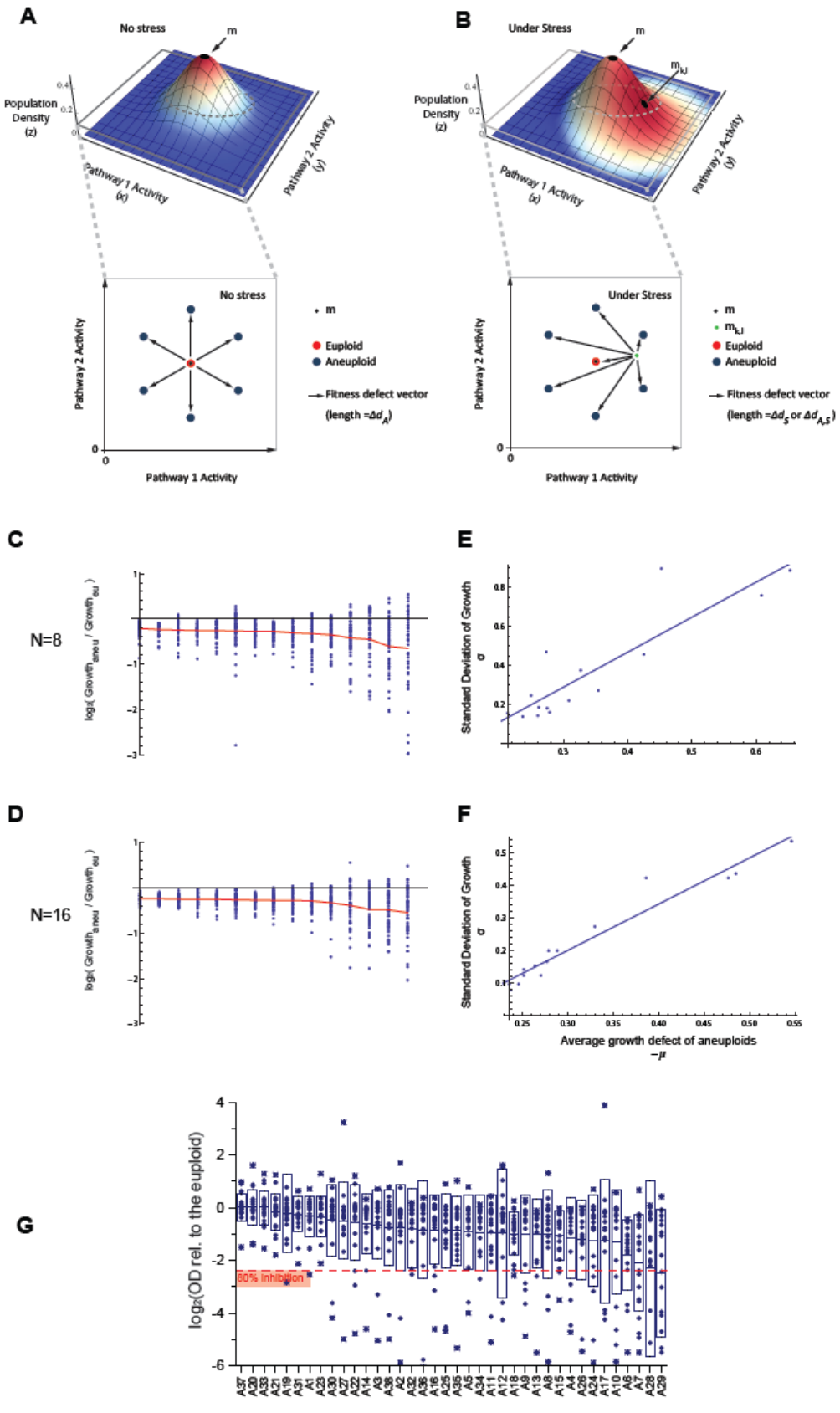
A
No stress
m
Population Density (z)
Pathway 1 Activity (x)
Pathway 2 Activity (y)
No stress
Pathway 2 Activity
Pathway 1 Activity
m
Euploid
Aneuploid
Fitness defect vector
(length =Δd_A)
B
Under Stress
m
m_k,l
Population Density (z)
Pathway 1 Activity (x)
Pathway 2 Activity (y)
Under Stress
Pathway 2 Activity
Pathway 1 Activity
m
m_k,l
Euploid
Aneuploid
Fitness defect vector
(length =Δd_S or Δd_A,S)
C
N=8
log2(Growth_aneu / Growth_eu)
D
N=16
log2(Growth_aneu / Growth_eu)
E
Standard Deviation of Growth σ
F
Standard Deviation of Growth σ
Average growth defect of aneuploids −μ
G
log2(OD rel. to the euploid)
50% inhibition
A37 A20 A33 A21 A19 A31 A1 A23 A30 A27 A22 A14 A3 A38 A2 A32 A36 A16 A25 A35 A5 A34 A11 A12 A18 A9 A13 A8 A15 A4 A26 A24 A17 A10 A6 A7 A28 A29

Figure 2. Additional Simulation Results and Experimental data for Diverse Aneuploids.

For simplicity of visualization, a two-pathway (N = 2) system is shown in the schematic representation. (A) Schematic representation of a horizontal section (bottom graph) of the 2D distribution (top graph) under stress-free condition, as explained in Figure 1A. Several different aneuploids located on the surface of the distribution within this section are shown along with the projected euploid and optimal fitness point m from the peak of the distribution. Growth defect of aneuploids is represented by the length of fitness defect vector (Δd) within the plane of the cross-section. (B) Stress moves the optimal fitness center ($m_{k,l}$) away from the euploid and increase the heterogeneity of fitness defect among aneuploids. Δd is further subdivided into three variants: Δd_A denotes the fitness shift caused by aneuploidy under the stress-free condition; Δd_s denotes the fitness shift caused by stress; $\Delta d_{A,S}$ denotes joint effect of Δd_A and Δd_s, which reflects the distance between aneuploids and the optimal fitness center ($m_{k,l}$) under stress conditions. **(C-D)** Example simulation results of the model of 50 random aneuploids under diverse stress conditions (governed by varying type k and magnitude l) for space with different number of dimensions. The relative growth is displayed similarly as the experimental data in Figure 1A. The red line shows the decrease of average $\log_2$ growth ratio from the simulated aneuploid population. Note the appearance of adaptive aneuploids under high-stress conditions (toward the right of the graph) and the correlation between the spread and growth suppression. (**E-F**) Plots of model simulations demonstrating the scaling between mean and standard deviation of relative growth given a range of N values. **(G)** Experimental data shows that each aneuploid has its own weakness. The log2 ratio of growth of aneuploid strains, compared to corresponding euploid, under diverse growth conditions, were plotted and binned by strain (as opposed to by growth condition in Figure 1A). Note that, for vast majority of the 38 individual aneuploid strains,

there was at least one of the tested conditions causing an 80% or higher growth suppression compared to the euploid, suggesting that individual karyotypes are targetable.

We used a multi-dimensional statistical model to investigate the theoretical generality of the above experimental observation. A simple schematic representation of the model is provided in Figure 1D and E and Figure 2A and B. Briefly, we assume that fitness, as measured by cell growth in defined time in the experimental analysis, is governed by *N* independent pathways (e.g. energy production, DNA replication, mitosis, etc.), reflecting the modular architecture of cellular systems. Given that aneuploidy affects the expression of hundreds of genes across the genome thus likely alters many components of each individual pathway, aneuploidy affects each pathway as a random process. Thus, for each individual pathway, the distribution of pathway activity with diverse karyotypes assumes a simple normal distribution with the euploid located at the peak (corresponding to the mean). Under the stress-free condition, the optimal fitness is reached by the euploid at the center and peak of the *N*-dimensional distribution (Figure 1D). The fitness of an aneuploid population with any karyotype can be located in the *N*-dimension normal distribution at positions away from the peak, reflecting reduced fitness compared to euploid in the absence of stress. In the presence of stress, however, the optimal fitness point moves away from the euploid position, reflecting changes in pathway activities needed for restoration of optimal growth, while the *N*-dimension normal distribution, determined by the genetic makeup of the cell population, remains the same (note that this model does not assume genetic changes under stress and thus examines the existing adaptability of the population) (Figure 1E). The distance between the position of each karyotype (including the euploid) and the optimal fitness point represents the fitness reduction caused by stress.

Simulation of this model with varying values of *N* and diverse types and levels of stress exerted on 50 random aneuploids revealed two properties of the system remarkably consistent with experimentally observed trends (Figure 1F,G). First, under stress conditions with sufficient

magnitude (thus large mean growth suppression toward aneuploids), even though most aneuploids have lower fitness than the euploid, there were always a fraction of aneuploids assuming fitness positions closer to the optimal fitness point than the euploid. The latter is reflected in the fraction of positive values of simulated log2 ratios of aneuploidy fitness over euploid fitness under a given stress condition. Second, the absolute value of the mean and standard deviation of the fitness ratios satisfy a positive linear correlation across diverse stress conditions and a range of *N* values that specify the complexity of the growth control system (Figure 1F,G and Figure 2C-F). The fact that such a simple model could qualitatively capture the experimental data suggests the observed phenomenon to be a general property of heterogeneous aneuploid populations irrespective of specific stress conditions applied. It implies that the evolvability of karyotypically divergent populations escalates with increased stringency of growth inhibition.

The practical implication of the above finding is that any effective strategy against heterogeneous aneuploids must also target the population's evolvability in addition to fitness. We reasoned that if a highly evolvable population with heterogeneous random karyotypes can be "channeled" toward a certain karyotypic characteristic under a designed selection (first treatment), thus drastically "shrinking" the population's evolvability, a second treatment may be added to eradicate the selected singular or limited karyotypes. Together these two treatments would form an "evolutionary trap" (ET) on the elusive aneuploid population. Supporting this idea, our analysis illustrated that, in contrast to the aneuploid cohort with diverse karyotypes, each specific aneuploid has its own unique weakness: for a given specific aneuploidy strain among the 38 examined, one or multiple conditions could be found for most strains that caused growth inhibition over 80% compared to the euploid control (Figure 2G).

Finding drugs forming an ET against heterogeneous aneuploid budding yeast

We used the budding yeast as a model to investigate the validity of ET against heterogeneous aneuploids. We first constructed a yeast population with high-degree karyotypic diversity by sporulation of a homozygous pentaploid yeast strain. Previous work showed that nearly 100% of all variable spores resulted from meiosis of pentaploid cells are aneuploids with random chromosome stoichiometry and ploidies mostly in the range of 2-3N [28]. 28 viable aneuploid meiotic products with ploidy above 1.9N (Figure 3) were mixed with isogenic diploid, triploid and tetraploid euploid cells in order to mimic karyotype heterogeneity observed in pathogenic fungi[85] or human cancers (97% of the 48,595 karyotypes recorded in Mitelman cancer cytogenetics database [20] were between 1.9N and 4N). Because most aneuploid karyotypes obtained from meiotic segregation are unstable [28,93,94], the degree of heterogeneity of this mixed population is likely to be far beyond 31 (28+3) karyotypes, as shown by DNA content profiles of individual aneuploids collected (Figure 3). We confirmed that this initial mixed population (referred to as "heterogeneous mix" for convenience) displayed a broad DNA content profile (Figure 4A) and did not show bias toward any specific chromosome gain or loss (Figure 4B,C).

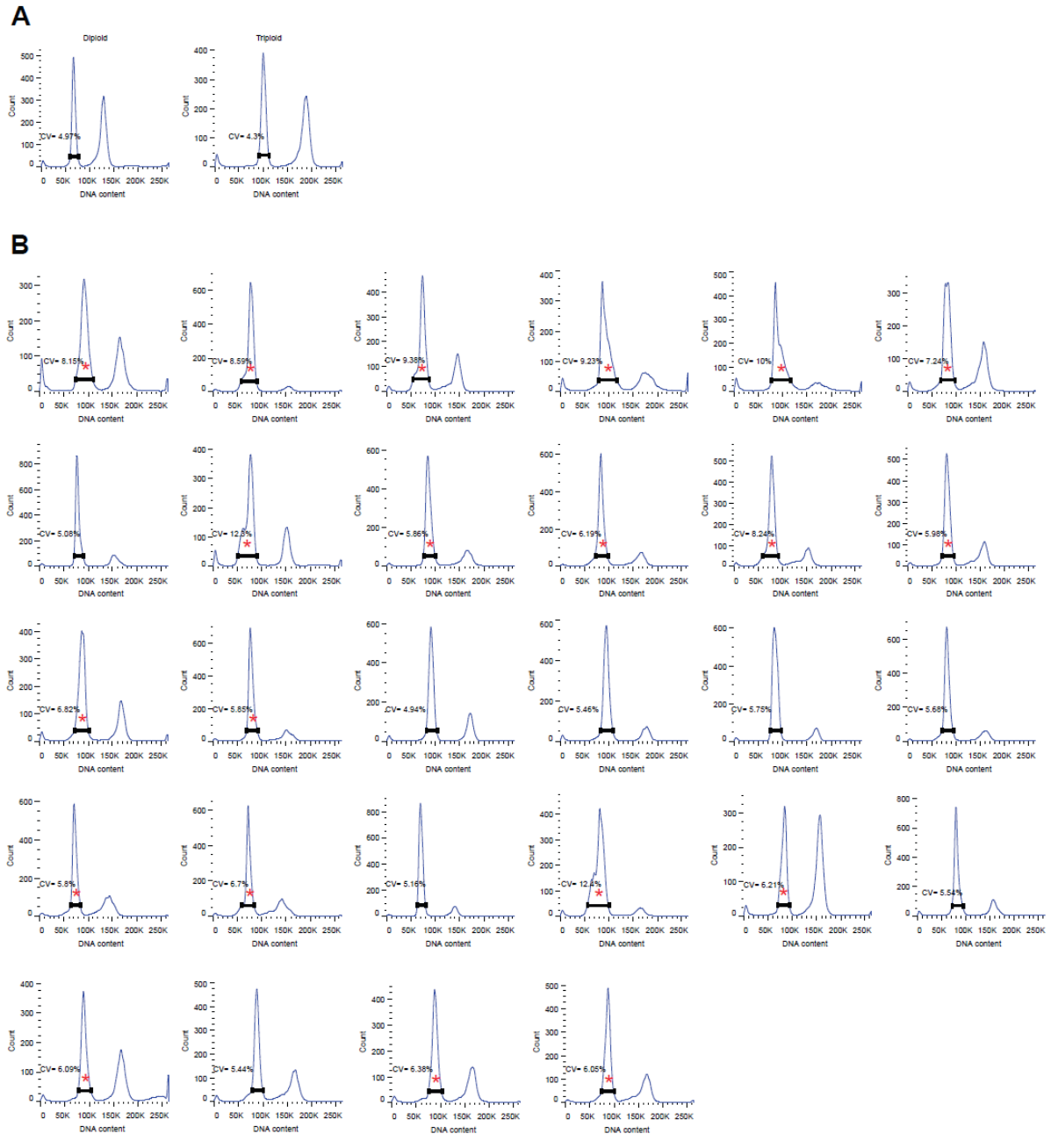

Figure 3. DNA Content Profiles of 28 Aneuploid Strains Demonstrating Karyotype Heterogeneity Between and Within Individual Strains

DNA content profiles of (**A**) Isogenic diploid (one representative figure of the two samples is shown) and triploid euploid control cells (**B**) 28 aneuploid strains by fluorescence-activated cell soring (FACS) are shown. On each profile, the G1 peak region (shown by the bracket) is defined by the G1 peak and its

surrounding area with the cell count higher than 10% of the peak position cell count. The mean and standard deviation of DNA content for the cells located in G1 peak region were calculated. Their ratio, coefficient of variation (CV), which reflects the internal karyotype heterogeneity within each strain, was marked. For 20 out of 28 aneuploids with a CV significantly higher than the euploid control (z-test, $p < 0.05$), a red star was marked.

To find a selective condition that could be used for channeling the diverse karyotypes toward a singular common characteristic, we took advantage of the previous finding that growth in high-concentration of radicicol, an inhibitor of Hsp90 chaperone, selects for aneuploids gaining extra copies of chromosome (Chr) XV [36]. Treatment of three independent populations of the heterogeneous mix with 50 μg/ml radicicol all predictably led to convergent evolution toward gain of Chr XV (Figure 4E), a signature enriched in neither the initial heterogeneous mix nor the non-drug control culture (Figure 4C,D). We further karyotyped six individual colonies derived from a culture that had grown to saturation in racidicol-containing medium. These colonies varied in both karyotype and ploidy but all shared Chr XV gain, confirming that radicicol caused a selective sweep in the heterogeneous mix (Figure 4F).

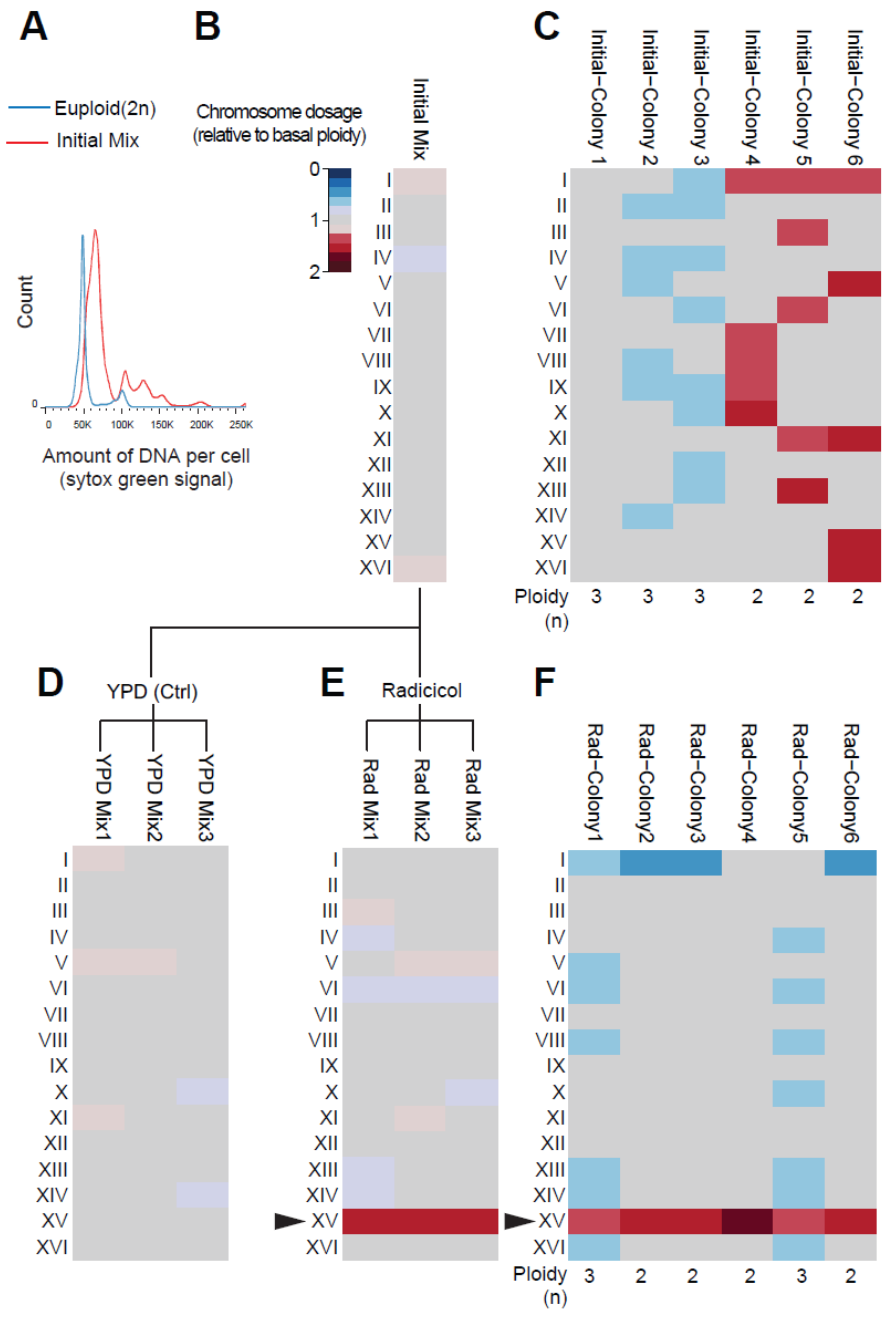

Figure 4. Evolution in the Presence of High-concentration Radicicol Channels Diverse Karyotypes into Karyotypes with The Common Feature of Chr XV gain.

A heterogeneous yeast population was constructed by mixing pentaploid meiotic progeny with different euploids (2n, 3n, 4n, each 10% at of total population). (**A**) DNA content analysis of the heterogeneous mix compared to diploid by FACS. (**B**) qPCR karyotyping of the heterogeneous

mix showing a lack of aneuploid karyotypic signature (thus euploid chromosome stoichiometry on the level of population average). (**C**) The karyotypes of six individual colonies from the initial heterogeneous mix were determined by qPCR assay showing lack of common signature prior to drug selection. (**D**,**E**) The population average karyotypes of the heterogeneous mix evolved in YPD or the presence of 50 μg/ml radicicol are shown, respectively. (**F**) 6 colonies isolated from Rad Mix1 were karyotyped. Arrowheads point to the Chr XV gain, which occurred in all 3 replicates of the heterogeneous mix cultured in liquid radicicol-containing media, as well as in all 6 karyotyped colonies derived from the evolved mix. Karyotypes in **B-F** are presented in the form of chromosome dosage relative to basal ploidy. The color key of heat maps color key is shown in **B** with blue representing loss and red gain.

The above results indicate that radicicol imposes a strong selection for a highly specific and thus likely more targetable aneuploid population. We then performed a screen for chemicals particularly effective toward Chr XV trisomy - the selected karyotypic feature. The growth of a Chr XV trisomy strain, in comparison to an isogenic diploid control strain, was assessed in the presence of a panel of 54 chemicals with previously verified potency against *S. cerevisiae* [95]. This screen identified hygromycin B, a translation inhibitor [96], as the most potent inhibitor of Chr XV trisomy relative to its effect on the diploid control (Figure 6). We further confirmed potent growth inhibition by hygromycin B for all 6 different karyotypes identified from radicicol-selected cultures sharing Chr XV gain (as shown in Figure 4F) (Figure 5A). It is important to note that even though hygromycin B effectively suppressed the growth of aneuploids that had gained Chr XV, this effect did not extend to all aneuploids. In particular, aneuploid strains with increased Chr II or IX dosage, but having a basal dosage of Chr XV, were associated with superior resistance to hygromycin B compared to euploid control (Figure 5B,C). Interestingly, the growth suppression by hygromycin B associated with Chr XV gain is dominant over drug resistance associated with Chr II or Chr IX gain, as strains with these features combined were highly sensitive rather than resistant to hygromycin B (Figure 5C).

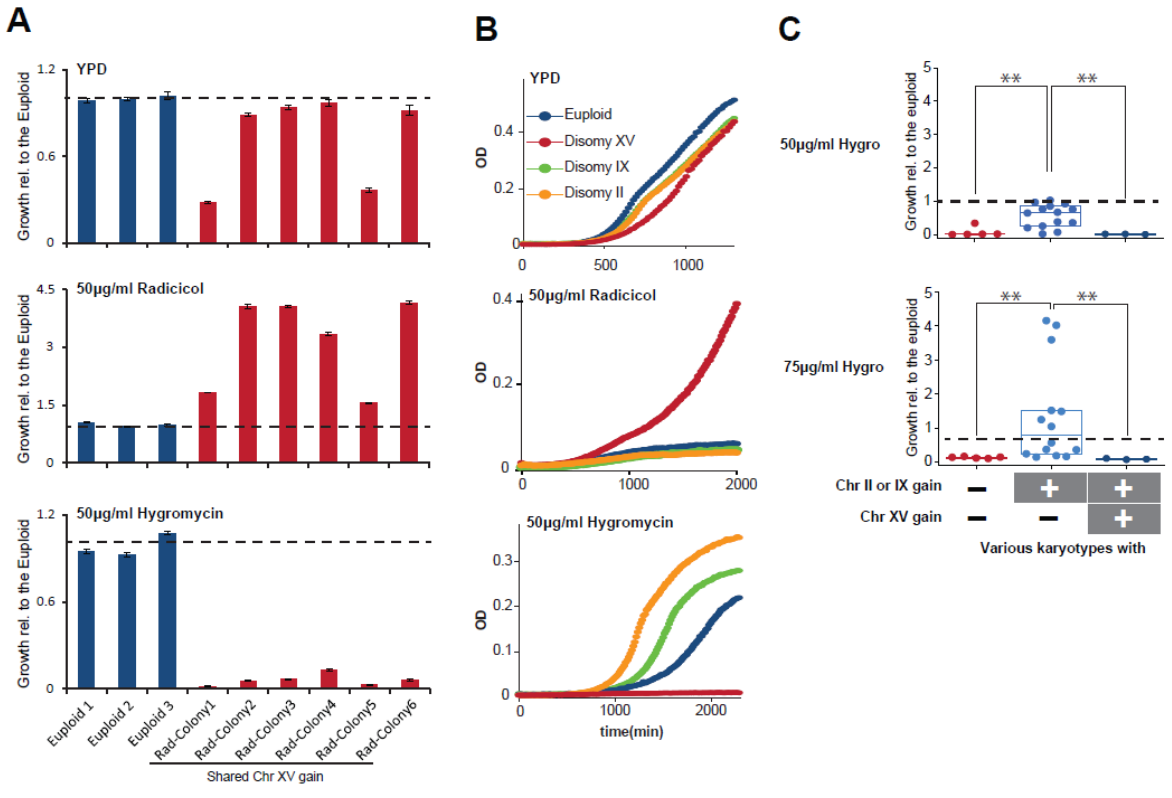

Figure 5. Different chromosome gains associated with hygromycin B sensitivity or resistance

(A) Six independent colonies isolated from radicicol-adapted population aneuploids with gain of Chr XV (as shown in Figure 4F) were grown under indicated conditions until saturation was reached in the fastest growing strain. Histograms show average amount of growth normalized to euploid and standard error of the mean (SEM) derived from 4 replicates. **(B)** Chr II and Chr IX disomy strains generated previously by genetic manipulation[1] exhibit resistance to hygromycin B yet are sensitive to radicicol. **(C)** Aneuploid strains generated by random triploid meiotic segregation with indicated karyotypic features were culture in different concentrations of hygromycin B. Box plots show growth relative to the euploid control with each dot representing an aneuploid strain. Karyotypes are categorized by their states of Chr II/IX/XV dosage, but other chromosome aneuploidy may also be present in these strains. The amount of growth (OD

increase) was normalized to the euploid with the nearest ploidy. The dashed line represents the average of normalized controls (equals to 1). ** indicates $p < 0.01$ according to Mann-Whitney U test.

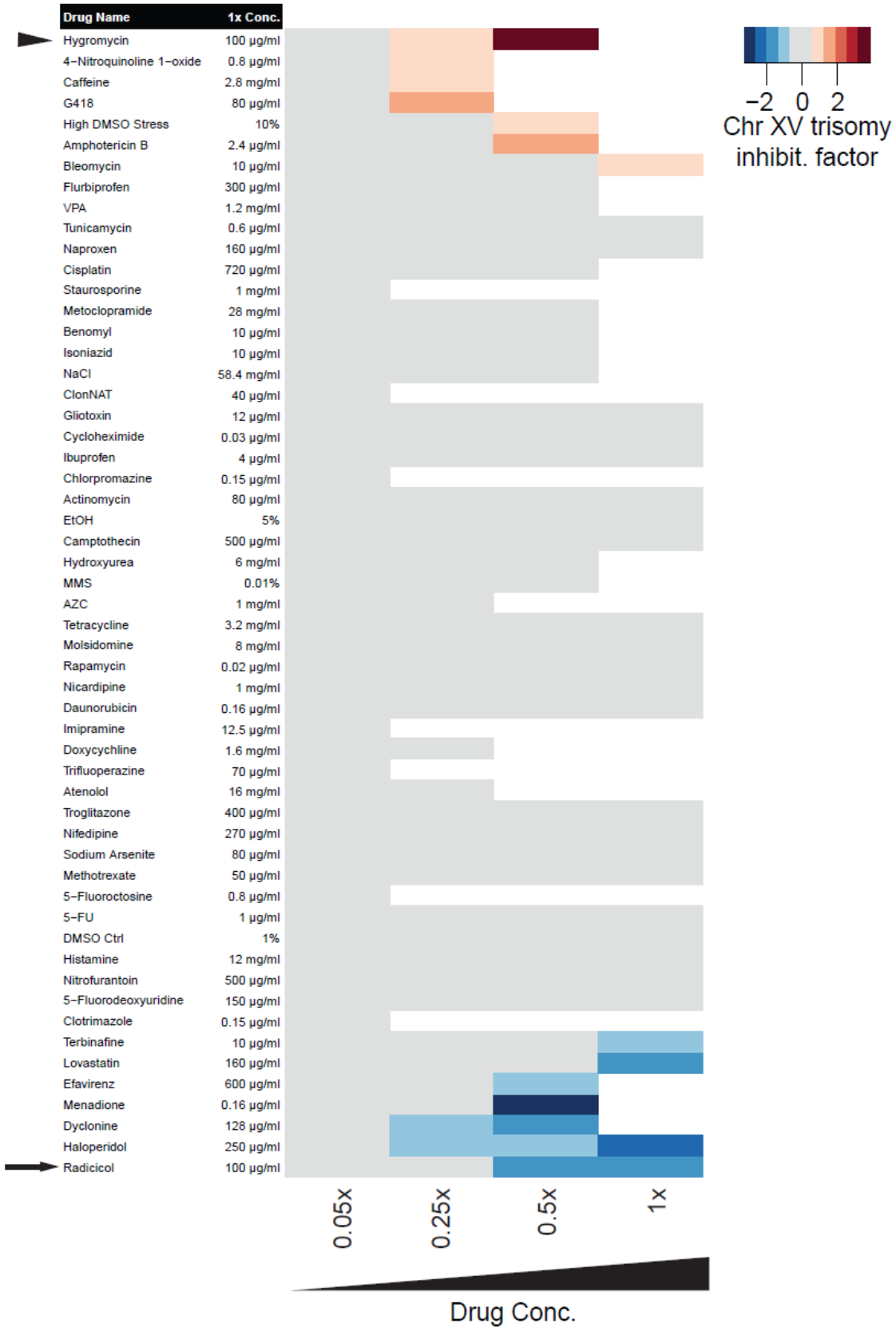

Figure 6. Drug Screen for a Chemical Specifically Targeting Chr XV Trisomy.

Diploid and Chr XV trisomy (with only Chr XV gain) were grown in YPD with 54 different chemicals at 4 different concentrations with concentration gradient from 0.05x to 1x. The 1x concentration is shown in the table. After overnight culture, inhibition of Chr XV trisomy compared to inhibition of the euploid was measured as

$Log_2[OD(Euploid) \ / \ OD(Chr\ XV\ trisomy)]$,

and shown in the heat map. Arrowhead, hygromycin. Arrow, radicicol.

We showed previously that dosage increase of *STI1* and *PDR5*, two genes present on Chr XV, are "driver mutations" underlying Chr XV gain-associated radicicol resistance [36]. However, the hygromycin B sensitivity was unrelated to dosage alterations of these two genes (Figure 7A,B). To understand why Chr XV-gain aneuploids are hypersensitive to hygromycin B, each of the 453 genes located on Chr XV with its original promoter and carried on a low-copy (centromeric) plasmid [97] was introduced into the diploid control strain and the growth was measured in media containing hygromycin B. Of 7 hits that reached a Z score -1.96 or lower (Z-test, $P < 0.05$), 5 plasmid transformants with genes located on Chr XV (*CRS5, RPS15, TRM11, RRP6, SER1*) were re-tested and verified in individual growth assay (Figure 7C, Figure 8). Furthermore, the integration of one copy of each gene associated with top 3 Z scores (*CRS5, RPS15, TRM11*) was able to partially recapitulate the hygromycin B-sensitivity of Chr XV trisomy in a diploid euploid background, demonstrating the strong dosage effect of these genes (Figure 7E).

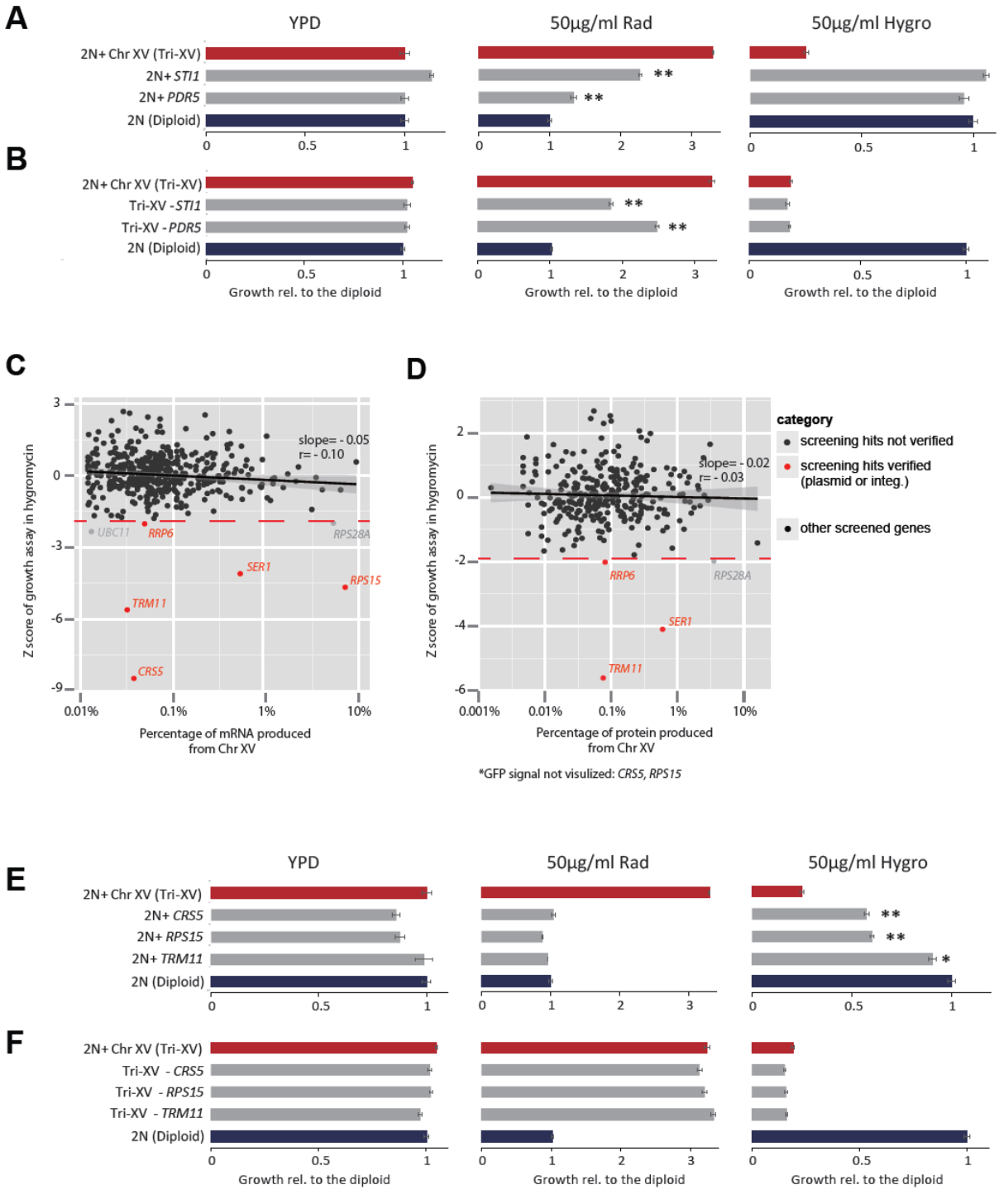

Figure 7. Hygromycin B selects against and radicicol selects for copy number increases of different sets of genes located on Chr XV

Copy number gain or loss experiments were performed to assess the impact of specific gene copy-number increase on hygromycin B sensitivity. The relative growth of different genetic

variants compared to the diploid euploid is reported in bar plots with the SEM derived from 3 replicates. Asterisks denote the genetic variants significantly different from the corresponding control background (the diploid euploid or the Chr XV trisomy (Tri-XV)) (*, $p< 0.05$; **, $p<0.01$; two-tail t-test). **(A-B)** Copy number gain or loss assays showing that increased copy numbers of STI1 and PDR5, which are both critical for radicicol resistance, do not contribute to the hygromycin B hypersensitivity caused by the additional whole chromosome XV. **(C-D)** Expression abundance is unlikely to explain the copy number effect of these genes towards hygromycin B. Each of 453 genes (available through MOBY library [97]) located on Chr XV, along with its original promoter and carried on a CEN vector, was transformed into a diploid strain. The mRNA (**C**) or protein (**D**) expression abundance of each tested gene in a wild type strain were mapped against its growth impact in the presence of 35 μg/ml hygromycin B, with Z scores denoting the deviation of growth of each strain from the population average. mRNA/protein expression abundance of genes was estimated using our RNAseq data (reads-per-million-per-kilobase, RMPK) or the published GFP measurement data [98]. Protein abundance data were not retrieved for 30% genes (including the hits *CRS5* and *RPS15*). The grey area shows the 95% confidence interval for the linear fitting. **(E)** Coy-number gain assays showing that the copy number increases of 3 genes (CRS5, RPS15, TRM11) on Chr XV were individually sufficient in a diploid euploid context to reproduce enhanced sensitivity to hygromycin B, but not radicicol resistance, contrasting copy number increase for STI1 and PDR5 as shown in **A**. **(F)** Copy-number loss assays showing that deletion of none of the 3 genes (CRS5, RPS15, TRM11) rescued Chr XV trisomy from hygromycin B hyper-sensitivity. In contrast, the deletion of either STI1 or PDR5 partially abolished the resistance of Chr XV trisomy to radicicol (**B**).

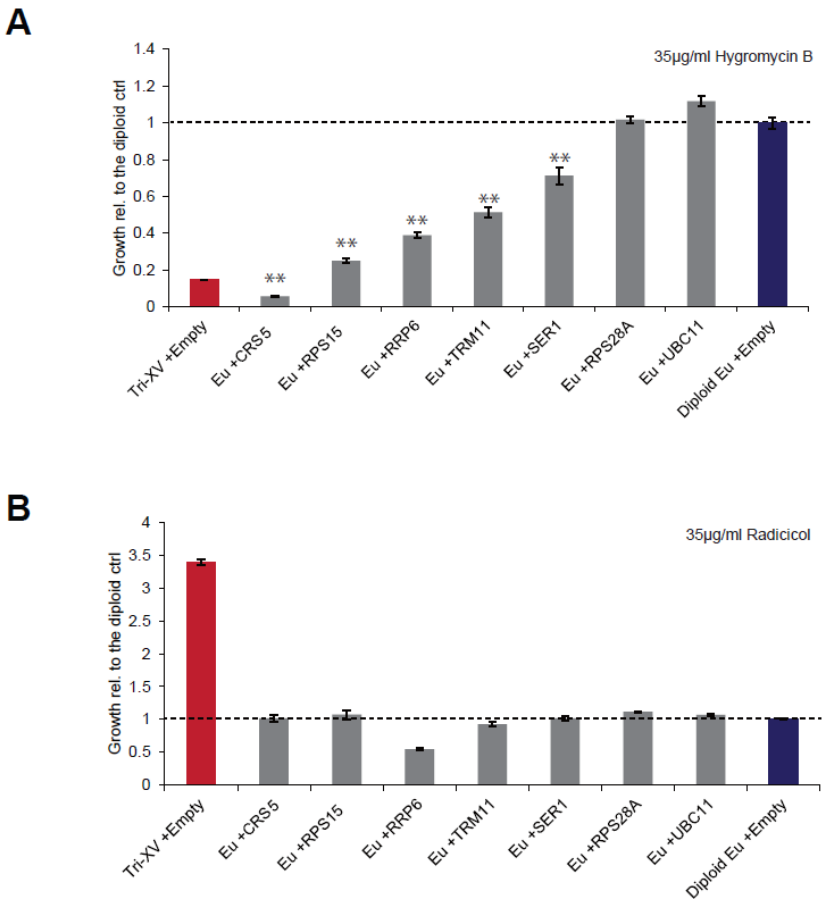

Figure 8. Increased Dosage of Individual Genes Located on Chr XV Causing Hygromycin Sensitivity in Diploid Yeast.

A screen was carried out on a library of transformants in which the diploid euploid strain was transformed with low-copy number (centromeric) plasmids (from MOBY library) containing each of the ORF located on Chr XV driven by its original promoter. The growth was monitored in hygromycin (Methods and Materials). (**A**) The seven hits from the screen which reaches statistical significance were retrieved from the library and retested in hygromycin. The increase dosage of 5 genes (*CRS5, RPS15, RRP6, TRM11, SER1*) were confirmed to reproduce 20% or more hygromycin sensitivity exhibited by Chr XV trisomy in comparison to the diploid control. None of these transformants however reproduced the increase in resistance to radicicol as observed for

Chr XV trisomy (**B**). Increased sensitivity toward hygromycin due to copy number increased of *CRS5, RPS15* and *TRM11* (genes with top 3 Z scores from the screen) was further verified by single copy genomic integration as shown on Figure 7E. Note: the concentrations of both radicicol and hygromycin were adjusted to produce growth delays for the diploid control with an empty MOBY (with *URA* marker) plasmid in SC-ura media with monosodium glutamate (MSG) as the nitrogen source (Methods and Materials) similar to the growth delay imposed on diploid in YPD media.

Hygromycin B as well as other proteotoxic agents were previously proposed to exaggerate the growth defect in aneuploids by augmenting the protein quality control deficit due to general imbalanced expression of large number of genes [1,99]. However, the verified genes whose dosage increase caused hygromycin B sensitivity were not highly expressed genes compared to the other genes located on Chr XV ($p = 0.56$ for transcripts, $p = 0.43$ for proteins, Mann-Whitney U test) (Figure 7C,D). Of note, the top hit *RPS15* encodes one of 30 proteins within the small ribosomal subunit to which hygromycin B binds [100], suggesting a direct gene-specific cause underlying the drug sensitivity. Importantly, the dosage increase of Chr XV genes redundantly produced hygromycin B sensitivity, since the deletion of a copy each of the three hits (*CRS5, RPS15, TRM11*) individually did not change hygromycin hypersensitivity or radicicol resistance of Chr XV trisomy (Figure 7F). Taken together, the mechanisms of radicicol-resistance and hygormycin-hypersensitivity are attributed to different sets of genes located on Chr XV. Furthermore, due to redundant effects and wide-spread gene locations (across both the left and right arms of Chr XV), an ET formed with radicicol and hygromycin B is not expected to be easily escapable through single-gene mutations or focal copy number changes.

Evolution dynamics of cell populations under single-drug treatment vs ET

Even though hygromycin B alone potently suppressed the growth of Chr XV trisomy strain initially, the treated cell population eventually adapted as indicated by growth takeoff after ~ 50 hr (Figure 9). Karyotyping of the adapted Chr XV trisomy culture revealed that the population is a mixture of euploid and aneuploid cells that no longer had Chr XV gain but some now carried an additional copy of Chr IX (Figure 9B,C), which was consistent with the result shown in Figure 9B,C. This observation reconfirmed the requirement for Chr XV gain in hygromycin B sensitivity and

demonstrated the ability of the population to escape single-drug treatment by continued karyotype changes. As expected, the condition that selected for Chr XV, i.e. 50 μg/ml radicicol, was highly toxic to all those survivors that had become hygromycin B resistant because they had lost the gained Chr XV (Figure 4D,E), supporting the rationale of combinatorial treatment with both radicicol and hygromycin B.

Indeed, the combination of both drugs led to the extinction of all 3 independent cultures first subjected to the radicicol selection (Figure 10A-C). The same drug pair was similarly effective against the heterogeneous aneuploid population (heterogeneous mix) when they were added simultaneously (Figure 10D-G, Figure 11). It is important to note that the opposite effects of these two drugs on the fitness of a karyotype feature (Chr XV gain in this case) were key to their combined effectiveness (Figure 10D-G). When the heterogeneous mix was treated with a single chemical, 10 out of 21 tested chemicals (for example, 0.08 μg/ml menadoine and 100μg/ml radicicol) imposed stronger growth suppression than 50 μg/ml hygromycin B (Figure 10F). Hygromycin B also ranked low among the drugs tested in suppressing euploid growth (Figure 10D). Yet, when combined with 50 μg/ml radicicol, hygromycin B, but not 0.08 μg/ml menadoine or 100μg/ml radicicol, led to the extinction of the heterogeneous mix (Figure 10G). Thus, the opposing selective effects of these two drugs on the channeled karyotype (Chr XV gain) imposed

an adaptive dilemma for the heterogeneous population, leading to its extinction.

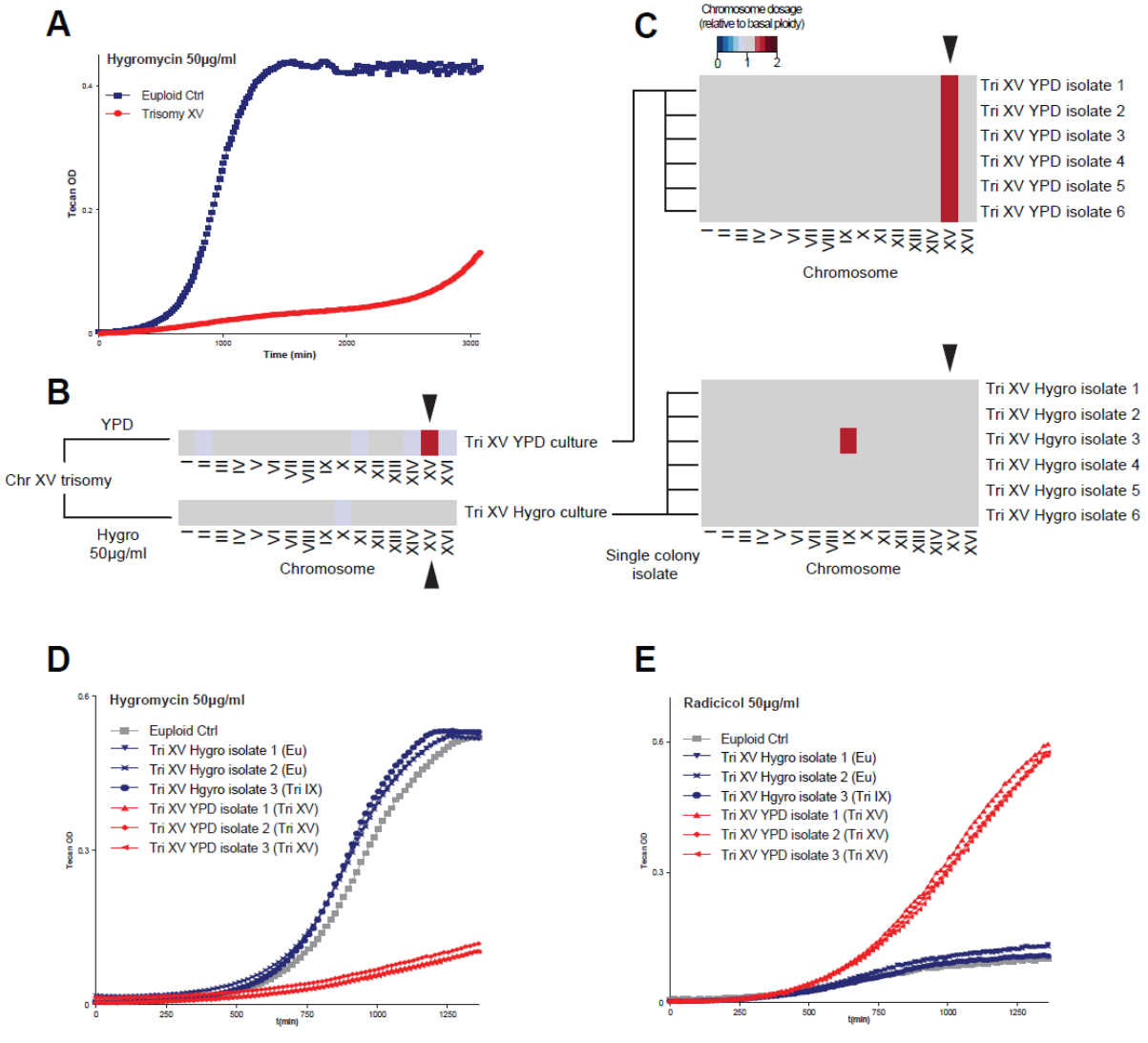

Figure 9. Chr XV trisomy escaped growth inhibition by hygromycin B through loss of the gained Chr XV

(A) The growth (represented by OD reading on a Tecan reader) of both the euploid control and the trisomy XV strain was monitored in media containing 50 µg/ml hygromycin B. **(B)** The additional copy of Chr XV was lost in hygromycin B culture but not in YPD culture, as shown by the heat map of karyotyping result of the final culture. **(C)** Karyotypes of 6 single colonies from the trisomy XV culture in YPD or hygromycin are shown, three of which were re-tested for growth

in the presence of hygromycin B **(D)** or radicicol **(E)**. Note radicicol sensitivity was re-established in all three adapted colonies from the trisomy XV culture in hygromycin, whereas isolates from the YPD culture remained radicicol resistant.

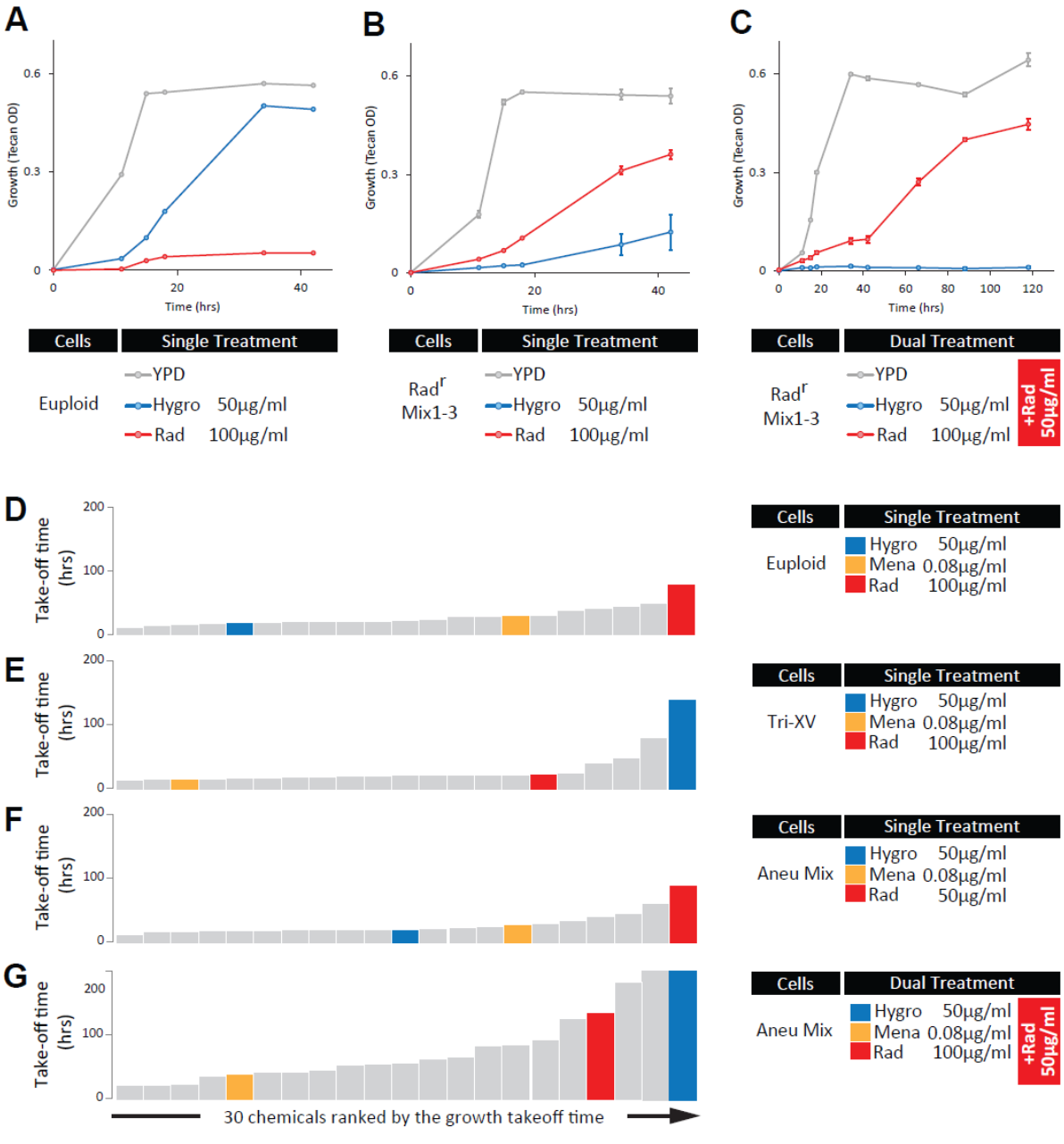

Figure 10. The combination of radicicol and hygromycin B extinct karyotypically heterogeneous population.

(A-C) Combination of hygromycin B and radicicol effectively eradicates the radicicol-preselected aneuploid population. **(A)** Growth curves (as OD600 measured in Tecan) of the diploid control strain under conditions as indicated. Note that 50 µg/ml hygromycin B alone had milder growth

suppression compared to 100 μg/ml radicicol. **(B)** Growth curves of 3 populations preselected independently in the presence of radicicol (Figure 4E) under indicated conditions. **(C)** Growth curves of the same 3 populations as in (b) under indicated conditions where each drug was combined with 50 μg/ml radicicol. Each data point in **B** and **C** shows the mean and SEM from 3 experiments. **(D-G)** Combination of hygromycin B and radicicol effectively eradicates the heterogeneous mix. Histograms show growth takeoff time, defined as the time it took for the designated cell culture to reach OD 0.2 (Tecan) under each growth condition.

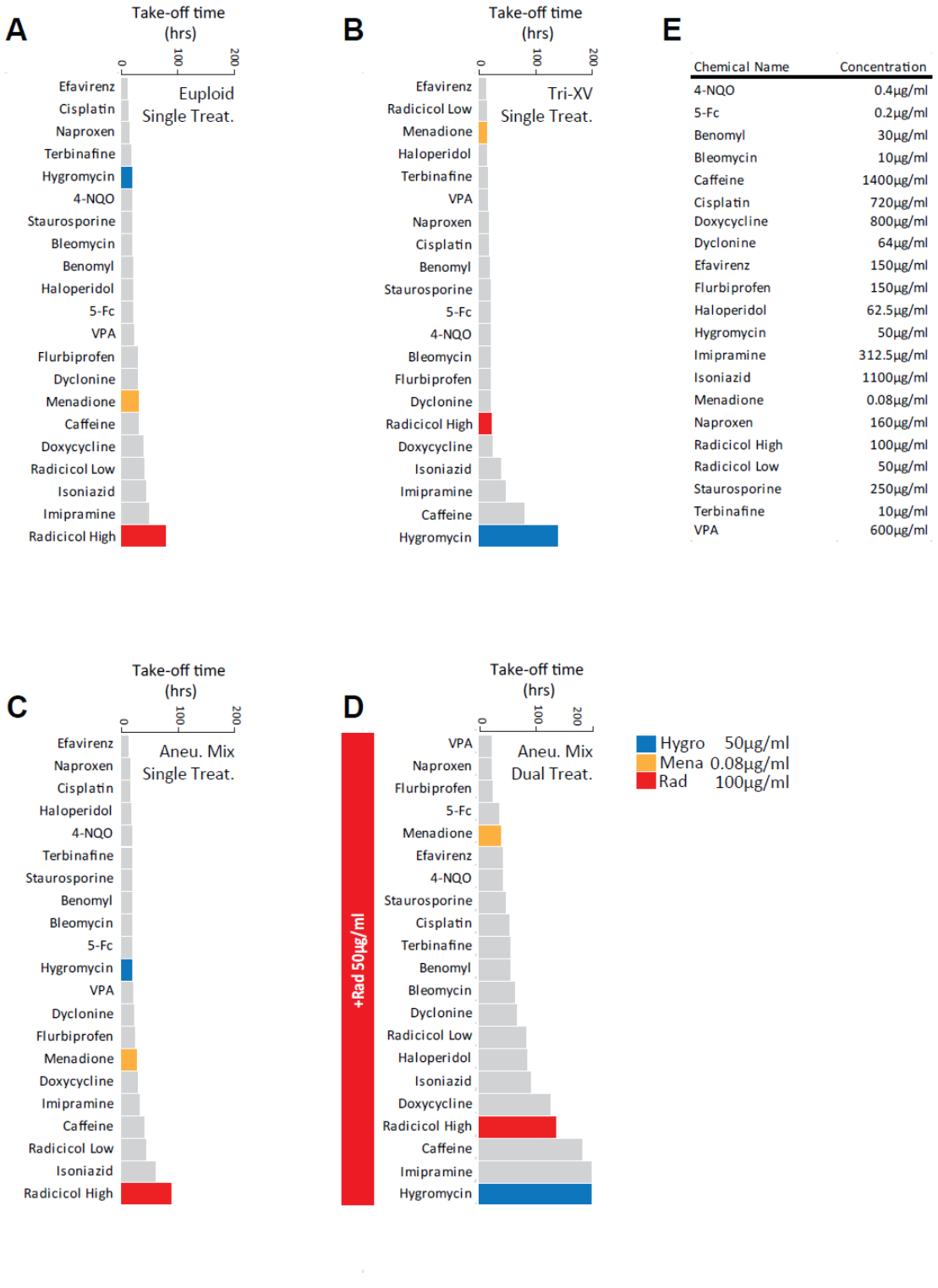

Figure 11. ET Effectively Suppressing the Heterogeneous Aneuploid Population.

Histograms show growth takeoff time, defined as the time it took for the cell culture to reach OD 0.2 (Tecan readings) under each growth condition. (**A-C**) three different cultures (euploid,

trisomy XV and heterogeneous mix) were treated with each chemical in single form, respectively. (**D**) The heterogeneous mix was treated with each chemical along with 50µg/ml radicicol. (**E**) A list of the concentration of each chemical used.

An azole-based ET for human pathogen *Candida albicans*

It was previously shown that a mechanism for human pathogen *Candida albicans* to confer resistance to fluconazole, a first-line medicine treating invasive candidiasis in immune-compromised patients, is gain of isochromosome 5L (i5L, which contains two copies of the left arm of Chr 5) [13]. This aneuploid feature was also recapitulated in a laboratory evolution experiment selecting for fluconazole-resistant *C. albicans* [101]. We therefore tested the possibility of using the evolutionary-trap strategy for more effective anti-fungal treatment. In this case, fluconazole serves as the "selection" drug, which would be used in combination with a second drug specifically targeting the i5L gain. To this end, we screened a chemical library that contained 1,713 FDA- or other regulatory agency-approved drugs, 580 natural compounds, and 420 other bioactive agents against an i5L-containing *C. albicans* isolate from a 30-year-old male who developed fluconazole-resistant candidemia, with its euploid derivative for comparison (See page 117 in appendix for experimental design details) [13,102]. We looked for chemicals that show much elevated potency against the i5L-containing strain compared to the euploid control, since such drugs were likely to be missed in previous screens against *C. albicans* without the drug-resistance karyotype [103,104].

A primary screen using a single concentration of 80 μM for each drug found that 3.5% of the compounds (100 out of 2713, Figure 13A) caused at least 80% growth suppression to either the i5L strain or the euploid, or both. For this set of compounds, we then profiled the drug-response curve for the pair of strains by growing them in a dilution series for each drug composed of 9 different concentrations. The concentration causing 80% growth suppression compared to solvent control (IC80) was determined for each drug and each strain. Figure 12A shows that

chromosome i5L copy number difference caused considerable variations in fitness in the presence of these compounds. In the presence of 26 or 11 conditions, the i5L strain showed significantly (Z-test, $p < 0.05$) higher (i.e., more resistant) or lower IC80 (more susceptible), respectively, than the euploid (Figure 12A). As expected, the i5L strain, originally selected for its resistance to fluconazole, exhibited increased resistance toward a panel of 7 other azole derivatives approved by FDA. The other end of the spectrum found pyrvinium pamoate (PP), a medication for pediatric pinworm infection (Figure 12A and Figure 13B). PP strongly suppressed the growth of the i5L strain at 10 μM but was ineffective against the euploid at concentrations as high as 80 μM after 48 hour culture on agar (Figure 12B). Given the possibility that euploid and i5L-gained Candida could co-exist in patients treated with fluconazole [29], we tested the combinatorial effect of PP with fluconazole in a 1:1 mixed population of both karyotypes. As shown in Figure 12C,D, at concentrations of PP that suppressed the growth of the i5L strain, the resistance to fluconazole regressed from > 256 μg/ml back to the same level exhibited by the euploid without PP (32-48 μg/ml), supporting the efficacy of the evolutionary-trap rationale to target the selected karyotype for combinatorial treatments.

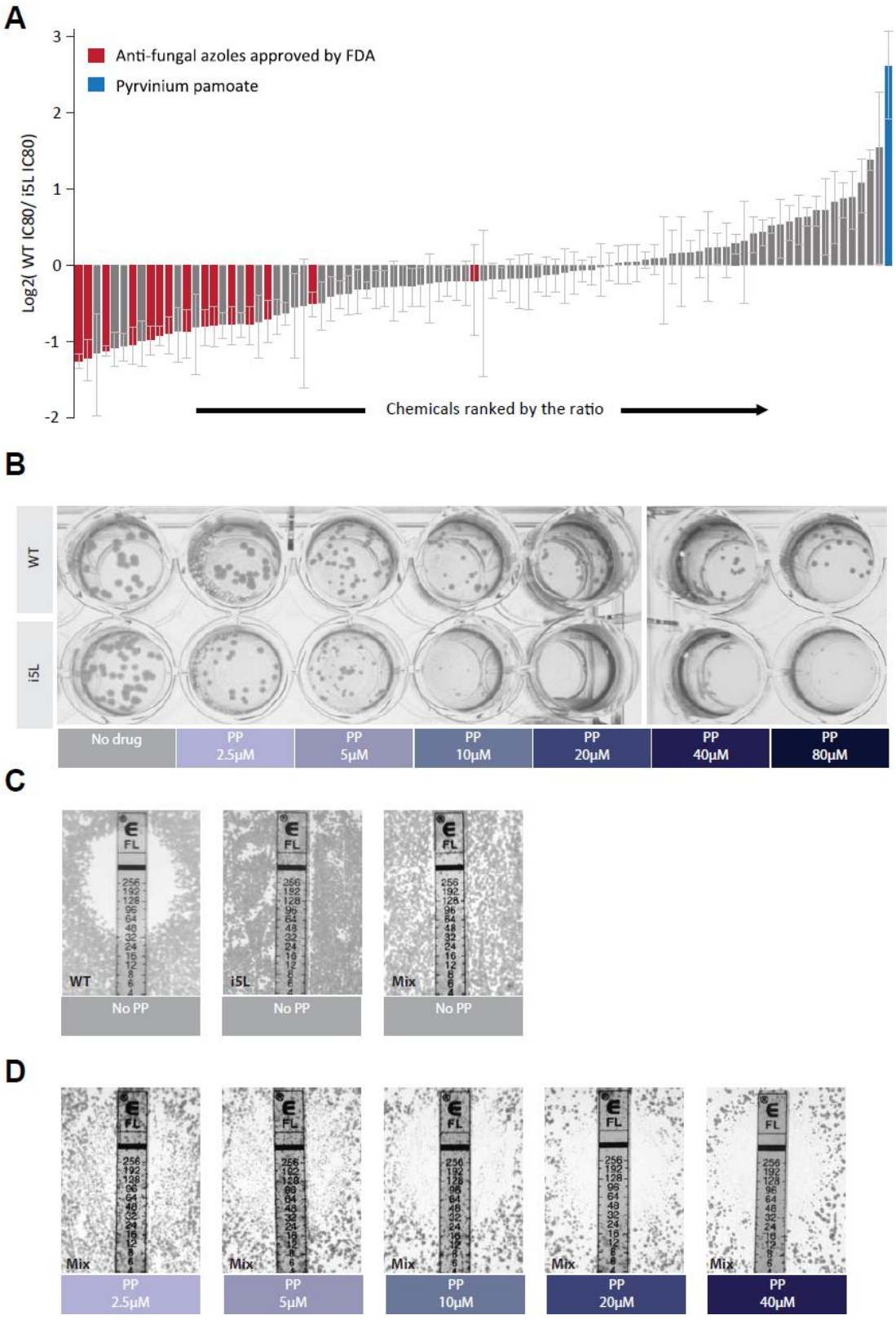

Figure 12. Pyrvinium pamoate (PP) effectively targets the fluconazole-resistant Candida

aneuploid.

(A) Relative IC80 (80% inhibitory concentration) of the diploid vs the i5L Candida strain for each of the hits of the primary drug screen. Note that i5L strain displayed higher IC80 toward all 8 anti-fungal azoles approved by FDA but much lower IC80 to pyrvinium pamoate (PP). **(B)** Images of agar plates showing selective effectiveness of PP toward i5L candida. **(C)** Resistance of the diploid, the i5L or the i5L+diploid mix population toward fluconazole. The results of fluconazole Epsilometer test (e-test) are shown with the size of the halo indicating the level of drug sensitivity. **(D)** PP at concentrations above 10 μM restored the sensitivity of the i5L+diploid mix population toward fluconazole in the e-test, in accordance to its singular form's activity against the i5L strain shown in **B**. Note even though the initial plating density was the same, due to the inhibition of the i5L cells, the overall growth was less in **D** compared to **C**. Note that our euploid strain also exhibited a reduced susceptibility to fluconazole compared to the clinical E-test standard strain, which may be attributed to other point mutations (such as the hyperactive *TAC1*) within this strain [13]. All plate images were taken after 48-hour culture.

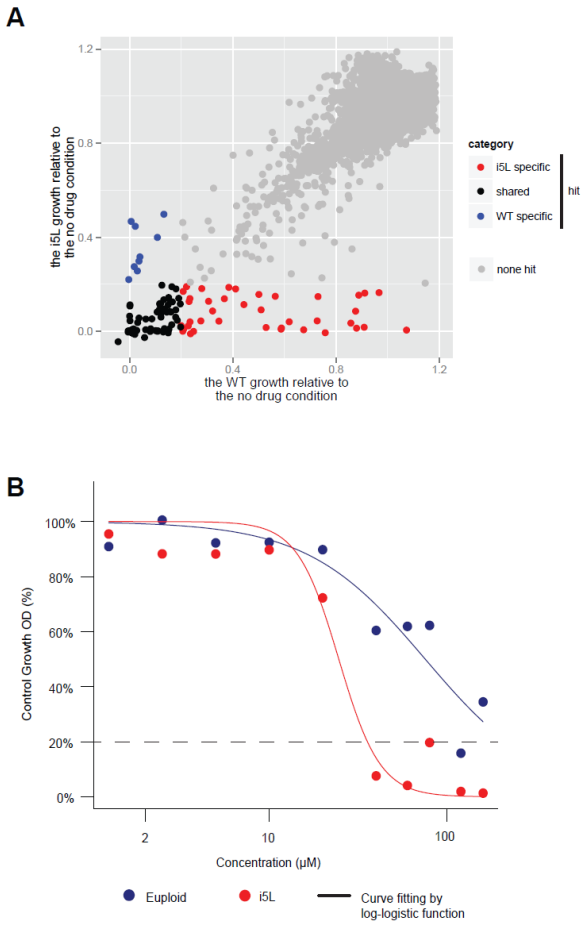

Figure 13. The Chemical Screen Searching for Chemicals Against i5L *C. albicans*.

(A) The scatter plot shows the result of relative growth measurement of 2 strains (diploid and i5L) in 3,600 assay conditions at a chemical concentration of 80μM. The assay number is higher than the total number of chemicals due to the partial overlapping between the chemical libraries used. As the libraries used (the Prestwick and the Spectrum collection) partially overlaps, these conditions represents 2713 different chemicals, as judged by distinct CAS registry numbers. 119 of the conditions, representing 100 distinct chemicals, caused an 80% or higher growth inhibition in at least one of the two strains tested. These hits are further categorized according to the strain toward which a chemical imposed 80% or higher growth inhibition. **(B)** As the top hit from the chemical screen against i5L, the drug response for pyrvinium pamoate was assayed for both the

euploid and the i5L strain at 9 different concentrations ranging from 1 μM to 160 μM in duplicates. The assay was carried in RPMI liquid media with 2% glucose added in 384-well format at 35 ^{o}C. The relative growth of each strain compared to the corresponding drug-free control was recorded and plotted from 24-hour culture, and fitted with a four-parameter log-logistic function. The average values from the duplicates are shown. 80% growth inhibition level is denoted by a dotted line.

Our experimental and theoretical findings argue on a general level that the difficulty of suppressing karyotypically heterogeneous cell populations is rooted in the large adaptive potential in the presence of severe stress. ET deals directly with this difficulty by reducing karyotypic heterogeneity through an evolutionary process. It is also motivated by the observation that even though no stress tested could kill all aneuploids in the population, the growth of specific aneuploids can be disproportionally inhibited or even eliminated under certain stress conditions. In our proof-of-principle experiments in budding yeast, this common aneuploid feature is gain of Chr XV, which harbors the "driver mutations" for radicicol resistance (selection) and multiple "passenger" genes whose copy number increase redundantly confers sensitivity to hygromycin B, the agent for extinction (Figure 14A, see following). The redundancy in genes whose copy number increase confers hygromycin B sensitivity and the requirement for multiple genes to achieve radicicol resistance predicted that escaping the trap is not easily attainable through single-gene mutations or copy number changes.

This strategy of treating aneuploidy is distinct from the idea of targeting a single characteristic trait of aneuploids, presently thought to be the proteome imbalance overwhelming the protein quality control system [1,34,99,105]. We note that both drugs used in the yeast ET, radicicol and hygromycin B, could perturb proteome homeostasis [1,69,96,99], but the responses of aneuploids to these drugs are karyotype-specific rather than uniform. Importantly, much of the hygromycin B hypersensitivity of Chr XV trisomy can be recapitulated with copy-number increase of a few specific genes producing only a small or even minute fraction of the expressed transcriptome or proteome from Chr XV. In this case, the aneuploid karyotype alters fitness by perturbing specific pathways rather than augmenting a general deficiency of aneuploids, such as the overload of protein quality control system. The rationale behind the dual drug treatments associated with

ET is also fundamentally different from the idea of synthetic lethality [106,107] or the use of dual drugs to target different aspects of the common defect of aneuploidy irrespective of the karyotype [105] , whose rationale is based on functional redundancy within an existing system without the anticipation of evolutionary changes. By contrast, radicicol and hygromycin B, or fluconazole and PP, pairs of drugs forming ET do not interfere with redundant processes but rather collaborate to force and interject a predicted evolutionary trajectory of the genome, which involves changes in the copy number of a chromosome that links pools of genes regulating divergent responses to the different drugs (Figure 14A, B).

Gain of Chr 5L is a genetic alteration prevalent in *C. albicans* with resistance to its first-line treatment, fluconazole[13]. Through screen, the study found that PP, a FDA-approved chemical may be highly toxic to *C. albicans* strains with additional copies of Chr 5L. Thus the combination of PP and fluconazole sets up an effective ET that may be able to eradicate the highly evovable aneuploidy *C. albicans* population in human patients. ET may have the potential to be utilized as a novel strategy to treat aneuploidy diseases.

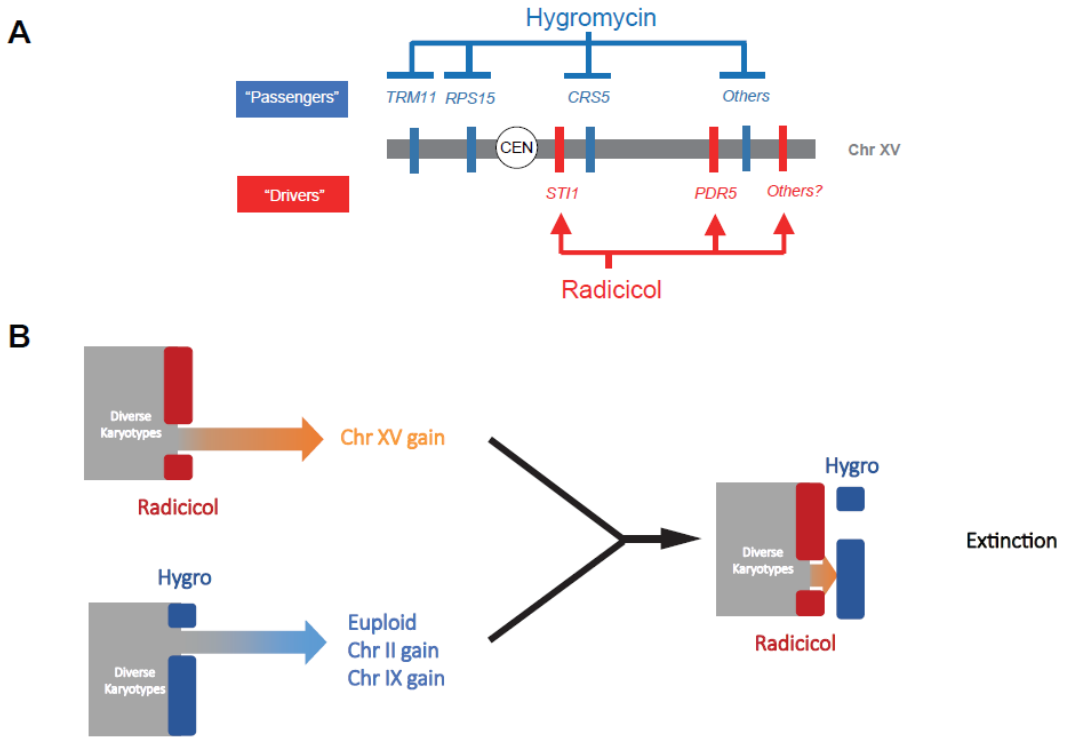

Figure 14. Graphic Summary of the evolutionary trap (ET)

(A) The molecular makeup of the yeast ET. Radicicol selects for gain of *STI1*, *PDR5* as well as other genes located on Chr XV, whereas hygromycin B selects against gain of *TRM11*, *RPS15*, *CRS5* and other genes (e.g. SER1, RRP6. See Figure 8) which are also located on Chr XV. For radicicol resistance, increased copy number of *STI1* and *PDR5* are driver mutations; in contrast, increase copy number of *TRM11*, *RPS15* and *CRS5* are passenger mutations, which are targeted by hygromycin B. The positions of genes are placed according to their relative locations on the chromosome. **(B)** The opposing selective effects of radicicol and hygromycin B on dosage increase of Chr XV impose an adaptive dilemma for the heterogeneous population with diverse karyotypes in budding yeast.

Chapter 4: Summary and Discussion

Summary

Aneuploidy population is often presented with more than a single karyotype but rather a heterogeneous group of diverse karyotypes. This is likely a consequence of how aneuploidy is generated, and the resulted heterogeneity can profoundly impact the cellular evolution process. In chapter 1, we showed that one consequence of strong Hsp90 inhibition, or in general CIN, is the production of a population with karyotypic diversity, which was shown in the study to promote rapid cellular adaptations to various stresses through karyotype selection. The superior adaptability of a heterogeneous aneuploidy population likely underlies the clinical challenge in the treatment of different diseases driven by eukaryotic cellular evolution, such as candidemia or cancer. In chapter 3, we proposed a novel strategy that eradicates the heterogeneous aneuploidy populations by targeting the trajectory of karyotype evolution and tested it in both lab yeast as well as the *Candida* clinical isolate.

Our analyses started from an exploration of the general response of karyotypically heterogeneous cell populations to diverse stress conditions and proceeded to the design of a strategy to extinct such cell populations that accounts for their adaptive potential. Our findings demonstrate that the phenotypic variation resulted from karyotype diversity of an aneuploid yeast collection scales directly with the degree of average population growth inhibition under diverse stress conditions. Mathematical simulations based upon a few logical and statistical assumptions supports the generality of our experimental observation. A more intuitive understanding of this phenomenon may lie in the highly pleiotropic nature of aneuploidy: as a result of its broad impact on gene expression, there is a high probability of a random aneuploid

karyotype to interact with a given stress condition, either exacerbating or alleviating the growth inhibitory effect of the stress. Such tendency may contrast that of most single-gene mutations affecting only one or a small number of cellular pathways and are thus much more likely to be phenotypically neutral toward a given stress condition.

The coexistence of karyotype heterogeneity and dominant karyotype features has been observed in both human cancer [4] and drug-resistant pathogenic fungi [13,85]. The prior selection that channels the karyotype change in these diseases may be leveraged as a part of an ET for therapeutic purpose. Our experiments with *Candida* provide a proof-of-principle case where PP, which selects against the gain of i5L, could enhance the efficacy of fluconazole, the prior selection favoring the gain of i5L. PP is extremely well tolerated (5mg per kg of body weight) in pediatric population for gastrointestinal treatment due to the near-zero absorption rate [108]. Interestingly, vast majority cases of *Candida* infection occurs on the outer or inner surface of the body [109], and the origin of rare but life-threatening systemic *Candida* infection may be traced back to resident gastrointestinal *Candida* flora [110]. Thus, the strategy of augmenting azole with PP to treat *Candida* infections is worthy of investigation in clinics.

Future Directions

Aneuploidy has been observed and documented in cancer more than a hundred years ago [111]. Recent genomics data reinforced the notion that aneuploidy is widespread in human cancers[4,112]. Statistical analysis on published data also found that a vast majority of solid tumors are aneuploid: 91.7% of 817 solid tumor cell lines surveyed by Cancer Cell Line Encyclopedia (CCLE) have at least 1 arm-level copy number variation, whereas 58.9% have more than 10. Yet, it remains elusive on how to target this hallmark of cancer. The large karyotype heterogeneity existing even in a single tumor further complicates the strategy design to use aneuploidy as a drug target. One proposal views aneuploidy as a group of mutations sharing similar molecular feature. For example, the excessive protein produced by the imbalanced chromosome may cause a universal proteotoxic stress response among aneuploids. And by extraggerating the proteotoxic stress, the growth of all aneuploids may be severely impaired[1,32,34,91,92,99,105].

Using budding yeast as the model organism, my current study challenged this view by showing that the phenotypic variation scales with the overall growth inhibition in the heterogeneous aneuploidy population (the scaling). A general multi-dimensional statistical model can produce similar behavior, suggesting the multi-pathway control of cellular growth may underlie the scaling. The scaling predicts that a single stress can hardly eliminate a heterogeneous aneuploidy population. Whether the scaling phenomena also exists in higher organisms remains unknown. It is of particular interest to investigate whether the scaling between phenotypic variation and overall growth inhibition exists in the population of cancer cells with diverse aneuploidy karyotypes. Such scaling can release phenotypic variation upon stress, thus enabling rapid cellular evolution. One way to examine such possibility is to leverage the widely available pharmacogenomics database in which a large number of cancer cell lines were tested against a wide spectrum of chemicals in different concentrations[113-116]. By examining the relationship

between standard deviation and mean of growth rates of a population of cancer cell lines under different conditions, it should become clear whether the scaling similar to what we observed in yeast aneuploids also happen in human aneuploidy cell lines.

If so, such observation will have a practical implication on how to target aneuploidy in cancer. As shown in our yeast model, instead of targeting general aneuploidy, aneuploidy population would become more approachable by first channeling the population into the one with a dominant karyotype feature. A second stress can then be applied to target the selected karyotype feature.

Interestingly, it is noticed that in some of the tumors even before any chemical treatment, the karyotypes are heterogeneous but non-random: a dominant karyotype emerges during the tumor evolution process. Thus, the natural tumor evolution process can serve as the first channeling selection. Under this condition, a chemical targeting the selected karyotype can set up an ET along with the tumor evolution. For example, karyotype channeling happens naturally in tumors such as glioblastoma even without chemical treatment: Chromosome 7 gain was observed in 80% of tumor samples collected from The Cancer Genome Atlas Pilot Project (TCGA) cohort of 219 patients [117,118]. Within individual tumors, arm-level or whole chromosome gain of chromosome 7 was detected in nearly all surgical sections examined, suggesting this event, unlike other heterogeneous genetic alterations, is an early critical event in clonal expansion [119]. Collectively, evidence at both inter- and intra-tumor levels suggest that the sweeping presence of karyotypic signatures in subtypes of tumors is likely to be a consequence of adaptation to the tissue micro-environment and/or the need for oncogenic transformation. It is interesting to speculate that this natural karyotypic selection combined with drug treatment targeting the passenger gene dosage changes associated with the gained or lost chromosomes may form an

ET on this elusive disease while minimizing the damage to normal euploid tissues. In order to find such chemical it will be necessary to establish the correlation between specific karyotype and drug response. One idea is to again utilize the cancer pharmacogenomic database consisting of both karyotype and drug response information.

In summary, data mining on existing cancer cell line pharmacogenomics database may provide a viable path to expand the strategy of ET into the field of cancer biology. Other experimental approach such as screening using a pair of euploidy and aneuploidy cells may also provide compound candidates which can be used to eradicate the dominant karyotype feature in cancer. Currently, the evolutionary trap strategy focuses on using two counter-acting compounds that select for and against the same karyotype feature. However, genetic features beyond karyotype alterations, such as point mutations, may also be utilized to set up the ET.

References

1 Torres, E. M. *et al.* Effects of Aneuploidy on Cellular Physiology and Cell Division in Haploid Yeast. *Science* **317**, 916-924, doi:10.1126/science.1142210 (2007).

2 Selmecki, A., Forche, A. & Berman, J. Genomic Plasticity of the Human Fungal Pathogen Candida albicans. *Eukaryotic Cell* **9**, 991-1008, doi:10.1128/ec.00060-10 (2010).

3 Pavelka, N., Rancati, G. & Li, R. Dr Jekyll and Mr Hyde: role of aneuploidy in cellular adaptation and cancer. *Current Opinion in Cell Biology* **22**, 809-815 (2010).

4 Gordon, D. J., Resio, B. & Pellman, D. Causes and consequences of aneuploidy in cancer. *Nat Rev Genet* **13**, 189-203 (2012).

5 Sheltzer, J. M. & Amon, A. The aneuploidy paradox: costs and benefits of an incorrect karyotype. *Trends in Genetics* **27**, 446-453, doi:10.1016/j.tig.2011.07.003 (2011).

6 Hughes, T. R. *et al.* Widespread aneuploidy revealed by DNA microarray expression profiling. *Nat Genet* **25**, 333-337 (2000).

7 Kvitek, D. J., Will, J. L. & Gasch, A. P. Variations in Stress Sensitivity and Genomic Expression in Diverse <italic>S. cerevisiae</italic> Isolates. *PLoS Genet* **4**, e1000223 (2008).

8 Codon, A. C., Benitez, T. & Korhola, M. Chromosomal polymorphism and adaptation to specific industrial environments of *Saccharomyces* strains. *Applied Microbiology and Biotechnology* **49**, 154-163, doi:10.1007/s002530051152 (1998).

9 Bond, U., Neal, C., Donnelly, D. & James, T. Aneuploidy and copy number breakpoints in the genome of lager yeasts mapped by microarray hybridisation. *Current Genetics* **45**, 360-370, doi:10.1007/s00294-004-0504-x (2004).

10 Borneman, A. R. *et al.* Whole-Genome Comparison Reveals Novel Genetic Elements That Characterize the Genome of Industrial Strains of <italic>Saccharomyces cerevisiae</italic>. *PLoS Genet* **7**, e1001287 (2011).

11 Infante, J. J., Dombek, K. M., Rebordinos, L., Cantoral, J. M. & Young, E. T. Genome-Wide Amplifications Caused by Chromosomal Rearrangements Play a Major Role in the Adaptive Evolution of Natural Yeast. *Genetics* **165**, 1745-1759 (2003).

12 Hu, G. *et al.* Comparative hybridization reveals extensive genome variation in the AIDS-associated pathogen Cryptococcus neoformans. *Genome Biology* **9**, R41 (2008).

13 Selmecki, A., Forche, A. & Berman, J. Aneuploidy and Isochromosome Formation in Drug-Resistant Candida albicans. *Science* **313**, 367-370, doi:10.1126/science.1128242 (2006).

14 Sionov, E., Lee, H., Chang, Y. C. & Kwon-Chung, K. J. <italic>Cryptococcus neoformans</italic> Overcomes Stress of Azole Drugs by Formation of Disomy in Specific Multiple Chromosomes. *PLoS Pathog* **6**, e1000848, doi:10.1371/journal.ppat.1000848 (2010).

15 Murray, H. W., Berman, J. D., Davies, C. R. & Saravia, N. G. Advances in leishmaniasis. *The Lancet* **366**, 1561-1577.

16 Rogers, M. B. *et al.* Chromosome and gene copy number variation allow major structural change between species and strains of Leishmania. *Genome Research*, doi:10.1101/gr.122945.111 (2011).

17 Akopyants, N. S. *et al.* Demonstration of Genetic Exchange During Cyclical Development of Leishmania in the Sand Fly Vector. *Science* **324**, 265-268, doi:10.1126/science.1169464 (2009).

18 Vanneste, E. *et al.* Chromosome instability is common in human cleavage-stage embryos. *Nat Med* **15**, 577-583 (2009).

19 van Echten-Arends, J. *et al.* Chromosomal mosaicism in human preimplantation embryos: a systematic review. *Human Reproduction Update* **17**, 620-627, doi:10.1093/humupd/dmr014 (2011).

20 Mitelman F, J. B. a. M. F. E. Mitelman Database of Chromosome Aberrations and Gene Fusions in Cancer (2012). doi:http://cgap.nci.nih.gov/Chromosomes/Mitelman (2012).

21 Weaver, B. A. A. & Cleveland, D. W. in *Current Opinion in Cell Biology* Vol. 18 658-667 (2006).

22 Ozery-Flato, M., Linhart, C., Trakhtenbrot, L., Izraeli, S. & Shamir, R. Large-scale analysis of chromosomal aberrations in cancer karyotypes reveals two distinct paths to aneuploidy. *Genome Biology* **12**, R61 (2011).

23 Duncan, A. W. *et al.* Frequent Aneuploidy Among Normal Human Hepatocytes. *Gastroenterology* **142**, 25-28 (2012).

24 Yurov, Y. B. *et al.* Aneuploidy and Confined Chromosomal Mosaicism in the Developing Human Brain. *PLoS ONE* **2**, e558 (2007).

25 Rehen, S. K. *et al.* Constitutional Aneuploidy in the Normal Human Brain. *The Journal of Neuroscience* **25**, 2176-2180, doi:10.1523/jneurosci.4560-04.2005 (2005).

26 Henry, I. M., Dilkes, B. P., Miller, E. S., Burkart-Waco, D. & Comai, L. Phenotypic Consequences of Aneuploidy in Arabidopsis thaliana. *Genetics* **186**, 1231-1245, doi:10.1534/genetics.110.121079 (2010).

27 Huettel, B., Kreil, D. P., Matzke, M. & Matzke, A. J. M. Effects of Aneuploidy on Genome Structure, Expression, and Interphase Organization in <italic>Arabidopsis thaliana</italic>. *PLoS Genet* **4**, e1000226, doi:10.1371/journal.pgen.1000226 (2008).

28 Pavelka, N. *et al.* Aneuploidy confers quantitative proteome changes and phenotypic variation in budding yeast. *Nature* **468**, 321-325 (2010).

29 Selmecki, A., Gerami-Nejad, M., Paulson, C., Forche, A. & Berman, J. An isochromosome confers drug resistance in vivo by amplification of two genes, ERG11 and TAC1. *Molecular Microbiology* **68**, 624-641, doi:10.1111/j.1365-2958.2008.06176.x (2008).

30 Rancati, G. *et al.* Aneuploidy Underlies Rapid Adaptive Evolution of Yeast Cells Deprived of a Conserved Cytokinesis Motor. *Cell* **135**, 879-893, doi:10.1016/j.cell.2008.09.039 (2008).

31 Gao, C. *et al.* in *Proceedings of the National Academy of Sciences* Vol. 104 8995-9000 (2007).

32 Williams, B. R. *et al.* Aneuploidy Affects Proliferation and Spontaneous Immortalization in Mammalian Cells. *Science* **322**, 703-709, doi:10.1126/science.1160058 (2008).

33 Upender, M. B. *et al.* Chromosome Transfer Induced Aneuploidy Results in Complex Dysregulation of the Cellular Transcriptome in Immortalized and Cancer Cells. *Cancer Research* **64**, 6941-6949, doi:10.1158/0008-5472.can-04-0474 (2004).

34 Torres, E. M. *et al.* in *Cell* Vol. 143 71-83 (Cell Press, 2010).

35 Tolliday, N., Pitcher, M. & Li, R. in *Mol. Biol. Cell* Vol. 14 798-809 (2003).

36 Chen, G., Bradford, W. D., Seidel, C. W. & Li, R. Hsp90 stress potentiates rapid cellular adaptation through induction of aneuploidy. *Nature* **482**, 246–250 (2012).

37 Sheltzer, J. M. *et al.* Aneuploidy Drives Genomic Instability in Yeast. *Science* **333**, 1026-1030, doi:10.1126/science.1206412 (2011).

38 Eyre-Walker, A. & Keightley, P. D. The distribution of fitness effects of new mutations. *Nat Rev Genet* **8**, 610-618 (2007).

39 Geiger, T., Cox, J. & Mann, M. Proteomic Changes Resulting from Gene Copy Number Variations in Cancer Cells. *PLoS Genet* **6**, e1001090 (2010).

40 Hanahan, D. & Weinberg, R. A. The Hallmarks of Cancer. *Cell* **100**, 57-70 (2000).

41 Roper, R. J. & Reeves, R. H. Understanding the Basis for Down Syndrome Phenotypes. *PLoS Genet* **2**, e50 (2006).

42 Merlo, L. M. F., Pepper, J. W., Reid, B. J. & Maley, C. C. Cancer as an evolutionary and ecological process. *Nat Rev Cancer* **6**, 924-935 (2006).

43 Heng, H. H. Q. *et al.* Genetic and epigenetic heterogeneity in cancer: A genome-centric perspective. *Journal of Cellular Physiology* **220**, 538-547, doi:10.1002/jcp.21799 (2009).

44 Holland, A. J. & Cleveland, D. W. Boveri revisited: chromosomal instability, aneuploidy and tumorigenesis. *Nat Rev Mol Cell Biol* **10**, 478-487 (2009).

45 Grimwade, D. *et al.* The Importance of Diagnostic Cytogenetics on Outcome in AML: Analysis of 1,612 Patients Entered Into the MRC AML 10 Trial. *Blood* **92**, 2322-2333 (1998).

46 Le Beau, M. M., Bitts, S., Davis, E. M. & Kogan, S. C. Recurring chromosomal abnormalities in leukemia inPML-RARA transgenic mice parallel human acute promyelocytic leukemia. *Blood* **99**, 2985-2991, doi:10.1182/blood.V99.8.2985 (2002).

47 Jones, L. *et al.* Gain of MYC underlies recurrent trisomy of the MYC chromosome in acute promyelocytic leukemia. *The Journal of Experimental Medicine* **207**, 2581-2594, doi:10.1084/jem.20091071 (2010).

48 Hasle, H., Clemmensen, I. H. & Mikkelsen, M. Risks of leukaemia and solid tumours in individuals with Down's syndrome. *The Lancet* **355**, 165-169 (2000).

49 Yang, Q., Rasmussen, S. A. & Friedman, J. M. Mortality associated with Down's syndrome in the USA from 1983 to 1997: a population-based study. *The Lancet* **359**, 1019-1025 (2002).

50 Zipursky, A., Brown, E. J., Christensen, H. & Doyle, J. Transient myeloproliferative disorder (transient leukemia) and hematologic manifestations of Down syndrome. *Clin Lab Med* **19**, 157-167, vii (1999).

51 Kirsammer, G. *et al.* Highly penetrant myeloproliferative disease in the Ts65Dn mouse model of Down syndrome. *Blood* **111**, 767-775, doi:10.1182/blood-2007-04-085670 (2008).

52 Ng, A. P. *et al.* Trisomy of Erg is required for myeloproliferation in a mouse model of Down syndrome. *Blood* **115**, 3966-3969, doi:10.1182/blood-2009-09-242107 (2010).

53 Navin, N. *et al.* Tumour evolution inferred by single-cell sequencing. *Nature* **472**, 90-94, doi:http://www.nature.com/nature/journal/v472/n7341/abs/10.1038-nature09807-unlocked.html#supplementary-information (2011).

54 Yuen, K. W. Y. *et al.* Systematic genome instability screens in yeast and their potential relevance to cancer. *Proceedings of the National Academy of Sciences* **104**, 3925-3930, doi:10.1073/pnas.0610642104 (2007).

55 Stirling, P. C. *et al.* The Complete Spectrum of Yeast Chromosome Instability Genes Identifies Candidate CIN Cancer Genes and Functional Roles for ASTRA Complex Components. *PLoS Genet* **7**, e1002057 (2011).

56 Sotillo, R. *et al.* Mad2 Overexpression Promotes Aneuploidy and Tumorigenesis in Mice. *Cancer Cell* **11**, 9-23 (2007).

57 Hanks, S. *et al.* Constitutional aneuploidy and cancer predisposition caused by biallelic mutations in BUB1B. *Nat Genet* **36**, 1159-1161 (2004).

58 Snape, K. *et al.* Mutations in CEP57 cause mosaic variegated aneuploidy syndrome. *Nat Genet* **43**, 527-529 (2011).

59 Weaver, B. A. A., Silk, A. D., Montagna, C., Verdier-Pinard, P. & Cleveland, D. W. Aneuploidy Acts Both Oncogenically and as a Tumor Suppressor. *Cancer Cell* **11**, 25-36 (2007).

60 Putkey, F. R. *et al.* Unstable Kinetochore-Microtubule Capture and Chromosomal Instability Following Deletion of CENP-E. *Developmental Cell* **3**, 351-365 (2002).

61 Duncan, A. W. *et al.* The ploidy conveyor of mature hepatocytes as a source of genetic variation. *Nature* **467**, 707-710, doi:http://www.nature.com/nature/journal/v467/n7316/abs/nature09414.html#supplementary-information (2010).

62 Stemmann, O., Neidig, A., KÃcher, T., Wilm, M. & Lechner, J. Hsp90 enables Ctf13p/Skp1p to nucleate the budding yeast kinetochore. *Proceedings of the National Academy of Sciences of the United States of America* **99**, 8585-8590 (2002).

63 Davies, A. E. & Kaplan, K. B. Hsp90-Sgt1 and Skp1 target human Mis12 complexes to ensure efficient formation of kinetochore-microtubule binding sites. *The Journal of Cell Biology* **189**, 261-274 (2010).

64 Rosenberg, S. M. Evolving responsively: adaptive mutation. *Nat Rev Genet* **2**, 504-515 (2001).

65 Spencer, F., Gerring, S. L., Connelly, C. & Hieter, P. Mitotic Chromosome Transmission Fidelity Mutants in Saccharomyces cerevisiae. *Genetics* **124**, 237-249 (1990).

66 Sharma, S. V., Agatsuma, T. & Nakano, H. Targeting of the protein chaperone, HSP90, by the transformation suppressing agent, radicicol. *Oncogene* **16**, 2639-2645, doi:10.1038/sj.onc.1201790 (1998).

67 Bohen, S. P. Genetic and Biochemical Analysis of p23 and Ansamycin Antibiotics in the Function of Hsp90-Dependent Signaling Proteins. *Mol. Cell. Biol.* **18**, 3330-3339 (1998).

68 Jarosz, D. F. & Lindquist, S. Hsp90 and Environmental Stress Transform the Adaptive Value of Natural Genetic Variation. *Science* **330**, 1820-1824, doi:10.1126/science.1195487 (2010).

69 Taipale, M., Jarosz, D. F. & Lindquist, S. HSP90 at the hub of protein homeostasis: emerging mechanistic insights. *Nat Rev Mol Cell Biol* **11**, 515-528 (2010).

70 McClellan, A. J. *et al.* Diverse Cellular Functions of the Hsp90 Molecular Chaperone Uncovered Using Systems Approaches. *Cell* **131**, 121-135 (2007).

71 Specchia, V. *et al.* Hsp90 prevents phenotypic variation by suppressing the mutagenic activity of transposons. *Nature* **463**, 662-665 (2010).

72 Gardner, R. D. *et al.* The Spindle Checkpoint of the Yeast Saccharomyces cerevisiae Requires Kinetochore Function and Maps to the CBF3 Domain. *Genetics* **157**, 1493-1502 (2001).

73 Niikura, Y. *et al.* 17-AAG, an Hsp90 inhibitor, causes kinetochore defects: a novel mechanism by which 17-AAG inhibits cell proliferation. *Oncogene* **25**, 4133-4146 (2006).

74 Lewontin, R. C. The Units of Selection. *Annual Review of Ecology and Systematics* **1**, 1-18, doi:10.1146/annurev.es.01.110170.000245 (1970).

75 Chen, G., Rubinstein, B. & Li, R. Whole chromosome aneuploidy: Big mutations drive adaptation by phenotypic leap. *BioEssays* **34**, 893-900, doi:10.1002/bies.201200069 (2012).

76 Ni, M. *et al.* Unisexual and Heterosexual Meiotic Reproduction Generate Aneuploidy and Phenotypic Diversity <italic>De Novo</italic> in the Yeast <italic>Cryptococcus neoformans</italic>. *PLoS Biol* **11**, e1001653, doi:10.1371/journal.pbio.1001653 (2013).

77 Marichal, P. *et al.* Molecular biological characterization of an azole-resistant Candida glabrata isolate. *Antimicrobial Agents and Chemotherapy* **41**, 2229-2237 (1997).

78 Ubeda, J.-M. *et al.* Modulation of gene expression in drug resistant Leishmania is associated with gene amplification, gene deletion and chromosome aneuploidy. *Genome Biology* **9**, R115 (2008).

79 Leprohon, P. *et al.* Gene expression modulation is associated with gene amplification, supernumerary chromosomes and chromosome loss in antimony-resistant Leishmania infantum. *Nucleic Acids Research* **37**, 1387-1399, doi:10.1093/nar/gkn1069 (2009).

80 Mannaert, A., Downing, T., Imamura, H. & Dujardin, J.-C. Adaptive mechanisms in pathogens: universal aneuploidy in Leishmania. *Trends in Parasitology* **28**, 370-376, doi:http://dx.doi.org/10.1016/j.pt.2012.06.003 (2012).

81 Llewellyn, M. S. *et al.* Extraordinary Trypanosoma cruzi diversity within single mammalian reservoir hosts implies a mechanism of diversifying selection. *International Journal for Parasitology* **41**, 609-614 (2011).

82 Minning, T., Weatherly, D. B., Flibotte, S. & Tarleton, R. Widespread, focal copy number variations (CNV) and whole chromosome aneuploidies in Trypanosoma cruzi strains revealed by array comparative genomic hybridization. *BMC Genomics* **12**, 139 (2011).

83 Davoli, T. *et al.* Cumulative Haploinsufficiency and Triplosensitivity Drive Aneuploidy Patterns and Shape the Cancer Genome. *Cell* **155**, 948-962, doi:10.1016/j.cell.2013.10.011 (2013).

84 Wang, Y. *et al.* Clonal evolution in breast cancer revealed by single nucleus genome sequencing. *Nature* **advance online publication**, doi:10.1038/nature13600

http://www.nature.com/nature/journal/vaop/ncurrent/abs/nature13600.html#supplementary-information (2014).

85 Harrison, B. D. *et al.* A Tetraploid Intermediate Precedes Aneuploid Formation in Yeasts Exposed to Fluconazole. *PLoS Biol* **12**, e1001815, doi:10.1371/journal.pbio.1001815 (2014).

86 Burrell, R. A., McGranahan, N., Bartek, J. & Swanton, C. The causes and consequences of genetic heterogeneity in cancer evolution. *Nature* **501**, 338-345, doi:10.1038/nature12625 (2013).

87 Maley, C. C. *et al.* Genetic clonal diversity predicts progression to esophageal adenocarcinoma. *Nat Genet* **38**, 468-473 (2006).

88 Lee, A. J. X. *et al.* Chromosomal Instability Confers Intrinsic Multidrug Resistance. *Cancer Research* **71**, 1858-1870, doi:10.1158/0008-5472.can-10-3604 (2011).

89 Sotillo, R., Schvartzman, J.-M., Socci, N. D. & Benezra, R. Mad2-induced chromosome instability leads to lung tumour relapse after oncogene withdrawal. *Nature* **464**, 436-440, doi:http://www.nature.com/nature/journal/v464/n7287/suppinfo/nature08803_S1.html (2010).

90 Gerlinger, M. *et al.* Intratumor Heterogeneity and Branched Evolution Revealed by Multiregion Sequencing. *New England Journal of Medicine* **366**, 883-892, doi:doi:10.1056/NEJMoa1113205 (2012).

91 Oromendia, A. B. & Amon, A. Aneuploidy: implications for protein homeostasis and disease. *Disease Models & Mechanisms* **7**, 15-20, doi:10.1242/dmm.013391 (2014).

92 Sheltzer, J. M., Torres, E. M., Dunham, M. J. & Amon, A. Transcriptional consequences of aneuploidy. *Proceedings of the National Academy of Sciences* **109**, 12644-12649, doi:10.1073/pnas.1209227109 (2012).

93 Zhu, J., Pavelka, N., Bradford, W. D., Rancati, G. & Li, R. Karyotypic Determinants of Chromosome Instability in Aneuploid Budding Yeast. *PLoS Genet* **8**, e1002719, doi:10.1371/journal.pgen.1002719 (2012).

94 Charles, J. S., Hamilton, M. L. & Petes, T. D. Meiotic Chromosome Segregation in Triploid Strains of Saccharomyces cerevisiae. *Genetics* **186**, 537-550, doi:10.1534/genetics.110.121533 (2010).

95 Lum, P. Y. *et al.* in *Cell* Vol. 116 121-137 (2004).

96 Singh, A., Ursic, D. & Davies, J. Phenotypic suppression and misreading in Saccharomyces cerevisiae. *Nature* **277**, 146-148 (1979).

97 Ho, C. H. *et al.* in *Nat Biotech* Vol. 27 369-377 (Nature Publishing Group, 2009).

98 Ghaemmaghami, S. *et al.* Global analysis of protein expression in yeast. *Nature* **425**, 737-741, doi:http://www.nature.com/nature/journal/v425/n6959/suppinfo/nature02046_S1.html (2003).

99 Oromendia, A. B., Dodgson, S. E. & Amon, A. Aneuploidy causes proteotoxic stress in yeast. *Genes & Development* **26**, 2696-2708, doi:10.1101/gad.207407.112 (2012).

100 Borovinskaya, M. A., Shoji, S., Fredrick, K. & Cate, J. H. D. Structural basis for hygromycin B inhibition of protein biosynthesis. *RNA* **14**, 1590-1599, doi:10.1261/rna.1076908 (2008).

101 Selmecki, A. M., Dulmage, K., Cowen, L. E., Anderson, J. B. & Berman, J. Acquisition of Aneuploidy Provides Increased Fitness during the Evolution of Antifungal Drug Resistance. *PLoS Genet* **5**, e1000705, doi:10.1371/journal.pgen.1000705 (2009).

102 Marr, K. A., White, T. C., van Burik, J.-A. H. & Bowden, R. A. Development of Fluconazole Resistance in Candida albicans Causing Disseminated Infection in a Patient Undergoing Marrow Transplantation. *Clinical Infectious Diseases* **25**, 908-910, doi:10.1086/515553 (1997).

103 Okoli, I. *et al.* Identification of Antifungal Compounds Active against <italic>Candida albicans</italic> Using an Improved High-Throughput <italic>Caenorhabditis elegans</italic> Assay. *PLoS ONE* **4**, e7025, doi:10.1371/journal.pone.0007025 (2009).

104 Spitzer, M. *et al.* Cross-species discovery of syncretic drug combinations that potentiate the antifungal fluconazole. *Mol Syst Biol* **7**, doi:http://www.nature.com/msb/journal/v7/n1/full/msb201131.html (2011).

105 Tang, Y.-C., Williams, B. R., Siegel, J. J. & Amon, A. Identification of Aneuploidy-Selective Antiproliferation Compounds. *Cell* (2011).

106 Kaelin, W. G. The Concept of Synthetic Lethality in the Context of Anticancer Therapy. *Nat Rev Cancer* **5**, 689-698 (2005).

107 Luo, J. *et al.* A Genome-wide RNAi Screen Identifies Multiple Synthetic Lethal Interactions with the Ras Oncogene. *Cell* **137**, 835-848, doi:10.1016/j.cell.2009.05.006 (2009).

108 Smith, T. C., Kinkel, A. W., Gryczko, C. M. & Goulet, J. R. Absorption of pyrvinium pamoate. *Clin Pharmacol Ther* **19**, 802-806 (1976).

109 Center for Disease Control and Prevention, U. Fungal disease statistics. (2014).

110 Nucci, M. & Anaissie, E. Revisiting the Source of Candidemia: Skin or Gut? *Clinical Infectious Diseases* **33**, 1959-1967, doi:10.1086/323759 (2001).

111 Boveri, T. in *J Cell Sci* Vol. 121 1-84 (2008).

112 Davoli, T. *et al.* Cumulative Haploinsufficiency and Triplosensitivity Drive Aneuploidy Patterns and Shape the Cancer Genome. *Cell* (2013).

113 Barretina, J. *et al.* The Cancer Cell Line Encyclopedia enables predictive modelling of anticancer drug sensitivity. *Nature* **483**, 603-307, doi:http://www.nature.com/nature/journal/v483/n7391/abs/nature11003.html#supplementary-information (2012).

114 Garnett, M. J. *et al.* Systematic identification of genomic markers of drug sensitivity in cancer cells. *Nature* **483**, 570-575, doi:http://www.nature.com/nature/journal/v483/n7391/abs/nature11005.html#supplementary-information (2012).

115 Heiser, L. M. *et al.* Subtype and pathway specific responses to anticancer compounds in breast cancer. *Proceedings of the National Academy of Sciences* **109**, 2724-2729, doi:10.1073/pnas.1018854108 (2012).

116 Daemen, A. *et al.* Modeling precision treatment of breast cancer. *Genome Biology* **14**, R110 (2013).

117 Bredel, M. *et al.* A network model of a cooperative genetic landscape in brain tumors. *JAMA* **302**, 261-275, doi:302/3/261 [pii]

10.1001/jama.2009.997 (2009).

118 Network, T. C. G. A. R. Comprehensive genomic characterization defines human glioblastoma genes and core pathways. *Nature* **455**, 1061-1068 (2008).

119 Sottoriva, A. *et al.* Intratumor heterogeneity in human glioblastoma reflects cancer evolutionary dynamics. *Proceedings of the National Academy of Sciences*, doi:10.1073/pnas.1219747110 (2013).

120 Bouchonville, K., Forche, A., Tang, K. E. S., Selmecki, A. & Berman, J. Aneuploid Chromosomes Are Highly Unstable during DNA Transformation of Candida albicans. *Eukaryotic Cell* **8**, 1554-1566 (2009).

121 Hieter, P., Mann, C., Snyder, M. & Davis, R. W. Mitotic stability of yeast chromosomes: A colony color assay that measures nondisjunction and chromosome loss. *Cell* **40**, 381-392 (1985).

122 Gerring, S. L., Spencer, F. & Hieter, P. The CHL 1 (CTF 1) gene product of Saccharomyces cerevisiae is important for chromosome transmission and normal cell cycle progression in G2/M. *EMBO J* **9**, 4347-4358 (1990).

123 Shero, J. H. *et al.* Analysis of chromosome segregation in Saccharomyces cerevisiae. *Methods in Enzymology*, 749-773 (1991).

124 Huh, W.-K. *et al.* Global analysis of protein localization in budding yeast. *Nature* **425**, 686-691 (2003).

125 Sinibaldi, R., O'Connell, C., Seidel, C. & Rodriguez, H. Gene expression analysis on medium-density oligonucleotide arrays. *Methods Mol Biol* **170**, 211-222, doi:10.1385/1-59259-234-1:211 [doi] (2001).

126 Smyth, G. K. Linear models and empirical bayes methods for assessing differential expression in microarray experiments. *Stat Appl Genet Mol Biol* **3**, Article3, doi:10.2202/1544-6115.1027 [doi] (2004).

127 Toussaint, M. & Conconi, A. High-throughput and sensitive assay to measure yeast cell growth: a bench protocol for testing genotoxic agents. *Nat. Protocols* **1**, 1922-1928 (2006).

128 Haase, S. B. & Reed, S. I. Improved Flow Cytometric Analysis of the Budding Yeast Cell Cycle. *Cell Cycle* **1**, 117-121 (2002).

129 Longtine, M. S. *et al.* in *Yeast* Vol. 14 953-961 (John Wiley & Sons, Ltd., 1998).

130 Gietz, R. D. & Schiestl, R. H. High-efficiency yeast transformation using the LiAc/SS carrier DNA/PEG methed. *Nat. Protocols* **2**, 31-34 (2007).

131 Ho, C. H. *et al.* A molecular barcoded yeast ORF library enables mode-of-action analysis of bioactive compounds. *Nat Biotech* **27**, 369-377, doi:http://www.nature.com/nbt/journal/v27/n4/suppinfo/nbt.1534_S1.html (2009).

132 Tong, A. H. *et al.* Systematic genetic analysis with ordered arrays of yeast deletion mutants. *Science* **294**, 2364-2368, doi:10.1126/science.1065810 (2001).

133 Muehlbauer, P. A. & Schuler, M. J. in *Mutation Research/Genetic Toxicology and Environmental Mutagenesis* Vol. 585 156-169 (2005).

Appendix 1: Methods for Chapter 2

Plasmids

pRLB473, a pRS305 based plasmid, was constructed to integrate an additional copy of *STI1* into the original locus and it was cloned as follows. Primers Cp073 and Cp074 were used to amplify a fragment of DNA by PCR from budding yeast genomic DNA, containing the *STI1* ORF and upstream/downstream sequences. This fragment was further amplified by using primers Cp078 and Cp079 to add a Not I cutting site to 5' and a Xho I to 3'. After restriction enzyme digestion, the fragment was inserted into pRS305. pRLB474, a pRS303 based plasmid, was constructed to integrate an additional copy of *PDR5* into the original locus. Primers Cp057 and Cp058 were used to PCR-amplify a fragment of DNA from budding yeast genome, containing the *PDR5* ORF and upstream/downstream sequences. This fragment was further amplified by Cp059 and Cp060 to add Not I to 5' and Xho I to 3', and inserted into pRS303. The above plasmids were sequenced to verify the absence of mutations in the ORF, by using primers Cs10-Cs18 and Cs21-Cs23.

Media

YPD media were made by mixing 10g Bacto-yeast extract (#212720), 20g Bacto-peptone (#211830), 20g Bacto-agar (#214010) together with 950ml water, autoclaved and adding 50ml 40% glucose. After cooled to 60-65 ^{o}C, YPD was supplemented with 1% (v/v) DMSO or drugs dissolved in DMSO, and the plates were poured.

***Saccharomyces cerevisiae* strains**

Standard techniques were used for yeast transformations. *STI1* and *PDR5* were deleted in Chr XV trisomy strain as follows. RLY6673, the Rad^{r} 3 in radicicol adaptation experiment with gain of only Chr XV, was streaked out from glycerol stock and karyotype-confirmed by qPCR. To delete one copy of *STI1,* Cp027

and Cp028 were used to amplify the *HPH* gene, a hygromycin resistance marker, from a pFA6a backbone plasmid. A DNA fragment with the marker and 45bp homologous sequences flanking the upstream and downstream of *STI1* was thus generated. RLY6673 was transformed with this fragment to generate RLY7011 where one copy of *STI1* was deleted by homologous recombination. To delete one copy of *PDR5*, Cp065 and CP066 were used following the same procedure as described above for *STI1* deletion. All deletions were verified by genomic PCR. As a previous report suggests transformation itself may induce aneuploidy [120], the karyotypes of the transformants were reconfirmed by qPCR karyotyping assay, and the ones retaining the original karyotype (Chr XV trisomy) were selected.

To integrate one copy of *STI1* into a haploid genome, RLB473 was linearized at BglII site and used to transform RLY2626. RLY2626 is a meiotic progeny with the *a* mating type of the diploid strain RLY2628 used in radicicol adaptation experiment. The integration of one copy *STI1* was verified by qPCR of genomic DNA using primers Cp088 and Cp089, yielding RLY7111. To integrate one copy of *PDR5* into RLY2627, a meiotic progeny with the α mating type of diploid RLY2628, RLB473 was linearized at SalI site before transformation. The integration of one copy *PDR5* was verified by DNA qPCR using primers Cp090 and Cp091, yielding RLY7114. RLY7111 was then crossed with RLY2627 to generate RLY7147, an a/α diploid strain with one additional copy of *STI1*. RLY7114 was crossed with RLY2626 to generate RLY7149, an a/α diploid strain with one additional copy of *PDR5*. RLY7111 was crossed with RLY7114 to construct RLY7148, an a/α diploid strain with one additional copy of both *STI1* and *PDR5*.

Colony color assay for detecting CF loss induced by diverse stresses

The CF is mostly a fragment of yeast Chr III, containing the left arm, the centromere, telomeres, and autonomous replication sequences [65]. It also contains *SUP11* and *URA3* marker on the right short arm. The transmission fidelity of the artificial chromosome was monitored by colony color. The background

haploid strain carries an ochre *ade2* mutation, *ade2-101*, and confers a red colony phenotype. This red pigment accumulation can be suppressed by *SUP11*, carried on the CF, generating a white colony phenotype. Chromosome loss events are manifested by the appearance of red colonies [54,121] .

White colonies with CF (RLY4029) from YPD plates were used to inoculate overnight cultures in the -ura synthetic complete (SC) media grown 30°C. The culture was then diluted to OD_{600} 0.1 in SC–ura media and grown for 6 more hours. The cells were then transferred to YPD media at the initial OD_{600} of 0.2 containing either vehicle control (1% DMSO) or different stress reagents. The cultures were incubated for 14-16 hours at 30°C and final OD was recorded. Yeast cells were diluted to an appropriate density (determined in pilot experiments) and plated onto YPD plates. After 3 days of incubation at 30°C, the plates were moved to cold room (4°C) to allow accumulation of red pigment for easy visualization. Total and red colony number were recorded. Due to the large number of plates, this experiment was performed in two batches with data combined.

Estimating chromosome loss rate (γ) from red colony frequency (α)

In order to estimate the chromosome loss rate (γ) per cell cycle, following parameters were measured:

b: The initial background frequency of rare cells giving rise to red colonies in -ura culture. To determine b, white cells with CF were cultured in SC-ura overnight and directly plated onto YPD plates. In 19608 colonies counted, 12 colonies were found to be red, so the frequency of red cells in SC–ura culture was estimated to be 0.06%.

n: The number of cell cycle in the liquid YPD media containing stress inducing agents or vehicle.

n was estimated from OD reading, as

$$n = \log_2(\frac{OD_{final}}{OD_{initial}})$$

α: The red colony frequency, which represents the percentage of the red colonies on the YPD plates after the incubation with vehicle or stress-inducing agents.

$$\alpha = \frac{R_n}{R_n + W_n} = 1 - \frac{W_n}{T_n},$$

where, W_n = the number of white cells, R_n =The number of red cells, and T_n= The total number of cells, at generation n.

As $W_x = (2-\gamma)W_{x-1}$, where γ = CF loss rate /division, it can be derived that $W_n = (2-\gamma)^n W_0$

Given $T_n = 2^n T_0$,

α can be expressed as:

$$\alpha = 1 - \frac{W_n}{T_n} = 1 - \frac{(2-\gamma)^n W_0}{2^n T_0}$$
$$= 1 - (1 - \frac{\gamma}{2})^n \frac{W_0}{T_0}$$

When γ<<1, the above expression can be approximated as:

$$\alpha \approx 1 - (1 - \frac{n\gamma}{2}) \frac{W_0}{T_0}$$

As the initial background frequency of rare red cells in SC-ura culture, b, can be expressed as:

$$b = \frac{R_0}{T_0} = 1 - \frac{W_0}{T_0}$$
$$\Rightarrow \frac{W_0}{T_0} = 1 - b$$

and thus,

$$\alpha = 1 - (1 - \frac{n\gamma}{2})(1 - b)$$

Resolving the above equation, the chromosome loss rate (γ) can be expressed as:

$$\gamma = \frac{2(\alpha - b)}{n(1 - b)}$$

As $b=0.6\times10^{-3}<<1$, $\gamma = \frac{2(\alpha - b)}{n}$

Using the above model, the loss rate of CF in YPD with vehicle control is computed to be 2.1×10^{-4}/division, similar to previous estimations based on sectoring assays [122,123].

Colony color assay for detecting heat-shock induced CF loss

RLY4029 (CF containing) cells cultured overnight in SC-ura media were transferred to YPD and OD adjusted to 0.5. 40µl aliquots of the resulting culture were tranferred into PCR tubes and heat-shocked for 90s. The cultures were then cooled down to 23 °C. 600 untreated cells or 6,000 heat-shocked cells were plated onto YPD plates. More heat-shocked cells were plated due to the high lethality. After 3 days of incubation at 30°C, the plates were moved to cold room (4°C) to facilitate red pigment accumulation.

Imaging analysis of Ndc10-GFP and Cep3-GFP localization after radicicol treatment

Yeast strains with C-terminal GFP tagging on *NDC10* or *CEP3* genes were retrieved from the GFP ORF tagging library [124]. All cultures were grown at 30 °C. Both strains were cultured overnight in SC media and dilute to OD 0.1 and further grown for 3 hours. The OD was again adjusted to 0.1 immediately prior to the addition of 1% Dimethyl sulfoxide (DMSO, vehicle control), 10 μg/ml radicicol or 100 μg/ml radicicol (final concentrations). After 4-6 hours incubations, Z-stack images were taken with an inverted Zeiss 200 m outfitted with a spinning-disc confocal system (Yokagawa) and an EM-CCD (Hamamatsu C9100), using a 100x oil objective lens.

To measure the intensity of the dot-like kinetochore localization of GFP signals, only large-budded anaphase cells with two distinct dots per cell were included, as prior to anaphase, the kinetochore signal varies depending on the status of DNA replication. Extraction of data from images was performed by Image J software. The background was first subtracted. For cells within the central field of the image, a circle slightly larger than a normal dot was specified, where average fluorescence intensity was measured. The same circle was used for all measurements.

Since at 100μg/ml radicicol, a large proportion of cells failed to localize Cep3 to the kinetochore, cells were scored for the presence of the Cep3-GFP or Ndc10-GFP kinetochore localization to distinguish cells with discrete dot-like GFP localization on kinechore from the ones with diffuse localization.

Selection for radicicol resistant yeast colonies

~600 diploid RLY2628 cells were plated onto plates containing 100 μg/ml radicicol (1st drug pate) while 10 fold fewer (~60) RLY2628 cells were plated onto plates with vehicle control. At this radicicol

concentration the cell survival rate as measured by colony formation was ~7%. After 7 days incubation at 30 ^{o}C, 3 largest colonies from each plate were picked and cultured, for roughly 5 generations, in drug-free YPD media overnight until saturation. This step was designed to diminish adaptation through non-genetic changes. The cultures were then plated again at ~400 cells/plate onto YPD media with radicicol (2nd drug plate) to re-test their drug resistance. After 3 days incubation at 30 ^{o}C, the images were taken. One colony randomly picked from each of triplicate of the 2nd drug plate was subjected to comparative genomic hybridization (CGH).

Comparative Genomic Hybridization

Array construction and hybridization were carried out as described previously [125]. The arrays consisted of 23.3k 70-mer custom oligonucleotides designed to tile the yeast genome with an average spacing of 528 bp. Genomic DNA was extracted using YeaStar™ Genomic DNA Kit (Zymoresearch), and then labeled for array analysis using the BioPrime Plus Array CGH Kit (Invitrogen). Data analysis was performed with the R programming language. Array intensities were background subtracted and normalized using the loess method from the limma package [126]. After global normalization, probe groups representing each chromosome were further adjusted by dividing each by the median of all chromosomes. The karyotype for each chromosome was determined by the median log2(test strain/wt) for all probes representing that chromosome. For visualization, the data were then sorted by chromosomal position and smoothed using a running median with a window size of 7 probes.

Quantitative growth Assays

The quantitative growth assays were performed with a previously reported protocol[127]. Cells were cultured to saturation in YPD or SC-His+100μg/ml G418 (used for genetically constructed Chr XV disomy and the control euploid strains[1]) and then were dilute 100 times into YPD with either vehicle control or drug (such as radicicol or tunicamycin)-containing media and split into 4 independent cultures as replicates. The 96-well or 48-well plate (Falcon) was filled with 100μl liquid and sealed with parafilm. The optical density (OD) at 595nm was continuously monitored at 30 ^{o}C using a Tecan Infinite M200 Pro. The data were extracted and analyzed by Magellan 7 software. For growth assay on strains with a known aneuploidy karyotype, each strain was streaked into single colonies and karyotyped again right before growth assay to make sure that the tested strains retained the original karyotype.

Determination of karyotype diversity caused by short-term radicicol treatment

All incubations were performed at 30 ^{o}C. RLY6864, a diploid strain in the same background as the CF strain was cultured in YPD overnight to reach saturation, diluted in fresh YPD and grown to OD 0.5. The cultures were then diluted to OD 0.05 in YPD media with 20μg/ml radicicol or vehicle control (1% DMSO). After 24 hours, the culture reached saturation and was diluted 100x and cultured further. The next day, the cultures were plated on YPD plates without drug to form single colonies, which were karyotyped by DNA qPCR.

Flow cytometry analysis of DNA content

A protocol optimized from that previously reported[128] was used to process yeast cells for DNA analysis by flow cytometry with improved ploidy resolution and throughput. As the purpose of this analysis was to identify changes in ploidy, cells were grown to saturation. The cells were harvested,

washed once with water, and fixed in 70% ethanol in a 96-well plate for 1 hour. Samples were then transferred into a 96-well polypropylene filter (Whatman), where the ethanol was removed by vacuum and the cells washed twice with water. 100 μl 2mg/ml RNase (Sigma) solution was then added to remove the RNA. After 2 hour incubation, 5mg/ml trypsin (Sigma) was added to digest the protein thoroughly. This procedure continued overnight at 37 ^{o}C and was the key for much improved DNA peak resolution over previous protocols. The cells were then washed in 50mM Tris 7.5 buffer and sonicated. 2μM Sytox Green dye (Invitrogen) was added to stain the DNA. The data was collected with the FITC channel on an Influx cytometer (BD Biosciences), and analyzed by Flowjo.

Karyotyping yeast cells by DNA qPCR

The detailed protocol used to karyotype yeast cells by DNA qPCR has been described elsewhere [28]. Briefly, a pair of qPCR primers was designed for each of the 2 pericentromeric regions flanking every centromere. By measuring the relative copy number of these pericentromeric DNA fragments through DNA qPCR in comparison to a known euploid strain, the number of each chromosome was determined.

Testing the adaptability of the population with karyotype diversity induced by Hsp90 stress

The initial pre-treatment process was essentially the same as described in the short-term radicicol treatment. Three lines of independent cultures were established, each from a single colony and split into

two groups: one with 20μg/ml radicicol, the other with 1% DMSO control. After the karyotype diversity was generated, each line of culture was washed with YPD 3 times and then diluted 100x in YPD without any drug. This recovery step lasted for 24 hours to recover from any non-genetic effects caused by radicicol pre-treatment. The cells were then plated either at 40,000 cells/plate onto new stress plates or at 40 cells/plate onto control YPD plates with 1% DMSO. The plates were incubated at 30 ^{o}C for around 7 days.

The plates were imaged by using a scanner (HP Scanjet 4070) and colony number and sizes recorded using an automatic colony identification software - imageQuantTL. All the colonies formed under the same stress conditions were ranked according to their sizes.

Assays to test the linkage between Chr XVI monosomy and tunicamycin resistance

Strain V-Tun-1a and V-Tun-1b were streaked out from glycerol stock into single colonies. From passage 1, one small colonies of each strain were karyotyped by qPCR and patched on YPD plates so that high density of cell colonies can form to enrich the rare big colonies. The patches were further streaked out to single colonies.

Single colonies with different sizes were karyotyped by qPCR. Colony growth was characterized right after karyotyping by both colony formation on solid plates and growth curve in liquid media. For colony formation assay, a portion of the fresh colonies were directly plated onto YPD plates with vehicle control or 2.5μg/ml tunicamycin at the same density of ~50 cells/plate. The plates were incubated in 30 ^{o}C for around 7 days before images were taken. Meanwhile, a small portion of colonies were cultured in YPD to saturation, karyotyped by qPCR again and then diluted 100x into YPD with either vehicle control

or 2.5µg/ml tunicamycin. 4 replicates of each colony from each condition were monitored for the growth by using a Tecan Infinite M200 Pro reader, as described above.

Appendix 2: Methods for Chapter 3

I. Strains and genetic manipulations

Plasmids construction

Plasmids used in this study are listed in Table S2 pGC881-883 were pRS306 based plasmids; constructed to integrate an additional copy of *TRM11*, *CRS5, and RPS15* into the original locus in the yeast genome. Primers WMG61 and WMG62 were used to amplify the ORFs using respective plasmids from MOBY-ORF collection. These PCR amplified ORFs were inserted into EcoRI digested pRS306 using In-Fusion® HD Cloning Kit (Cat. # 638909). Primers WMG37 and WMG38 were used to verify the absence of mutations in the ORF of plasmids PGC881-883. pGC884 was a MOBY-ORF library plasmid without ORF.

***Saccharomyces cerevisiae* strains**

Strains used in this study are listed in Table S1. Standard techniques were used for yeast transformations and deletion[129,130]. RLY8338 and RLY8410 were derived by transforming pGC884 into RLY2628 and RLY6673 respectively. RLY8344, RLY8345, RLY8411, RLY8412, RLY8415 and RLY 8416 were derived by transforming RLY2628 with a MOBY-ORF library plasmid containing *RRP6*, *TRM11, CRS5, RPS15, SER1* and *RPS27A* respectively. To verify the absence of mutations in *RRP6*, *TRM11, CRS5 and RPS15,* ORFs used for above transformations were sequenced using primers WMG37 and WMG38. In case of *RRP6* two additional primers, WMG44 and WMG46 were used to cover entire region of the ORF. RLY8339 was derived from RLY2628 by replacing *leu2-3* with *HIS3* and used as a marker control for other strains with the *HIS3* marker. RLY8340, RLY8343, RLY8346, RLY8413, RLY8414 strains were derived from Chr XV trisomy strain as follows. RLY6673 was streaked out from glycerol stock, grown at 23°C and karyotype-confirmed by qPCR karyotyping assay. One copy of respective gene was deleted by transforming RLY6673 with a DNA fragment containing *HIS3* and 45bp homologous sequences flanking the upstream and downstream of

ORF. All deletions strains were verified by genomic PCR. The karyotype of the strains derived from RLY 6673 were reconfirmed by qPCR karyotyping assay and the ones retaining the original karyotype (Chr XV trisomy) were selected.

RLY8417 was constructed by transforming *NcoI* digested *pRS306* into *MATα* strain RLY2626. Further, integration of one copy of URA3 was verified by qPCR of genomic DNA using primers WMG63 and WMG64, based upon copy number of Ampicillin. To integrate one copy of *TRM11*, *MfeI* digested *pGC881 was* transformed into *MATα* strain RLY2627; integration was verified by qPCR of genomic DNA using primers WMG67and WMG68, resulting into RLY8419. RLY8420 was constructed by transforming *NruI* digested *pGC882* into *MATα* strain RLY2626; integration of one copy of *CRS5* was confirmed by qPCR of genomic DNA using primers WMG69 and WMG70. One copy of *RPS15* was integrated into *MATα* strain RLY2627 by transforming *BclI* digested *pGC883* and integration was verified by qPCR of genomic DNA using primers WMG71 and WMG72, resulting in RLY8421. RLY8417 and RLY8420 were crossed with haploid strain RLY2627, to generate diploid strains RLY8431 and RLY8433, containing one additional copy of *URA3* and *CRS5* respectively. RLY8419 and RLY8421 were crossed with haploid strain RLY2626, to generate diploid strains RLY8432 and RLY8434, containing one additional copy of *TRM11* and *RPS15* respectively.

MOBY library transformation for *Saccharomyces cerevisiae*

MOBY plasmid library which contains centromeric plasmids carrying individual ORFs in the yeast genome driven by respective native promoters was constructed by Charles Boone lab[131] and resourced from Thermo Open System. For Chr XV, the library covered 465 ORFs out of 529 non-dubious ones (88% coverage). MOBY ORFs-carrying *E. coli* were inoculated into 2ml Deep Well Plates containing 1.8 ml/well of LB + 5 µg/ml tetracycline, 100 µg/ml kanamycin, and 12.5 µg/ml chloramphenicol. Plates were grown overnight in a New Brunswick Scientific shaking incubator set to 220 rpm and 37°C. Following growth,

plasmids were purified using a Tecan EVO liquid handling robot and the Wizard Magnesil Tfx System (part # TB314) from Promega.

The plasmids were transformed into the diploid wild-type strain RLY2628 following the standard high-throughput transformation protocol using the robot Biomek FX. The transformants were spotted onto SD-ura plates and incubated at 30°C for 3 days. 454 out of 465 plasmids (97.6%) were successfully transformed.

II. Yeast and *C. albicans* growth and lab evolution experiments

Cell culture media

Budding yeast was cultured using standard media. *C. albicans* cells recovered from frozen glycerol stocks were grown on YPD plate. For bulk liquid culture prior to drug sensitivity assays, SC media with additional 80mg/L uridine was used. RPMI1640 + 0.165M MOPS buffer + 0.2% glucose without bicarbonate (Lonza) was used for 96-well culture according to the Clinical Laboratory and Standards Institute (CLSI) standard M27-A3. For 384 well cultures, additional 2% glucose was added to accelerate the growth. Agar plates were prepared using RPMI1640 with MOPS without bicarbonate powder (US Biological) supplemented with 2% glucose and 1.5% agarose, following the E-test strip manufacturer's guideline (bioMerieux).

Chemical reagents

Radicicol powder was purchased from AG Scientific. Hygromycin B solution (100mg/ml) was prepared by media facility at Stowers Institute for Medical Research from powder purchased from Sigma. Small batch to batch variations were noticed for hygromycin B and effective drug concentration was adjusted based

on the growth delay it causes. Effective 50 μg/ml hygromycin B in YPD causes the wild type euploid overnight growth rate to reduce 50% so that from the same initial OD, it takes twice the time for the euploid cells to reach saturation under 50 μg/ml hygromycin B compared to in drug-free media. The hygromycin B solution was aliquoted and stored in -20°C. Chemicals used in screening process are described later under the screening section.

Flow cytometry analysis of DNA content

A protocol optimized from that previously reported[36] was used to process yeast cells for DNA analysis by flow cytometry with improved ploidy resolution and throughput. As the purpose of this analysis was to identify changes in ploidy, cells were grown to saturation. The cells were harvested, washed once with water, and fixed in 70% ethanol in a 96-well plate for 1 hour. Samples were then transferred into a 96-well polypropylene filter (Whatman), where the ethanol was removed by vacuum and the cells washed twice with water. 100 μl 2mg/ml RNase (Sigma) solution was then added to remove the RNA. After 2-hour incubation, 5mg/ml trypsin (Sigma) was added to digest the protein thoroughly. This procedure continued overnight at 37 °C and was the key for much improved DNA peak resolution over previous protocols. The cells were then washed in 50mM Tris 7.5 buffer and sonicated. 2μM Sytox Green dye (Invitrogen) was added to stain the DNA. The data was collected with the FITC channel on an Influx cytometer (BD Biosciences), and analyzed by using Flowjo software.

Yeast karyotyping by DNA qPCR

The detailed protocol for karyotyping budding yeast cells by DNA qPCR has been described previously[28]. Briefly, a pair of qPCR primers was designed for each of the 2 pericentromeric regions flanking every

centromere. By measuring the relative copy number of these pericentromeric DNA fragments through DNA qPCR in comparison to a known euploid strain, the number of each chromosome was determined.

Growth assays for budding yeast

Cells were inoculated in a 96-well plate in non-stress media (YPD or SC with the appropriate selective condition) at 30°C for 24 hours. The cultures were then diluted 100 times and incubated for another 24 hours to allow all strains entering saturation. Aneuploid strains were cultured at 23°C before growth experiments, the incubation temperature was lowered to 23°C to minimize stress and the dilution factor was reduced to 10x so that all different strains can similarly reach saturation. The OD of the cultures were taken on a Tecan M200Pro reader and adjusted by OD before the growth experiment. 100x dilutions of the pre-cultures were inoculated into the media with or without different chemicals in 96-well or 384-well plate for growth profiling.

For continuous OD monitoring, cultures were set up in a 96-well sealed with parafilm and loaded into a Tecan M200Pro reader. Orbital shaking was set to 336rpm and 1.5 mm in magnitude. OD at wavelength 595nm was taken every 15 minutes and analyzed using the Magellan 7 software (Tecan). For cultures whose OD reading was taken intermittently every several hours, the plate containing the cultures were placed in non-shaking incubator within a wet chamber to keep the moisture and before each reading, the plate was agitated with a Microplate Genie (Scientific Industries Inc.) for 10 seconds. The OD at wavelength 595nm was recorded by a Tecan M200Pro reader and the data files were processed by R. The growth assays lasted until the fastest grower reached saturation, at which time the last OD readings of all strains were recorded.

The drug concentrations of hygromycin B and radicicol were adjusted for different media (e.g., YPD vs SC-ura) and/or the strain background, so that the wild-type control show the same growth

delay as was observed in YPD media contained the stated drug concentration. The growth of genetic variants was normalized to the according wild-type controls.

For quantitative growth measurement in liquid, OD readings less than 0.02 are not reliable. Thus, any OD readings lower than this threshold were adjusted to 0.02 to avoid spurious log2 values.

Growth assays of MOBY transformants with extra copies of genes located on Chr XV

Transformants of 465 MOBY plasmids carrying Chr XV genes (testing strains) along with the control strain RLY8410(diploid wild-type strain RLY 2628 transformed with an empty MOBY plasmid pGC8410) were inoculated in SC-ura media in 96-well plate and cultured in 30 °C for 24 hours to reach saturation. The cultures were diluted 100 times and grew further in the same condition for another 24 hours until all strains reached saturation. The first OD reading (time zero OD) was taken at this moment reflecting small variations in saturation OD among different transformants. The saturated cultures were then diluted 100 times into SC-ura media with MSG (monosodium glutamate) as nitrogen supplement with 35 μg/ml hygromycin B. This concentration of hygromycin B was used because it caused similar growth delay (as measured by the time it takes to grow from OD 0.05 to saturation) of the control strain to double in SC-HIS+MSG media, comparable to the effect of 50μg/ml hygromycin B on the wild type control strain in YPD media. MSG was used in the SC-ura media to replace ammonium sulfate as the latter reduces the efficacy of hygromycin B probably due to high salt concentration, which was noted previously also for G418[132].

The growth assays were performed in 384-well plates, with the strains aligned in a way such that each testing strain was neighbored by the control strain. OD readings were taken every 3-6 hours on a Tecan M200Pro reader until the control strain cultures reached saturation. Data analysis was performed using R. Several layers of normalization were performed. First, the growth of testing strains was normalized to the neighboring control strains to eliminate positional effect across the plate. Second, the growth of

testing strains was also normalized to the time zero OD to adjust for the minor variations among the initial cell mass input. Third, the Z score was calculated for the growth of each testing strains to record its deviation from the mean value of growth of all testing strains on the same plate.

$$Z_x = \frac{OD_x\text{-}Mean(OD)}{SD(OD)}$$ **SD* and *Mean* were calculated for each plate.

This step was taken because it appeared that the median growth value for testing strains varied from plate to plate and was unlikely to be driven by a biological process relevant to hygromycin B sensitivity. The Z scores were then ranked from low to high with the lowest Z-scores (negative) associated with genes whose increased dosage leads to the strongest growth inhibition by hygromycin B in the diploid context.

Top hits were picked from the yeast-transformant library and verified in 4 replicates by using a 96 well plate growth assay. The identities of the plasmids were further verified by sequencing the plasmids extracted from the transformants. The verified hits were further tested by gain and loss-of-copy number assays after gene integration or deletion.

Statistical analysis

Scatter plot, linear fitting and correlation statistical analysis were all performed using R. The GFP intensity data was downloaded from a previous publication[98] and the gene IDs were matched with those corresponding to MOBY transformants growth data using R.

Construction of and lab evolution experiments on heterogeneous aneuploid mix

Euploid pentaploid RLY6959 was sporulated in the super sporulation media, as previously described[28]. Individual tetrads were dissected and 40 viable colonies were characterized for ploidy through FACS with

28 selected with ploidy higher than 1.9N. The selected aneuploids were cultured to saturation in individual wells and then mixed. We note that inherent instability of most of the aneuploid spores[28,93] was likely to lead to further population heterogeneity. This mix was further supplemented with 10% diploid, triploid and tetraploid each to generate a heterogeneous population with diverse karyotypes and ploidies.

For evolution in the presence of radicicol, the heterogeneous mix was inoculated in either YPD or YPD with 50 μg/ml radicicol after 1/100 dilution from the saturated pre-culture. The cultures were grown at 30 °C for 4-5 days until the radicicol culture reached saturation. After the lab evolution, the cultures were diluted and plated onto YPD plate without drug to allow single colony formation. Both the liquid culture and 6 random single colonies from the radicicol culture were karyotyped.

To test if the radicicol-selected population could be extinct with the addition of hygromycin B, the Rad^r populations 1-3 from the above lab evolution experiments were recovered from glycerol stocks and colonies were combined and precultured in YPD at 23°C, as described in "Growth assays for budding yeast". Four pre-cultures (RLY2628 diploid and the Rad^r Mixes 1-3) were then inoculated into different conditions: YPD, or YPD with 50μg/ml hygromycin, 50μg/ml radicicol or both drugs together. The growth was performed in a 384-well plate with 35 μl media per well at 30°C in a humidity chamber. OD was monitored by using a Tecan M200Pro reader.

To test the effects of single and dual drugs on heterogeneous aneuploidy mix population, the drug-containing YPD media were prepared following the same procedure for screening for agents against Chr XV trisomy (see below) and kept frozen at -80°C. Additional radicicol for the combinatorial treatment was added after thawing before the experiment. Three saturated pre-cultures (RLY2628 diploid, RLY6673 Chr XV trisomy and the heterogeneous aneuploid mix) were inoculated into different media by 100 x dilution into 384-well dish with 35 μl media per well. There were 2 replicates for each condition. The incubation was maintained in 30°C in a humidity chamber. The OD readings were taken by using Tecan

M200Pro and results were analyzed with R. Linear fitting was done between the last reading time point with OD below 0.2 and the first reading time point with OD above 0.2 to determine the time that the culture reached OD 0.2, as the growth takeoff time.

Lab evolution experiments to monitor the escape of Chr XV trisomy in hygromycin B-containing culture

RLY6673 (Chr XV trisomy strain) and control diploid strain (RLY 2628) were cultured in YPD with 50 µg/ml hygromycin B. The cultures were grown at 30 °C until the trisomy culture showed significant growth. The trisomy culture was then diluted and plated onto YPD plate without drug to allow single colony formation. Both the liquid culture and 6 random single colonies were karyotyped.

Plating assays and E-test for *C. albicans*

C albicans colonies, recovered from the glycerol stock, were first karyotyped with qPCR to confirm the correct karyotype. Colonies were then streaked out on a fresh YPD plate and incubated at room temperature for 48 hours to allow single colony formation. ~2mm colonies were picked up, re-suspended in 1ml 0.82% sodium chloride solution with the final OD adjusted to 0.0005. 10 µl of the resulting suspension was plated to give rise to ~100 colonies per plate. The plate was incubated at 35°C in a humidity chamber for 2 days before the images were taken.

Cell resuspensions generated using the above procedure were adjusted to OD 0.02. The i5L and euploid strains were mixed 1:1 to make the “mix” cell population. 100 µl solution was plated onto each plate to reach 40,000 colonies per plate and the plate was allowed to absorb the excessive moisture at room temperature for 20 min. The E-test strips were applied according to the manufacturer's guideline (bioMerieux) and the plates were incubated in a wet room at 35°C for 48 hours before imaging.

III. Screens

Screening for agents against Chr XV trisomy

The 100x stock solution for each drug from various venders was prepared from the powder using DMSO or water or ethanol as the solvent. The stock was added into YPD media to make the YPD media with highest concentration possible for the drug, using robot Platemate Plus (Thermo Matrix). The YPD stock was further diluted, by robot Tecan EVO, into lower concentrations in YPD.

The cells (the euploid RLY2628 and the Chr XV trisomy RLY6673) were inoculated into drug-containing media using the robot Biomek FX. The starting OD reading of the culture is 0.05. The euploid and the Chr XV trisomy were arrayed in 384-well plates so that they neighbored to each other to control for positional effect. OD readings were taken by using a Tecan M200Pro reader. The data files were pooled and analyzed in R. The drug selectivity against Chr XV trisomy is defined as the log ratio at 17 hours (when both strains reached saturation under the non-stress condition):

$$\mathrm{Log}_2[\mathrm{OD(Euploid)} \,/\, \mathrm{OD(Chr\ XV\ trisomy)}]$$

Screening for agents against euploid or i5L *C. albicans*

To screen for compounds affecting the growth of euploid or i5L *C. albicans* in liquid culture, RPMI1640 medium (with MOPS and 2% glucose without bicarbonate, Lonza) was added to 384-well V-bottom

microplates (Axygen). Two libraries were used: the Microsource Spectrum Collection and Prestwick Chemical library[133], containing 2320 and 1280 small molecules, respectively, with a total of 2713 unique CAS registry numbers included. The compounds were added to RPMI+MOPS without bicarbonate +2% glucose using a positive displacement syringe head on a Platemate Plus (Thermo Matrix) to generate 112 µM stocks (60 µl total volume). Plates were agitated on a plate shaker to mix and then centrifuged at 1000 rpm for 5 min. Subsequently, media were mixed with disposable tips using a 384 air displacement head on Platemate Plus prior to pipetting 25µl of the stock into 384-well microplates with flat-bottom, round-shaped wells (Genetix). DMSO (8 wells, 0.8%) controls as well as fluconazole controls at varying concentrations (16 µg/ml, 32 µg/ml, 48 µg/ml or 64 µg/ml final concentration) were included on each plate.

Overnight cultures of *C albicans* strains in SC+uridine (the euploid and the i5L strain) were adjusted to the same OD_{600} and added into drug media by using a Thermo Matrix Equalizer multi-channel pipettor. 10 µl culture of 100 cells was added into each well containing 25 µl to bring the final concentration of each compound from 112 µM to 80 µM. A total of 3600 assay conditions were distributed into 2 sets (one for the euploid and the other for the i5L strains) of 17 384-well plates with the edge wells skipped without cells. The plates were incubated in a humidity chamber at 35 °C with OD readings taken with a Tecan M200Pro reader. The OD readings were analyzed in R. Drugs that repressed the growth of either the euploid or the i5L strain for more than 80% compared to the non-drug controls were selected as hits for the second round of screening extending the assay to multiple concentrations (see below).

Culture plates were prepared and incubated the same way as described above, except that each drug was assayed at 9 different concentrations ranging from 1 µM to 160 µM and two replicates for each strain and each drug were assayed. The OD reading was taken at 24-hour and analyzed using R. OD readings of each strain under a series of different concentrations of the same drug were normalized to the non-drug control and fitted by a four-parameter log-logistic curve using drc package in R[133]. IC80 values derived from the

fittings were compared between the euploid and the i5L strain. Not all chemicals' drug response curves could be fitted and IC80 of these chemicals were missing. For example, flucytosine killed both the euploid and the i5L across all concentrations tested including the lowest at 1 μM.